TECHNISCHE UNIVERSITÄT MÜNCHEN

Lehrstuhl für Verkehrstechnik

A Mesoscopic Emission Model to Assess the Impact of ITS Measures on the Spatial Distribution of Traffic Emissions in Urban Road Networks

Yingjie Wu, M.Sc.

Vollständiger Abdruck der von der Ingenieurfakultät Bau Geo Umwelt der Technischen Universität München zur Erlangung des akademischen Grades eines Doktor-Ingenieurs genehmigten Dissertation.

Vorsitzender: Prof. Dr.-Ing. Stephan Freudenstein

Prüfer der Dissertation:

1. Prof. Dr.-Ing. Fritz Busch
2. Prof. Dr.-Ing. Keping Li, Universität Tongji

Die Dissertation wurde am 15.07.2020 bei der Technischen Universität München eingereicht und durch die Ingenieurfakultät Bau Geo Umwelt am 30.11.2020 angenommen.

Beijing, 2019.06.23

Acknowledgments

I sincerely appreciate all the help and support from all the people in my doctoral research way. I would like to express my sincere gratitude to Prof. Busch, who has accepted me as the doctoral candidate of the TUM, as well as supervised the research and my personal growth. I have greatly appreciated his inspirations, guidance, positivity, open-mindedness, patience, and financial support. Without these, I can hardly complete the doctoral research. I am also very thankful for Prof. Li, who has given me valuable inputs and suggestions on the improvements as well. I also greatly appreciate daily sharing and support from the research group I belonged to, especially my mentor, Dr.-Ing. Antonios Tsakarestos.

I would also like to thank the CSC (China Scholarship Council) for its financial support. Owing to it, I can come to Germany for my further study.

Last but not least, I would say thanks to my family and friends who encourage me and motivate me a lot as always.

Yingjie Wu

Abstract

Air quality issues and traffic-related emissions draw increasing attention from public authorities and governments. In the context of communication technologies and digitalization, Intelligent Transport Systems (ITS) are emerging, which can not only improve traffic efficiency and safety but can also reduce emissions at the same time. In order to choose ITS under consideration of changes in emissions, careful emission impact assessments need to be conducted. For such assessments, a wide range of emission models have been developed and integrated with different levels of traffic models. The macroscopic emission models can estimate the emissions either at the country, regional, or street level. Although these models require less detailed data and have a lower computation cost, they cannot identify emission hot spots on which traffic management and control could focus. In contrast, microscopic emission models can estimate emissions more accurately in higher temporal and spatial resolution while demanding a larger amount of data and more intensive computation. To help assess the impact of ITS on emission, a more user-friendly and feasible emission model needs to be developed, taking into account the required resolution, the validity of the assessment, as well as resulting costs. To this end, this thesis aims to develop a time- and data-efficient mesoscopic emission model that can distinguish local emission changes resulting from different ITS measures. Following this objective, the main research questions are how to divide streets and intersections into small segments and how to estimate the emission changes in each small segment.

To investigate all possible cases of the speed variation, various causes of the speed change are considered by designing typical scenarios, including the infrastructure layout, the traffic control, and the traffic condition. Since the emission factor for the passenger car and truck differs significantly, the truck percentage is included in the study. In order to develop the model, the research identifies the important types and parameters of traffic flow variations and the corresponding causes and quantifies their effects on local emissions. By integrating the emission model with a mesoscopic traffic model, it is possible to assess the changes in the emission distribution in an urban road network. By linking this combined mesoscopic traffic and emission model with ITS control measures, it is possible to assess the different emission impacts of ITS measures and allow for a comparison of their effects on emissions, which is important to facilitate decision making in traffic management under environmental objectives. Additionally, the emission model can be integrated with dispersion models to generate air quality maps – this is not elaborated in detail but shows an operational application option of the new mesoscopic approach.

As field-measurements are by far too difficult to conduct and therefore fall outside the scope of this study, the use of simulation as virtual reality was chosen instead. VISSIM, a microscopic traffic simulation, and PHEM, a detailed physical emission model, are used as a linked framework; both simulators represent current state-of-the-art models for high-resolution investigations in traffic flow and emission determination. By analysis of literature and some preliminary studies, meaningful variables of traffic and infrastructure are defined for the model

development, including lane type, traffic volume, turning ratio, truck percentage, cycle time, green ratio, and speed limit. Using the experimental design method, various scenarios with these variables are designed. The spatial data mining methods are reviewed, and the Local G* method is chosen for the segment division. Based on the distribution and variance of the segment boundaries for each lane type, the rules to divide the road into smaller segments are defined. The traffic volume, percentage of the trucks, capacity, speed limit, conflicting traffic volume, and its truck percentage, average speed, and cycle time are used as the predictors. The regression modeling method is chosen to select variables and estimate parameters for the emission function. Linear, interaction, and stepwise models are applied. The emission regression function is optimized to minimize the prediction error and ensure the sign of the effect of each prediction reasonable. The results show that there are four major segments along the road: the midblock, the segment close to the stop line, the segment on which vehicles cross the intersection, and the segment where vehicles leave the intersection to drive towards the midblock. Each segment can be further categorized according to the lane type, including separate lanes or mix-used lanes, as well as driving directions.

The test environment consists of a small road network with four intersections with different layouts and link lengths. Among the intersections, the approach that consists of the types of lanes for modeling development is chosen to compare different emission models. The size of the high-emission area is compared with the one from the Local G* method. The tested results show that the rules can identify the high-emission area before the stop line on the lane of straight-through and right-turning traffic as well as the straight-through lane. It slightly overestimates the size of the high-emission area on the left-turning lane, while it underestimates the size of the area after crossing the intersection.

The emission estimation by the developed model is compared with the one from HBEFA as well as from the high-resolution models VISSIM and PHEM. The result of the integration of the VISSIM and PHEM is the baseline. Generally, the developed model performs better than HBEFA on the hot spots, lanes, and approaches. The predictivity of the developed model is suggested to be improved by considering the length of crossing lanes and the turning radius. The accuracy of traffic volume is important to ensure the good performance of the emission model on the segment emissions, especially when there are multi-lanes. The developed emission model and HBEFA perform similarly on the absolute differences in the estimation of the stream emissions from PHEM. To estimate the impact of the rerouting on the emission factor of NO_x, the developed model performs better than HBEFA at the segment-, lane-, approach-level. The result of the stream emissions from the HBEFA is only slightly different from the developed emission model.

The developed model can identify the segments with significantly high or low emissions. It can estimate the changes in the emissions as a result of the ITS in urban traffic management and control to help choose ITS. It is also introduced how to estimate the near-road air quality by integrating between the developed emission model and a dispersion model. The model concept and research methodology can be applied to other types of intersections, such as

three-ways junctions, ramps, non-signalized intersections, and roundabouts. It is suggested that a dynamic prediction model can be developed to better estimate the size of the segment after crossing an intersection. In the future study, the impact of the length of the crossing lane, the turning radius, pedestrians, cyclists, public transportation, road slope, and road width should also be investigated by using a more detailed traffic flow model and emission model. Future research can also investigate if the developed model concept can estimate the ADAS and autonomous driving.

Zusammenfassung

Luftqualitätsfragen und verkehrsbedingte Emissionen ziehen die zunehmende Aufmerksamkeit von Behörden und Regierungen auf sich. Im Zusammenhang mit den Kommunikationstechnologien und der Digitalisierung entstehen intelligente Verkehrssysteme (ITS), die nicht nur die Effizienz und Sicherheit des Verkehrs verbessern, sondern auch Emissionen reduzieren können. Um die Entscheidungsfindung über den Einsatz von ITS unter Berücksichtigung der Emissionsänderung zu erleichtern, ist die Durchführung einer sorgfältigen Emissionsverträglichkeitsprüfung erforderlich. Für solche Bewertungen wurde eine Vielzahl von Emissionsmodellen entwickelt und mit verschiedenen Ebenen von Verkehrsmodellen integriert. Makroskopische Emissionsmodelle können die Emissionen entweder auf Länder-, Regional- oder Straßenebene schätzen. Doch während dieser Modelle weniger detaillierte Daten benötigen und geringere Berechnungskosten haben, eignen sie sich nicht zur Identifikation von Emissions-Hotspots, auf welche sich das Verkehrsmanagement und die Verkehrsregelung konzentrieren könnten. Im Gegensatz können mikroskopische Emissionsmodelle Emissionen in höherer zeitlicher und räumlicher Auflösung genauer abschätzen, erfordern jedoch auch viel größere Datenmengen und intensivere Berechnungen. In Anbetracht der erforderlichen Auflösung, Aussagekraft der Bewertung und der Kosten, wie sie in dieser Doktorarbeit angestrebt werden, muss ein benutzerfreundlicheres und praktikableres Emissionsmodell entwickelt werden, um die Auswirkungen von ITS auf die Emissionen zu bewerten. Ziel dieser Forschung ist es, ein mesoskopisches Emissionsmodell zu entwickeln, das die lokalen Emissionsänderungen aufgrund verschiedener ITS-Maßnahmen unterscheiden kann, jedoch mit geringem Daten- und Zeitaufwand. Zur Erreichung dieses Ziels gilt es insbesondere die Forschungsfrage zu beantworten, wie Straßen und Kreuzungen in kleine Segmente geteilt und wie Emissionsänderungen in jedem kleinen Segment abgeschätzt werden können.

Um alle möglichen Fälle von Geschwindigkeitsänderungen zu untersuchen, werden verschiedene Ursachen für eine Geschwindigkeitsänderung anhand typischer Szenarien wie Infrastrukturlayout, Verkehrssteuerung und Verkehrssituation in Betracht gezogen. Da sich der Emissionsfaktor für Pkw und Lkw stark unterscheidet, wurde der Lkw-Anteil in die Studie miteinbezogen. Zur Entwicklung des Modells identifiziert die Doktorarbeit die wichtigsten Arten und Parameter sowie die entsprechenden Ursachen von Verkehrsflussschwankungen und quantifiziert deren Auswirkung auf die lokalen Emissionen. Durch die Integration des Emissionsmodells mit einem mesoskopischen Verkehrsmodell ist es möglich, die Veränderungen der Emissionsverteilung in einem städtischen Straßennetz zu beurteilen. Durch die Verknüpfung dieses kombinierten mesoskopischen Verkehrs- und Emissionsmodells mit ITS-Steuerungsmaßnahmen können verschiedene Emissionsauswirkungen von ITS bewertet und ein relativer Vergleich ihrer Auswirkungen gezogen werden. Dies ermöglicht eine erleichterte Entscheidungsfindung im Rahmen des Netzverkehrsmanagements unter Umweltgesichtspunkten. Darüber hinaus kann das Emissionsmodell mit Ausbreitungsmodellen integriert werden, um Luftqualitätskarten zu

erstellen - dies wird nicht im Detail erläutert, sondern zeigt operative Anwendungsmöglichkeiten des neuen mesoskopischen Ansatzes.

Da das Durchführen von Feldmessungen viel zu aufwendig wäre und über die Möglichkeiten dieser Doktorarbeit hinausgehen würde, wurde beschlossen, die Simulation als Virtual Reality durchzuführen. VISSIM, eine mikroskopische Verkehrssimulation, und PHEM, ein detailliertes physikalisches Emissionsmodell, werden als vernetztes Framework eingesetzt; beide Simulatoren stellen aktuelle State-of-the-Art-Modelle für hochauflösende Untersuchungen in der Verkehrsfluss- und Emissionsbestimmung dar. Durch die Analyse von Literatur und einigen Vorstudien werden für die Modellentwicklung aussagekräftige Verkehrs- und Infrastrukturvariablen definiert, darunter Fahrspurtyp, Verkehrsaufkommen, Wendeverhältnis, Lkw-Anteil, Zykluszeit, Grünanteil und Tempolimit. Mit Hilfe einer experimentellen Entwurfsmethode werden verschiedene Szenarien mit diesen Variablen entworfen. Die räumlichen Data-Mining-Methoden werden überprüft und für die Segmentaufteilung wird die lokale G*-Methode gewählt. Basierend auf der Verteilung und Varianz der Segmentgrenzen für jeden Spurtyp werden die Regeln für die Aufteilung der Straße in kleinere Segmente definiert. Als Prädiktoren werden das Verkehrsaufkommen, der Prozentsatz des Lkw-Anteils, die Kapazität, das Tempolimit, das entgegengesetzte Verkehrsaufkommen und sein Prozentsatz des Lkw-Anteils, die Durchschnittsgeschwindigkeit und die Zykluszeit verwendet. Das lineare, interaktive und schrittweise Modell wird getestet. Die Emissionsregressionsfunktion ist optimiert, um den Vorhersagefehler zu minimieren und sicherzustellen, dass das Vorzeichen der Wirkung jedes Prädiktors sinnvoll ist. Die Ergebnisse zeigen, dass es vier Segmente entlang der Straße gibt: das obere Segment, das Segment nahe der Stopplinie, das Segment für die Überquerung und das Segment von nach der Kreuzung bis zu dem oberen Segment. Jeder Segmenttyp könnte zusätzlich nach Spurenart, wie beispielsweise nach getrennten oder gemischten Fahrspuren sowie Fahrtrichtung kategorisiert werden.

Die Testumgebung besteht aus einem kleinen Straßennetz mit vier Kreuzungen mit unterschiedlichen Layouts und Verbindungslängen. Das Testfeld besteht aus einer Kreuzung mit den gleichen Arten von Fahrspuren wie in der Modellentwicklung. Die Größe des Hochemissionsbereichs wird mit der Größe des lokalen G*-Verfahrens verglichen. Die getesteten Ergebnisse zeigen, dass die angewandten Regeln den emissionsreichen Bereich vor der Stopplinie auf der Fahrspur des geradeausfahrenden und rechts abbiegenden Verkehrs sowie auf der Fahrspur des geradeausfahrenden Verkehrs identifizieren können. Sie überschätzen leicht die Größe des emissionsreichen Bereichs auf der links abbiegenden Fahrspur, während die Größe des Emissionsbereichs nach Überqueren der Kreuzung unterschätzt wird.

Die Emissionsschätzung des entwickelten Modells wird mit der der HBEFA sowie mit den hochauflösenden Modellen VISSIM und PHEM verglichen. Das Ergebnis der Integration von VISSIM und PHEM ist die Grundlinie. Im Allgemeinen schneidet das entwickelte Modell bezüglich Hotspots, Fahrspurebene und Anflugebene besser ab als die HBEFA. Die

Vorhersagekraft des entwickelten Modells kann durch Berücksichtigung der Länge der kreuzenden Fahrspuren und des Wenderadius verbessert werden. Die Genauigkeit des Verkehrsaufkommens ist wichtig, um eine gute Leistung des Emissionsmodells in Bezug auf die Segmentemissionen zu gewährleisten, insbesondere bei mehrspurigen Strecken. Das entwickelte Emissionsmodell und HBEFA schneiden bei den absoluten Unterschieden in der Schätzung der Stromemissionen aus dem PHEM ähnlich ab. Um die Auswirkungen der Umleitung auf den Emissionsfaktor von NO_x abzuschätzen, schneidet das entwickelte Modell auf der Segment-, Fahrspur- und Anfahrebene besser ab als HBEFA. Das Ergebnis des Stromes aus dem HBEFA unterscheidet sich nur geringfügig von dem entwickelten Emissionsmodell.

Es wird geschlussfolgert, dass das entwickelte Modell Segmente mit signifikant hohen oder niedrigen Emissionen identifizieren kann. Zudem ermöglicht es eine Abschätzung der Emissionsveränderungen die infolge des ITS im städtischen Verkehrsmanagement und in der Verkehrssteuerung auftreten, und kann somit bei der Auswahl des richtigen ITS helfen. Des Weiteren wird dargelegt, wie die Luftqualität in Straßennähe durch Integration des entwickelten Emissionsmodells mit einem Ausbreitungsmodell abgeschätzt werden kann. Das Modellkonzept und die Forschungsmethodik können auf andere Kreuzungstypen angewandt werden, wie z.B. Drei-Wege-Kreuzung, Rampen, nicht signalisierten Kreuzungen und Kreisverkehren. Es ist vorschlagt, dass ein dynamisches Vorhersagemodell entwickelt werden kann, um die Größe des Segments nach dem Überqueren eines Schnittpunkts besser abzuschätzen. In einer zukünftigen Studie sollten auch die Auswirkungen der Kreuzungsspurlänge, des Wenderadius, der Einfluss von Fußgängern, Radfahrern und des öffentlichen Verkehrs sowie der Straßenneigung und der Straßenbreite ebenfalls mit Hilfe des detaillierten Verkehrsfluss- und Emissionsmodells untersucht werden. In der weiteren Forschung kann zudem untersucht werden, ob das entwickelte Modellkonzept das ADAS und das autonome Fahren abschätzen kann.

Table of contents

1. Introduction

1.1 Background

Huge populations often suffer from bad air quality. It is estimated that 90% of people are exposed to severely polluted air (World Health Organization, 2018). In cities, road traffic emissions are the main sources of air pollutions, including nitrogen oxides (NO_x), particulate matter (PM), carbon monoxide (CO), and hydrocarbons (HCs) (Transportation Research Board, 2002; Zhang & Batterman, 2013). These pollutants could have adverse effects on human health, including “mortality, nonallergic respiratory morbidity, allergic illness and symptoms, cardiovascular morbidity, cancer, pregnancy, birth outcomes, and male fertility”(Heinrich et al., 2005, p.125). Thus, road traffic emission and air quality have attracted lots of attention from the public and the government. Nowadays, decision-makers have to consider not only traffic congestion and safety but also emission issues. In order to support the deployment of traffic measures under consideration of emissions, it is necessary to conduct an emission impact assessment.

Intelligent transport systems (ITS) as emerging technologies mainly aim to solve traffic congestions and improve safety. They also play a potential role in emission reduction, for example, by smoothing traffic flow or facilitating route choice. Since the cause and effect of ITS on congestion, safety, and emissions are different, the impact of ITS on these issues should also be conducted separately. ITS may follow conflicting objectives, and the solutions they provide may result in trade-offs, such as route assignment to minimize both travel time and emissions (Macedo et al., 2020). In order to prioritize the consideration of emissions in the deployment of ITS, it is necessary to conduct an emission impact assessment of ITS. The applications of the information, communication, and sensor technologies in the ITS provide the possibility for more dynamic decision-making in traffic management. On the one hand, the dynamics of ITS require that the emission impact assessment is based on real-time estimations. On the other hand, it also supports the realization of the real-time estimation of emissions.

On the one hand, the distribution of emissions shows spatial and temporal heterogeneity on the urban road network. On the other hand, local air quality is a more meaningful estimator of the hazard exposure level. Thus, further knowledge is required on how the spatial distribution of emissions changes, especially with regard to the location of high-emission zones, area size, and emission level, rather than merely measuring total emissions on roads or a network. Otherwise, it would be impossible to identify where exactly higher emissions occur, as emission levels would be averaged over the entire area, which may consist of both short high-emission distances and long low-emission distances. However, most of the existing emission impact assessments focus only on the total changes in emissions over a road or a city.

In terms of assessment scale, local traffic and emissions cannot only be influenced by local traffic measures, but also by network or surrounding measures. Therefore, the assessment of ITS should be conducted on a larger scale. A large scale of assessment may, however, lead to a more data-consuming and cost-intensive assessment.

Nowadays, the common emission impact assessment is conducted via the integration of one traffic simulation model and one emission model. The traffic simulation model serves to generate traffic data, while the emission model consists of emission factors. Traffic data from the traffic simulation model would be used as an input in the emission model to estimate emissions. There are three major types of emission estimation methods based on the aggregation level of the traffic data: the average speed-based emission estimation, traffic situation-based, and instantaneous (engine or driving dynamics-based) emission estimation. The average speed-based and traffic situation-based emission estimation approaches can provide regional and urban emission inventory or emissions estimation for long roads. However, they cannot account for the detailed spatial and temporal distribution of emissions, because they do not sufficiently consider the effect of driving dynamics on emissions. The instantaneous emission models, in turn, can provide more accurate short-segment emissions but are limited in scalability due to the consumption of large amounts of data and computation time. Furthermore, a more detailed complex model cannot always offer higher accuracy because the uncertainty arising from the larger amount of data may become a bigger issue.

1.2 Research motivation

On the one hand, the emission impact assessment should focus on the more detailed emission distribution while considering a bigger urban network. On the other hand, the emission estimation framework can reflect the level of the emission change due to ITS and help pre-select some types of ITS before detailed design and more accurate emission estimation are carried out. Conducting two stages of emission impact estimation can improve the efficiency of the decision-making, reduce the cost, and ensure the validity of the assessment. Moreover, the more detailed emission distribution can be used as an input in the dispersion model to estimate the changes in air quality near roads. As the existing emission models cannot simultaneously fulfill the needs of both validity and efficiency, a new emission model needs to be developed.

1.3 Research objectives and questions

The study aims to develop a feasible emission model for assessing the impact of ITS on emissions. It should be able to distinguish between road segments with high and those with low emissions. The model should further be sensitive to ITS to help compare different ITS measures. It would also be user-friendly and ensure that the emission estimation is closest to the best achievable results. Two main research questions should be answered to develop such

a model. One is what is the effective resolution to identify the hot emissions and represent the spatial emission variation. Another is how to derive the emission changes on each road segment due to ITS without knowing each vehicle's speed profile.

1.4 Research structure

Fig. 1.1 shows the structure of the study. In chapter 2, the characteristics and spatial distribution of the road traffic emissions are described, the methodology of the emission impact assessment of ITS, and the existing road traffic emission models are systematically reviewed based on literature analysis. The experience and knowledge of emission impact assessment derived from this analysis will inform the development of a new emission model concept. In chapter 3, the model concept and development methodology are described, including road divisions, emission estimations, and the design of scenarios. Additionally, the results of the road division and emission function of each segment type are shown and discussed. The rules of the segment division and emission functions are tested on an intersection in a small network environment. The detailed test scenarios and test results are described in chapter 4. Chapter 5 introduces the integration between the developed emission model and a dispersion model to estimate air quality near roads. In chapter 6, the conclusions and outlooks are addressed, including transferability, limitations, contributions, and future work.

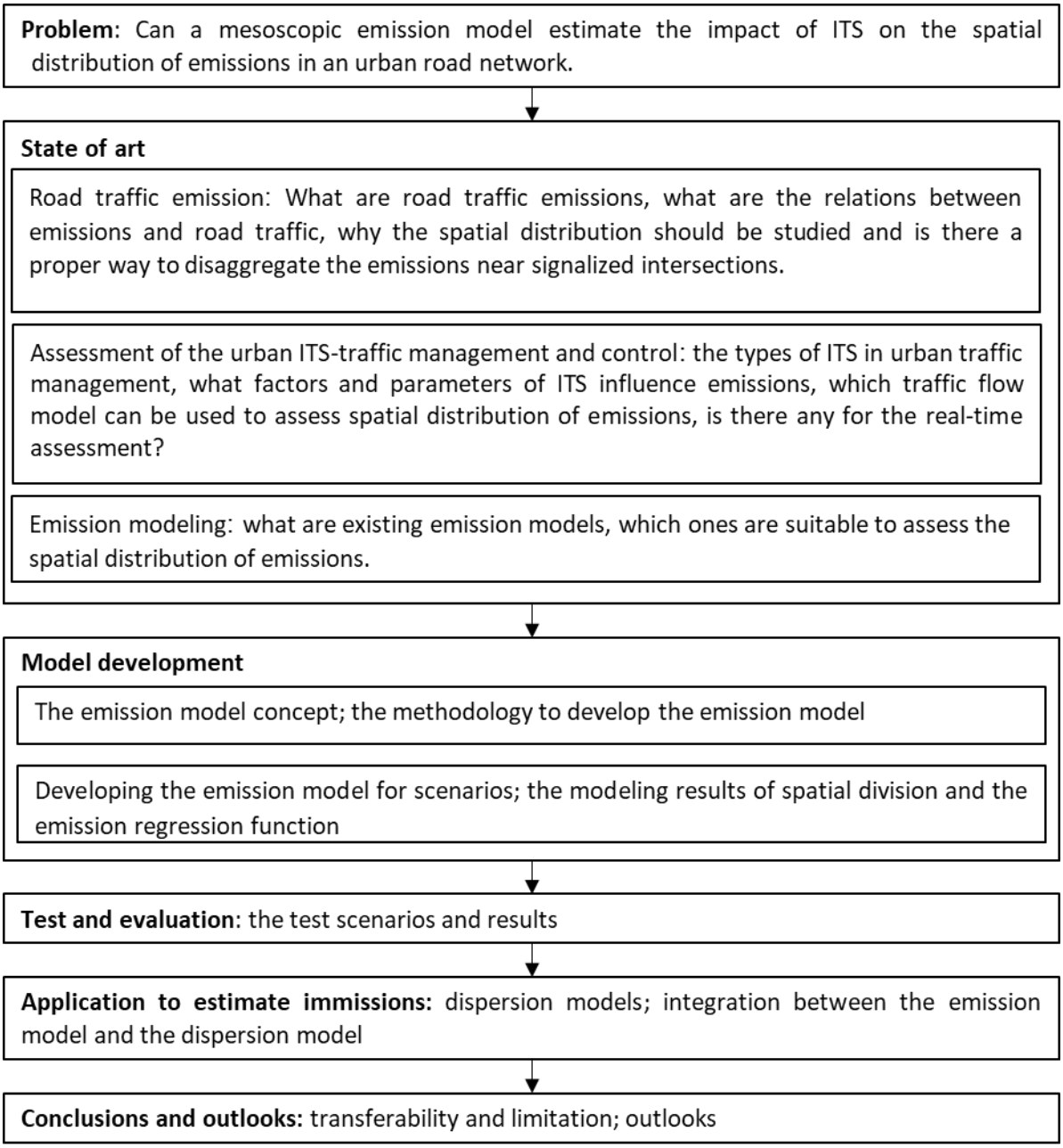

Fig. 1.1 Research structure

2. State of the art: road traffic emission estimation

In this chapter, the context and existing studies about road traffic emissions are summarized. It includes the cause and effect between the ITS for urban traffic management and road traffic emissions and the methods of the emission impact assessment. It explains why the spatial distribution of emissions should be estimated, how to appropriately divide the road in order to distinguish between high and low-emission areas, whether the simulation models are used for the modeling development, how the ITS for urban traffic management influences the emissions, and what the potentials and limitations of the existing estimation methods are. In each sub-chapter, the relevant literature and studies are summarized, and conclusions will be addressed in the end.

2.1 Road traffic emissions

This subchapter will answer the questions of what road traffic emissions are, what factors influence these emissions, how emissions are spatially distributed, why spatial distribution should be studied, and, finally, whether there exists any proper way to disaggregate emissions spatially.

2.1.1 Types of road traffic emissions

The main road traffic emissions are NO_x, PM, CO, HCs, and sulfur oxides (SO_x) (Hülsmann, 2014). Road traffic can produce tailpipe emissions and non-tailpipe emissions. Non-tailpipe emissions are the emissions due to the wear and tear of the road surface, brakes, and tires. Tailpipe emissions are emitted from combustion engines. They may result from incomplete combustion, high temperatures, fuel impurities, or evaporation. Since tailpipe emissions are the primary source of road traffic emissions, they form the focus of the study. Tailpipe emissions can be categorized into hot stabilized emissions, warm-start emissions, and cold-start emissions(Environmental Protection Agency, 1993). Hot stabilized emissions are emitted when both engine and catalytic converters are around operating temperatures; warm-start emissions are emitted when only the engine is hot; cold-start emissions are defined when both engine and catalytic converters are cool (Environmental Protection Agency, 1993).

The main difference between cold-start emissions and hot stabilized emissions is caused by the different fuel/air ratios and the emission control equipment (Ding, 2000). Several studies show that the percentage of cold-start emissions depends mainly on the ambient temperature, the average trip length, driving dynamics (the speed and acceleration rate), and the operating temperature of the emission control system (Joumard & Andre, 1990; Matthaios et al., 2019). By using a real-world collection of driving profiles, emission measurement equipment, and a detailed emission model, it was found that warm- and hot-start emissions are significantly

influenced by the driving dynamics, road gradient, fuel type, as well as vehicle and engine characteristics (Avetisyan, Miller-Hooks, Melanta, & Qi, 2014).

2.1.2 Influencing factors on emissions

Urban road traffic constitutes a complex and dynamic system. Agents in the system can be categorized into infrastructure, traffic modes (non-motorized and motorized), and users. The natural environment (e.g., weather) also plays a role in the system. The interaction of agents in the system results in spatial-temporal distributions of emission levels. Some researchers grouped influencing factors into traffic, road, and vehicle characteristics, and identified the parameters in each group (Pandian et al., 2009). The effect of these factors on emissions depends on the type of air pollutant. For example, emissions of HC and CO are larger, when significant acceleration occurs at high speeds, while emissions of NO_x do not show such an effect(Ding, 2000). Local emissions are the total emissions of several vehicles within a defined area and time interval. Local emissions are generally predicted by the multiplication of an emission factor with corresponding traffic activity data. Smit (2006, p.98) described that "emission factors quantify the amount of pollutant[s] emitted" by being "usually expressed as mass per unit distance (e_x) at the link or network level and as mass expressed per unit time (e_t) at the vehicle level". The factors that influence emissions depend on the level of analysis. In the study by Smit (2006), the influencing factors were summarized separately at the vehicle-, link-, and network-levels. In this study, the influencing factors are categorized for an individual vehicle, traffic over a short street segment, traffic over an entire lane, traffic across an intersection, and traffic within a whole network. After reviewing existing studies, the factors found to influence emissions at different levels are summarized below.

Emissions of a vehicle at a certain point in time are influenced by the following list of factors:

- fuel characteristics (gasoline, diesel, electric vehicle) (Delavarrafiee & Frey, 2018)
- vehicle age, size, weight, and load (Pandian, Gokhale, & Ghoshal, 2009)
- engine load and capacity (Pandian, Gokhale, & Ghoshal, 2009) and deterioration of the engine (Organ et al., 2020)
- emission control technology (Mera et al., 2019) and the deterioration of its components (Mera et al., 2019)
- engine speed and torque (Lozhkina & Lozhkin, 2016)
- use of auxiliary equipment (Zachiotis & Giakoumis, 2019)
- road gradient (Prakash & Bodisco, 2019)
- ambient temperature and humidity (Hall et al., 2020)
- air density of the location (Smit, 2006; Sturm et al., 1996)

Emissions of a certain vehicle type driving across an intersection are influenced by the following list of factors:

- on-road geometric and operational characteristics: speed limit, vehicle's position in a queue, road gradient, traffic volumes on downstream lanes and upstream lanes,

distance from the closest downstream signalized intersection, and the ratio of heavy-duty vehicles (Hallmark et al., 2002).
- type of the intersection (signalized intersection and roundabout) (Gastaldi et al., 2017).
- driving style: an aggressive, conservative, professional, or experienced driver (Lu et al., 2017); eco-driving (J. Sun et al., 2013).
- road type or facility type(freeway segments, ramps, local streets, collectors) (Christopher Frey et al., 2006)

Emissions on a lane: the total emissions of a group of vehicles could be theoretically obtained by summarizing the emissions of all relevant vehicles. However, this is not very practical, as it would demand large amounts of data and due to the limitations of data collection techniques. Therefore, the average emission factor is used instead as an approximation of the individual vehicle's emission factor. The vehicles are classified into several groups based on emission-influencing factors like vehicle types, fuel types, and emission standards (Smit, 2006). Apart from the road gradient, the average emission factor is further influenced by the following factors:

- the composition of vehicle classes (Smit, 2006)
- the traffic flow pattern (Schreckenberg et al., 2015)

Emissions near an intersection area are the total emissions from the vehicles that drive on all the approaches of the intersection. Apart from the composition of vehicle classes and the road gradient, some studies have investigated the influencing factors at the macroscopic level:

- macroscopic traffic flow factors: delay time, number of stops, queue length, and average speed (Guo & Zhang, 2014); Level of service (Papson et al., 2012)
- type of the intersection (signalized intersection and roundabout) (Salamati et al., 2015)
- pedestrians and cyclists: a few studies have been carried out on modeling the impact of the interaction between cyclists, pedestrians, and vehicles on emissions (Paulo Fernandes & Coelho, 2017; Li & Sun, 2014). They focused on the cyclist volume, pedestrian volume, traffic density, and yielding rate.
- platoon ratios and early or late arrival (Lv & Zhang, 2012)

Emissions in a network are defined as the total emissions of all vehicles driving on the roads consisting of several intersections. Apart from the composition of vehicle classes and the road gradient, the average emission factor could be influenced by the following factors:

- space between intersections (Fernandes, Coelho, & Rouphail, 2017)
- levels of interruptions and congestions on the roads (Choudhary & Gokhale, 2019)

There may be some other factors that influence emissions at a specific level that need to be addressed. However, they have not been well studied, since there exists either no valid methodology to measure or model these factors, or there exists a resource constraint. Such factors include the detailed interaction behavior among traffic modes like cars, trucks, buses, bicycles, and pedestrians.

Based on the relationship of these factors across various levels, the multi-level cause and effect relationship between traffic and tailpipe emissions is summarized in Fig. 2.1. In the traffic system, factors that may influence driving and engine behavior include the traffic management and control, type of road and intersection, infrastructure layout and geometry, traffic volume, vehicle composition, and driver type. The engine behavior influences the emission factor directly. Additionally, the vehicle characteristics and weather influence the emission factor as well. In the end, local emissions are the result of the multiplication of the emission factor with the traffic activity data (traffic volume and travel time or distance).

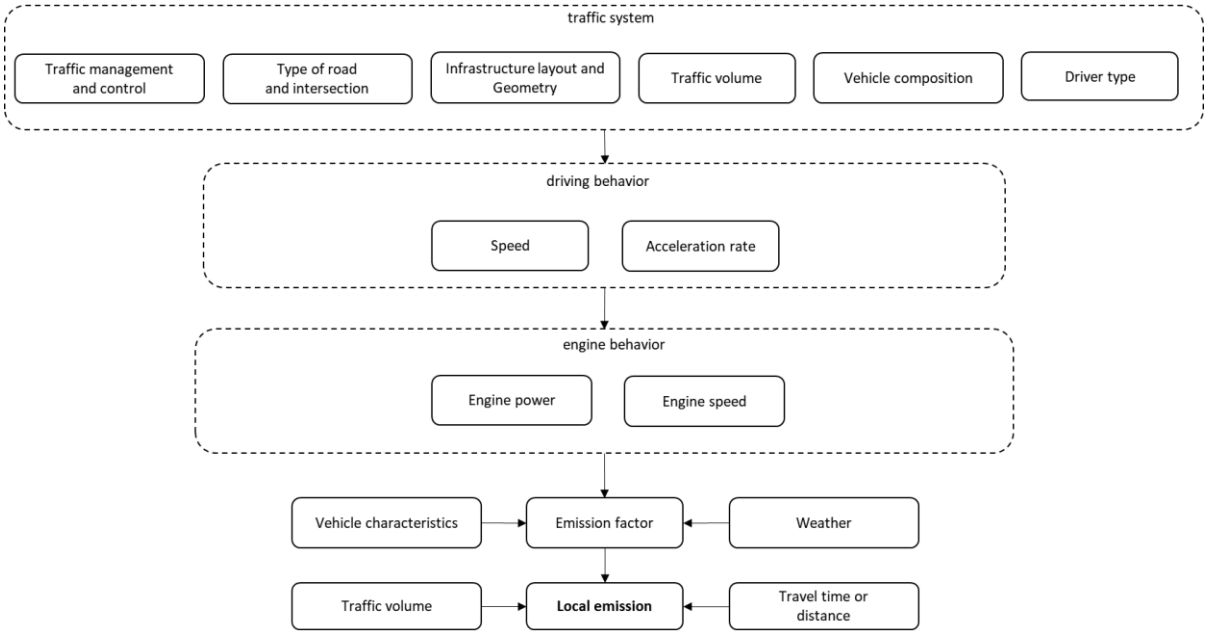

Fig. 2.1 Framework for the integration of all factors that influence tailpipe emissions

2.1.3 Emission distribution on the urban road network

The identification and evaluation of high-emission areas are the most critical, as they may negatively affect air quality and human health. The distribution of emissions shows spatial and temporal heterogeneity on the urban road network (Freedman, 1984; Sun, Zhang, & Shen, 2018). The level of the emissions varies not only at street-level but also between individual road segments. The level of the fine particulate matter($PM_{2.5}$) varied largely every ten meters (Targino et al., 2016). Various studies on onboard measurements and simulations show that emission hot spots in urban locations mainly occur near intersections and especially during stop-and-go situations (Unal, Frey, Rouphail, & Colyar, 2001; Unal, Frey, & Rouphail, 2004). High NO_x emissions are located near intersections and increase in the vicinity of bus stops (Tate & Connors, 2012). High NO_x emissions near intersections are the result of a high traffic density and interruptions of the traffic flow. NO_x emissions near a bus stop increase because buses as heavy diesel vehicles need to accelerate additionally to depart from a bus stop (Tate & Connors, 2012). Targino et al. (2016) conducted a study to measure the concentrations of black carbon and $PM_{2.5}$ through mobile sampling carried by cyclists on several urban roads. They found that concentrations of black carbon and $PM_{2.5}$ showed skewed distributions and

that the pollutants were concentrated near signalized intersections as well as bus stops (Targino et al., 2016). Due to complex wind flow and dynamic speed changes, the average concentration of particle numbers measured at a signalized intersection can be up to one order higher than the average value at roadsides and street canyons (Goel & Kumar, 2014). The measured PM concentration on the street decreases exponentially the further away from the center of the intersection (the measure points are 10, 20, 30, 45, and 60 meters away from the center, respectively) (Goel & Kumar, 2016). Furthermore, it has been found that pedestrians who cross an intersection are exposed to a high level of air pollutants (Borge et al., 2016). Based on these studies, we can conclude that vehicles emit high levels of pollutants in the vicinity of intersections. It can be the result of a high traffic density, an interruption of traffic flow through traffic control measures, conflicting traffic flows, and turning traffic. Besides, the topology of the intersection, built-up area, and environmental factors like wind speed and wind directions further contribute to the concentration of pollutants at the intersection. The ITS can influence the traffic near intersections by impacting the traffic density, fleet composition, and driving conditions through measures like traffic signal control, routing, demand access management, speed limit, etc. The resulting changes in traffic can influence emission levels and exposures to pollutants near intersections. Since intersections are areas with high traffic emissions and exposure levels and because the ITS can influence traffic near intersections, areas around intersections should be seen as key areas for assessing the impact of ITS on emissions and exposures.

The ambient concentration depends strongly on local emissions and meteorology. Due to the variation of local emissions and meteorology, the ambient concentration varies strongly with the locations and time. A detailed estimation of emissions and dispersions is required to capture the variation of the air quality. It has been shown that when estimated emissions are used as inputs of the dispersion model to predict the near-road air quality, different spatial resolutions of emissions can lead to different predicted ambient concentrations (Ritner et al., 2013). Thus, to evaluate the impact of ITS on emissions and air quality, a proper spatial resolution for the emission estimation is required.

Most of the existing emission impact assessments focus on changes in area-wide emissions or street emissions. However, they cannot distinguish emission levels between smaller road segments. Some studies have investigated emissions near intersections at a detailed spatial level. Some have divided the street near the signalized intersection based on fixed distances (Lee et al., 1983). Tate and Conors (2014) studied the spatial variation in emissions based on fixed segment sizes (each a length of 10 meters). While the results of the study indicate that the spatial resolution of each 10-meter segment can reflect the locations of high and low emissions, they also show that similar levels of emissions exist on several connected road segments (Tate and Conors, 2014). That suggests that these connected segments could be aggregated into a single larger segment to reduce data and time expenditure for the emission and air quality assessment. In another study, a roundabout corridor was divided into segments and sub-segments (Fernandes, Salamati, Rouphail, & Coelho, 2015). In this study, the street was divided into four segments based on the vehicle’s speed pattern: 1. the circulation lane;

2. the section after crossing the roundabout, where vehicles accelerate to the cruising status; 3. the section where vehicles are driving at cruising speed; 4. the section where vehicles decelerate to drive towards the downstream roundabout (Fernandes, Salamati, Rouphail, & Coelho, 2015). The location of high emissions depends on whether or not the space between the roundabouts is equal. This method requires information on the vehicle's speed profile to calculate the boundaries between smaller segments. In order to identify the hot spots and help estimate the near-road air quality when there exists no information on speed, the question remains how streets with intersections should be divided appropriately.

2.1.4 Summary

Road traffic is the dominant anthropogenic source of NO_x, CO, and HCs in urban areas. Vehicle tailpipe emissions are the primary source of road traffic emissions. Emission-influencing factors can be distinguished at different levels of analysis, and the factors between these levels are correlated. The distribution of emissions shows spatial and temporal heterogeneity on the urban road network. Signalized intersections constitute high-emission areas. There exists a gap in the literature on how to properly measure the aggregation of emissions to distinguish between high and low-emission areas near signalized intersections.

2.2 Assessment of the urban ITS-traffic management

This subchapter answers the questions of which types of ITS are applied in the urban traffic management, through which factors these ITS influence emissions, the assessment methodology, and the traffic flow model used to conduct a real-time assessment of the impact of the ITS on the spatial distribution of emissions.

2.2.1 ITS in urban traffic management

The urban road traffic environment typically features a road network made up of intersections, streets and cross-walks, parking places, and traffic management and control (Perallos et al., 2015, p.251). Travelers move through the urban road network to reach their destinations via different transport modes, including cars, trams, buses, motorcycles, bicycles, walking, and trucks (for goods transport). Sometimes a traveler needs to use multi-modal transport to move from door to door. Since a road network has certain road lengths, as well as a limited number of lanes and fixed lane widths, the capacity of the road network for travelers at any given point in time is constrained. The interaction of travelers and transport modes can result in traffic accidents, long waiting times, or slow-moving traffic. In addition, vehicles emit air pollutants. Traffic management has to find a balance between "the travelers' needs and network capacity" (Jimenez, 2017, p.9). Urban traffic management has to apply measures to balance the travel demand and network capacity to improve traffic efficiency, increase traffic safety as well as reduce emissions. Urban traffic management measures typically include signal control, ramp metering, speed limit, lane management, routing, and pricing. These measures have different scopes and focuses. In major German cities, urban arterials are mostly controlled by signals

(Wolfermann et al., 2019, p.45). In small German cities, roundabouts are commonly installed (Wolfermann et al., 2019, p.46). The main types of roundabouts include mini-roundabouts, one-lane roundabouts, two-lane compact roundabouts, and two-lane larger roundabouts (Brilon, 2005). Signalized roundabouts are rare (Tang et al., 2019, p.210).

In order to design appropriate measures, data needs to be collected on traffic flow, vehicle types, and speed. The collected data will then be processed to estimate and predict traffic conditions. Subsequently, specific measures will be designed and implemented. This process requires data collection equipment, data transmissions, algorithms, modeling, and communication interfaces. Travel demand varies over time due to changes in land use or traveler activities. Changes in the road network may occur due to lane or zone closures, construction work, or accidents. These changes may be long-term and in place for several years, or consist of only short-time adjustments that take only a few hours to resolve. The variations of travel demand and adjustments of a road network require dynamic traffic management to respond quickly to the changes in the traffic environment.

ITS has emerged around the 1980s, in parallel with the development of information and communication technologies (Andersen & Sutcliffe, 2000). Ni (2016) defines ITS as the application of "information, communication and sensor technologies to vehicles and transportation infrastructures to provide real-time information for road users and transportation system operators to make better decisions" (p.3). Roadside cameras, loop detectors, mobile GPS, and other wireless technologies that enable the communication between vehicles as well as between vehicles and infrastructures can help to quickly obtain, process, and transmit more information to realize real-time effective traffic management. Real-time traffic management can respond to situations including travel demand, traffic congestion, vehicle type, weather, incidents, and issues with the road network. Some examples of real-time traffic management are adaptive signal control, bus priority, dynamic route guidance, speed limits, etc. On the road, the ITS can cover all the transport modes for passenger and freight transport, inter-city, and urban transport. The ITS for urban traffic management can be applied to different scopes: sections, corridors, and networks.

The ITS can be categorized according to service functions: navigation and travel information (such as variable message signs, dynamic on-trip routing, and smart parking), traffic management and control (such as green wave, adaptive signal control, dynamic speed limits, ramp metering, lane management, prioritization, and route clearance), demand and access management (such as congestion charge, road-pricing, restricted traffic zones, and tolling system), advanced driver assistance and automotive driving (such as adaptive cruise control, safety, and emergency system), and logistics and fleet management (Consortium, 2013). The first three types of ITS belong to urban traffic management. Since urban traffic management is the target of the study, the first three types of ITS are taken into consideration for this research.

Adaptive signal control helps to optimize signal settings responding to current and forecasted traffic situations, thereby helping to optimize the traffic flow. Wireless communication tools like dedicated Short Range Communications (DSRC) can provide real-time information on "vehicle

class, position, speed, and acceleration on each approach" and other factors, such as "Wi-Fi, 3G/4G, and Bluetooth enabled Smartphones" and can also detect approaching pedestrians and cyclists (Office of the Assistant Secretary for Research and Technology (OST-R), n.d.).The early detection of vehicles through wireless communications helps to "forecast the queue length and arrival patterns" and enables the optimization of "signal control even before vehicles arrive at the stop line" (Priemer & Friedrich, 2009). The detection of vehicles, pedestrians, and cyclists can support the optimization of multi-modal signal control (Office of the Assistant Secretary for Research and Technology (OST-R), n.d.). Adaptive signal control can be applied to one intersection, several intersections on an arterial road, or network-wide intersections. Many algorithms have been developed for the design of adaptive signal control, with changing parameters of cycle length, phase split, phase sequence, and offset to improve traffic performance. A summary and review of methods of adaptive signal control using wireless technologies can be found in the study by Jing et al. (2017). Adaptive signal control can help reduce delay time, number of stops, accidents, and emissions. The performance of adaptive signal control depends on several factors: reductions of delay and emissions are dependent on traffic volume (Feng et al., 2018); the increase of average travel speed varies with time of day and travel direction (Slavin et al., 2013); the reduction of average delay time and improvement of travel time reliability on the corridor deployed with adaptive signal control is correlated with signal density (Hu et al., 2016). Signal coordination or "Green Wave" is a design where signal settings on several intersections along a route or a network are coordinated to allow a group of vehicles to drive through these intersections without meeting red lights. It is often applied on main roads or in high traffic demand situations. The category and description of signal coordination can be found in the book (D. Ni, 2020, p.293-295). The main optimization objectives are reduction of delay, number of stops, and queue length. While the calming green wave aims at improving safety by avoiding excessive acceleration of travelers to catch the next green light (De Coensel et al., 2012; Ellenberg & Bedeaux, 1999), the reduction of acceleration can also reduce emissions. The offset, defined as the time difference between the beginning of green light at one intersection and the beginning of green light at an adjacent successive intersection, is set by considering the distance between intersections and driving speed. When vehicles meet a red traffic light, the vehicles will stop and form a queue. When the traffic light turns green, the group of vehicles will cross the intersection and move towards the downstream intersection. The group of vehicles is called a platoon. While driving downstream, the platoon disperses due to different driving speeds and delays. The longer the distance, the higher the probability of the platoon dispersion. Apart from different desired speeds, other factors that influence the scale and speed of platoon dispersions include traffic volume, percentage of heavy-duty vehicles, and the number of lanes (Bie et al., 2013). The platoon's dispersion needs to be considered to optimize signal coordination. The traffic density, the distance between intersections, and the arrival pattern of vehicles can influence the performance of signal coordination. The improvement in traffic efficiency is impeded when travel demand or traffic density is high (D. Huang & Huang, 2003; Ye et al., 2015). Signal coordination performs well when the distance between intersections is short (Jiang & Wu, 2005). Additionally, congestion, side-street traffic, percentage of heavy duty

vehicles, pedestrians, and public transport prioritization can result in poor performance of a green wave (Bert De Coensel & Botteldooren, 2011).

Ramp metering serves to control the number of vehicles within a time slot on a ramp entering a freeway (metering rate) by using a signal control built on the ramp. There are two types of ramp metering: a local ramp metering applied on an isolated freeway section with only one ramp to control the local traffic conditions and systemwide ramp metering applied on several ramps to control network traffic conditions (Kachroo & Ozbay, 2003, p.3). Ramp metering as part of ITS can adjust the traffic flow entering the freeway to the actual traffic conditions by using real-time traffic information.

The variable speed limit serves to change the speed limit on roads. The adjusted speed limit is shown on variable speed limit signs. The detectors installed measure traffic conditions surrounding the sign. A control algorithm is then needed to design the speed limit to control the traffic flow. This solution has been mainly applied to urban motorways when an incident occurs, traffic flow is close to capacity, and when there are high levels of exhaust emissions (Grumert et al., 2018).

In the case of dynamic lane management, lanes are allocated to specific vehicle types (busses, trucks, alternative fuel vehicles, autonomous vehicles) at a certain time to optimize lane use. The lane allocation strategy depends on the prediction of traffic conditions and traffic demand. Examples include high occupancy vehicle lane management, which gives priority of lane use to vehicles with passenger numbers above a certain threshold such as carpooling and busses; dynamic lane assignment at signalized intersections which assigns lane use based on turning traffic demand; and lanes dedicated to vehicles on alternative fuels. The connected vehicle environment provides the information required to design lane management and help transmit the measures.

Dynamic traffic routing serves to direct vehicles to choose their travel routes based on forecasted traffic conditions. ITS applications for routing, such as dynamic route guidance, can help to collect real-time information on traffic situations and compute the best routes with reasonable computation costs (Yusof et al., 2015). Routing can help optimize logistics and reduce the cost of passenger transport. Although the main objective of dynamic traffic routing is to avoid traffic congestions, increasing awareness of the need for environmental protection has led to the development of eco-routing, which takes into account the reduction of traffic emissions during route selection.

Dynamic pricing helps to adjust prices that users need to pay for the mobility service. It can influence the choices of users in a way that balances the capacity of the traffic system with transport demand. The main applications of dynamic pricing in ITS are congestion charging, parking pricing, charging/discharging pricing for electric vehicles, and fare pricing (Saharan et al., 2020).

All these ITS applications can influence road traffic emissions. Their respective effect depends on the context and design of each specific ITS. Some studies specified the factors and parameters through which an ITS can influence emissions, dividing them into four groups:

parameters defining traffic demand (e.g., trip origination, destination, transport mode, route); parameters defining driving behaviors and vehicle's performance (e.g., driving speed, lane use, time or distance headway, tire pressure); indirect factors (e.g., travel cost, capacity of the infrastructure); long-term effects (e.g., inducing demand) (Mahmod et al., 2015).

Based on the existing literature, the commonly used ITS in urban traffic management, as well as the influencing parameters and factors on the emissions are summarized in Tab. 2.1. Routing, speed limit, signal control, and lane management are the major ITS at the signalized intersection. They influence emissions not only through the average speed but also through speed variation and the distribution of driving modes. Because the average speed itself cannot sufficiently represent the ITS's effect on emissions, the speed variation should be considered as well.

ITS	Parameters influenced by ITS	Factors that influence ITS performance
dynamic on-trip routing	average speed and steadiness of the speed (Y. Huang et al., 2018)	road type, road gradient, traffic condition, vehicle type, and penetration rate of eco-routing (Y. Huang et al., 2018)
Adaptive signal control	acceleration and average vehicle speed (De Coensel & Botteldooren, 2011; Pandian et al., 2009; Y. Wang et al., 2018)	
coordinated signal control		larger platoon ratio [1] and later platoon arrival (the last few platoon vehicles arriving during a red light phase) can reduce more emissions (Lv & Zhang, 2012); Traffic volume, and green split (De Coensel & Botteldooren, 2011)
dynamic speed limit	speed variation and the fluctuations in headways	driver compliance level (Cohen et al., 2014);

[1] Highway Capacity Manual (Transportation Research Board (TRB), 2010) defined the platoon ratio as the ratio of vehicles arriving during green time to the green time ratio.

	during traffic congestions (H. Yang et al., 2018); average speed acceleration and decelerations (Grumert et al., 2015)	
lane management (high occupancy vehicles, lanes dedicated to vehicles on alternative fuels)	traffic volume and percentage of cleaner vehicles (Fontes et al., 2014)	road type, traffic volume, fleet composition, and average vehicle occupancy rate (Fontes et al., 2014); traffic condition and lane configuration (Boriboonsomsin & Barth, 2008)
ramp metering	smooth vehicle maneuver (Du et al., 2018)	level of congestion (Pasquale et al., 2014)
congestion charging	vehicle kilometers traveled and average speed (Beevers & Carslaw, 2005)	levels of public transit service and size of the charging zone (Wu et al., 2017)

Tab. 2.1 Impact of ITS-measures for urban traffic management on emissions based on the existing – literature

2.2.2 Performance assessment methodology

The design and deployment of a specific ITS measure need to assess the performance of the ITS measure. The assessment method can consist of models or field trials. Models include a driving simulator and a traffic flow simulation model. Field trials can consist of driving in the real-world or on a closed testbed. The choice of the performance assessment method needs to take into consideration “cost, safety, repeatability, scale, and technological requirements” (d’Orey & Ferreira, 2014). Since models have advantages with regard to these indicators, they are the main methods to assess the ITS.

To model the ITS in the road transportation network, several models need to be integrated. The basic models include the function of the ITS to be tested and the traffic model that represents the behaviors of vehicles on a road transport network. Since ITS such as an advanced diver-assistance system, involves the driver’s features, a driver model may be needed to evaluate the type of ITS. The traffic model includes the demand model to represent the traveler’s trip generations, destinations, departure time, and transport means, the supply model to analyze the road capacity, the assignment model to choose the routes, and the traffic flow model to represent the interactions of the vehicles. Based on the level of granularity of the traffic flow, the traffic flow models can be commonly classified into macroscopic, mesoscopic, microscopic, and submicroscopic models (Fig. 2.2).

The macroscopic traffic model represents road traffic as an aggregated flow of vehicles driving through the links and intersections. Its representation is based on the relationship between the average speed of traffic, traffic density, and traffic flow (Elefteriadou, 2014, p.138). The macroscopic traffic model can describe the dynamics of the traffic flow, such as the formation and dissipation of queues, while it is incapable of distinguishing individual vehicles. Since it can save time and cost, it is suitable for the modeling of traffic flow in a large geographical area, such as in an urban road network.

The mesoscopic traffic model specifies an individual vehicle's behavior while activities and interactions are based on the macroscopic relationship. While a well-calibrated mesoscopic traffic model can estimate with sufficient accuracy the average speed of each vehicle, it does not reproduce the approximate speed changes (Kuwahara et al., n.d.). The platoon dispersion model serves to estimate a vehicle's arrival profile based on the dispersion effect and discharge flow from an upstream intersection. The most widely used dispersion model is Robertson's dispersion model (Robertson, 1969). The platoon dispersion model can be integrated into mesoscopic traffic models like TRAFFMED to represent platoon dispersion (Cantarella et al., 2019; Pace et al., 2017).

The microscopic traffic model describes the interaction between vehicles to represent driving behaviors. The characteristics of the driver and vehicle can be defined in the model, such as the aggressiveness of the driver and vehicle type. The typical microscopic traffic models include the car flowing model, the lane-changing model, and the route choice model. In the paper of Maerivoet and De Moor (2005), the main microscopic traffic flow models are summarized. There are mainly four types of car-following models: safe-distance models, such as that of Gipps (1981) and Krauß (1998); stimulus-response models such as that of Reuschel (1950), Pipes, and Forbes; psycho-spacing models such as that developed by Wiedemann (1974) and Fritzsche (1994); and cellular automata models such as the Nagel-schreckenberg model (Nagel & Schreckenberg, 1992). The lane-changing model considers two types of lane change behaviors: necessary lane changes, for example, due to route choice and traffic regulation; and free lane change, such as due to overtaking to reach the desired driving speed. Typical lane-changing models are those developed by Sparmann (1978), Gipps (1986), Krajzewicz (2010), and Ehmanns (2014). Since the typical time resolution of the car-following model is in the orders of 0.1-0.01 second, the car-following model can reproduce the smooth changes of the driving speed (Kuwahara et al., n.d.). As a consequence, this type of model can help obtain emissions in seconds. Since the cost of data and computation increases with the size of the road network, the microscopic traffic flow model is suitable to simulate an area with several links and intersections (Grote et al., 2016).

The submicroscopic model simulates the behavior of the vehicles and drivers by considering more detailed physical characteristics such as detailed gearbox operations (Maerivoet & De Moor, 2005). It can model the impact of the road condition (slope and wetness), air drag, wind resistance, car weight, and tire wear on the vehicle behavior more realistically than other types of traffic flow models mentioned above (Maerivoet & De Moor, 2005). However, this type of

model also requires a deeper understanding of the details, more input data, and longer simulation time than other traffic flow models.

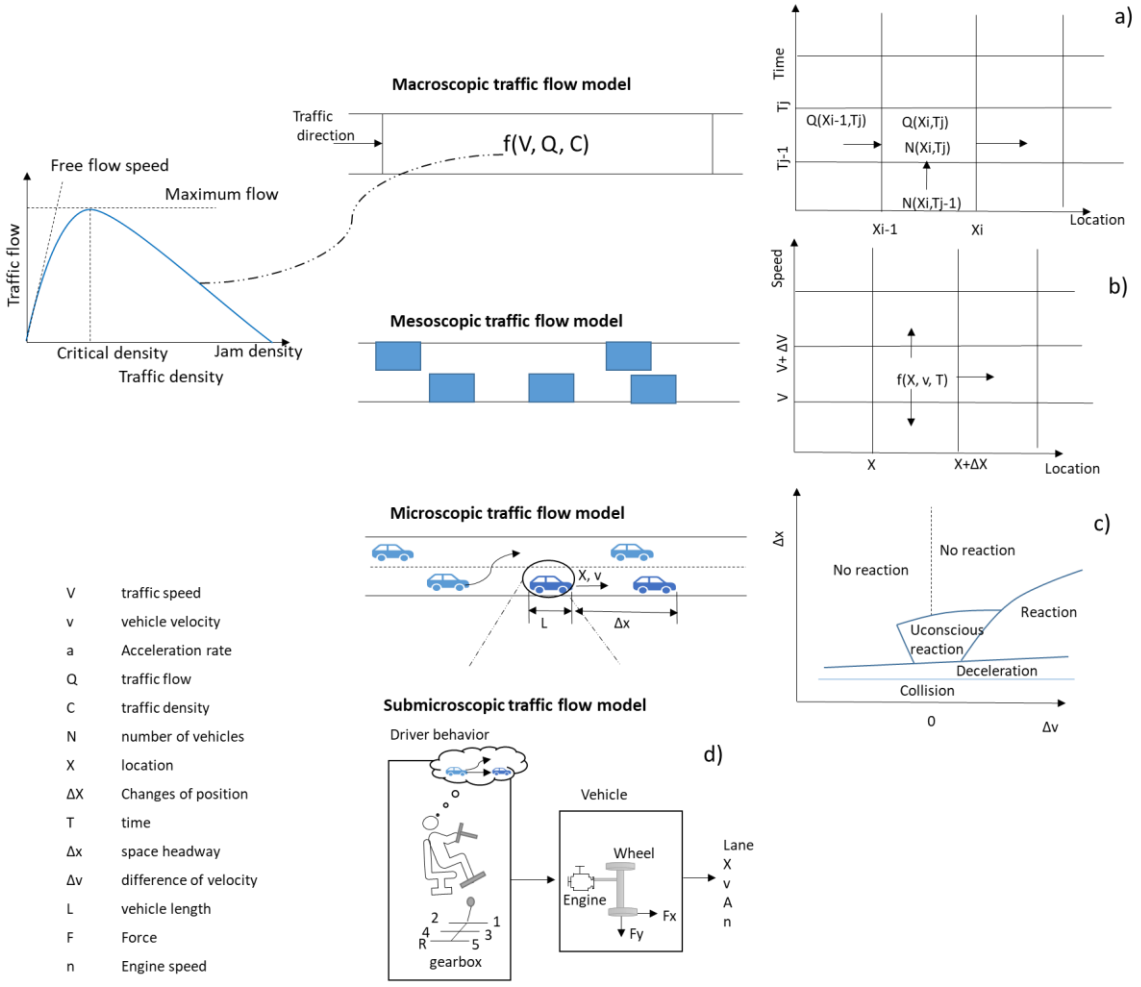

Fig. 2.2 Illustration of different levels of traffic flow models. a) and b) adapted from Ni (2011); c) a – representative Wiedemann car-following model, adapted from Wiedemann(1974) and PTV – Planning Transport Verkehr AG (2011); d) adapted from Neunzig et al. (1998).

When choosing the traffic flow model to assess emissions, several aspects need to be considered. Firstly, the traffic factors that influence emissions should be obtained through a traffic flow model. Since the traffic flow model can produce the vehicle trajectories at different granularities, it can generate different levels of influencing factors. The macroscopic traffic flow model would be one option allowing for the use of aggregated traffic flow variables to assess emissions. However, the macroscopic traffic model is unsuitable when driving speed is measured second by second to assess emissions. In this case, different levels of traffic factors have to be integrated into the model, necessitating the application of a specific traffic flow model. Secondly, the traffic flow model can take into account the resolution of the emission estimation. By using different levels of traffic models, emissions can be estimated at different spatial-temporal levels. For example, when using the microscopic simulation model, which produces speed trajectories every 0.1-0.01 second, emissions per second can be estimated based on the dynamics of the vehicle. This data can be further aggregated into bigger spatial

and temporal resolutions. Thirdly, the choice of the traffic flow model needs to consider resource constraints in terms of money, time, and data. On the one hand, the application of the ITS in traffic management should be assessed in large-scale scenarios rather than at a small number of intersections since the application areas interact with their surroundings. On the other hand, the ITS allows for real-time information communication, which enables real-time traffic management. Consequently, the speed of data collections, calibrations, and simulations for the flow model has to be fast enough to enable the real-time assessment of the ITS for traffic management.

2.2.3 Summary

Common ITS in traffic management can influence emissions not only through average speed but also by speed variations.

To choose or design ITS measures to account for emissions, the impact of ITS on emissions needs to be estimated. The evaluation has to be based on the traffic flow model and emission model. According to the level of granularity of traffic flow, the traffic flow model can be classified as a macroscopic, mesoscopic, microscopic, and submicroscopic traffic flow model. The macroscopic traffic model cannot represent the individual vehicle speed dynamics but can save time and data when modeling the aggregate traffic flow variables of a big urban network. The mesoscopic traffic models can represent the traffic flow characteristics over short distances but are incapable of simulating fine-grained vehicle trajectories. The microscopic traffic simulation model can provide the fine-grained vehicle trajectories for estimating the individual vehicle emissions at the second level but at high data and time expenditure, making it inappropriate for the real-time simulation of a large urban network. The submicroscopic traffic model can simulate road conditions, traffic environment, and detailed vehicle operating characteristics but is time and data-consuming. To assess the real-time spatial distribution of emissions, the submicroscopic and microscopic traffic simulation models encounter problems related to data costs, duration, and quality of the data for calibration and validation; and the macroscopic traffic model lacks accuracy in traffic flow characteristics over short distances and thus lacks accuracy in the estimation of emissions. In contrast, the mesoscopic traffic model comes at lower data and time costs than both the microscopic and submicroscopic simulation models. Moreover, the mesoscopic traffic model can better simulate traffic flow dynamics than the macroscopic traffic flow model. Thus, it has the biggest potential for the assessment of the real-time spatial distribution of emissions.

2.3 Emission modeling

This chapter will investigate the existing emission models to answer which ones are most suitable for assessing the spatial distribution of emissions and the real-time emission impact of the ITS.

2.3.1 Requirements of the emission impact assessment by ITS

Emissions can be assessed by conducting field experiments, real-world measurements, laboratory studies, or emission models. Data acquired from fields, laboratories, and other real-world measurements are limited in terms of time and location. Emission models are required when the detailed spatial and temporal distribution of emissions throughout the urban road network has to be considered. Emission models can also predict emission levels in situations that do not yet exist or occur and thus cannot be measured. The ITS to be assessed in this research is designed for decision-making, but not yet for implementation. Therefore, an emission model is required for emission estimation.

Emission models help to estimate emissions in real-world scenarios. Each emission model consists of algorithms and requires data inputs and certain computation time to generate results. To apply an emission model, the model must meet several requirements. Foremost, the model must be able to represent the targeted phenomenon. Secondly, it needs to be operationally within a reasonable scope when considering the cost of computation and data acquisition. Thirdly, the result of the emission model needs to be valid enough for the targeted problem and situations. Within an emission model, the emission factor or emission rate is the function of various influencing factors. Each influencing factor and its extent in the model differ between emission models. Each emission model involves a certain degree of uncertainty, sensitivity, resolution, and cost. Therefore, any specific emission model is suitable only for some limited purposes and situations.

To check whether an existing model can estimate the impact of ITS in real-time on the spatial distribution of emissions and can estimate the spatial distributions of emissions, the represented emission models are examined from the aspects of sensitivity, validity, operationality, and resolution. The sensitivity is tested to check if the model can estimate emission changes resulting from a specific type of ITS. The validity is tested to check if the model can estimate emissions at a certain resolution level, including at the level of a short segment, a street, a road network, or at the regional level. The operationality is tested to check if the model can be applied in real-time to a road network with a certain size, ranging from several signalized intersections to several corridors to an entire urban road network. Resolution can range from yearly regional emissions to hourly street-emissions and from emissions resulting from an individual vehicles' entire trip to second-by-second emissions. Moreover, the source and causes of errors are examined to help understand the limitations of these models and gain insight on possible improvements. These aspects will be investigated by reviewing the literature on model development, application studies, and thoughts of other researchers. In the end, this knowledge and experience will be synthesized to develop a new emission model concept for this study and inform the model development methodology.

2.3.2 Existing emission models

According to how the emission is represented, the emission model could be categorized into macroscopic emission models, traffic situation-based emission models, mode decomposition emission models, and instantaneous emission models.

Macroscopic emission models: there are two types of macroscopic emission models. The first uses traffic layouts and signal controls instead of traffic flow variables. The second uses traffic flow variables, typically average speed.

For the first type, one study has developed a regression function of the number of lanes, presence or absence of a left-turn lane, cycle time, green ratio of the major street, lane volume, volume of the left-turn vehicles, percentage of the truck on a major street, and those on the minor street (Lee et al., 1983). The developed predictive emission models have more than 60 terms, including first and second order of the main effect and two-factor interaction effects (Lee et al., 1983). Although it shows a good fit for regression, the performance of the predictive models is not examined with a new dataset. A regression model with too many terms may result in an overfit, which causes the prediction to have large variances. If other or more predictors are added into the regression model, the number of the regression terms would dramatically increase, which may lead to a higher prediction bias. Thus, it is necessary to develop a good predictive emission model that has relatively few terms but can consider the effect of more emission sensitive variables.

For the second type, the average emission factor is a function of average speed. The emission function is based on the real-world collection of driving cycles that are sets of vehicle speed points versus time. Typical models are EMFAC (Ca, 2015) and COPERT (Gkatzoflias et al., 2007). This type of emission model has large or systematic differences in the emission estimation for some pollutants due to the measurement method, driving situation, test environment, and vehicle characteristics (Smit, 2006). This type of emission model has a large prediction error of a few tens of percentage points at low speed and short links (Negrenti, 1999). A dynamometer test shows that the average speed cannot sufficiently explain the variation of NO_x emission (Kent & Mudford, 1979). To improve emission estimation, TEE (Traffic Emissions and Energy) corrected average speed model was developed, and the kinematic correction factor is used to express the effect of speed variability (Negrenti et al., 2007). The kinematic correction factor is a product of four independent functions in which the predictors are average speed, green time fraction, density, and link length, respectively (Negrenti, 1999). The model showed a better estimation of CO concentration than COPERT 3 (Negrenti et al., 2007). Some researchers distinguish between emission estimation functions for speed limits, link lengths, control types, and percentages of trucks (Klunder et al., 2013). Some researchers used the average speed distribution to offer a better explanation for traffic flow dynamics than would be possible based on a single average speed value (Aguiléra & Tordeux, 2011). It was found that based on average speed distribution, COPERT was able to reduce deviations of emissions from the instantaneous emission model, but still underestimated emissions in congested urban traffic networks (Lejri et al., 2018).

By looking into the model structure and studies on model accuracy mentioned above, it can be concluded that macroscopic emission models are insensitive to emission changes resulting from driving dynamics. Thus, they are unsuitable for assessing the corresponding traffic measures that lead to changes in the driving speed. Since these models have higher

uncertainty on shorter links, they are unsuitable for the emission estimation of short segments either.

Traffic Situation-based emission model: typical models are HBEFA (S Hausberger et al., 2009) and ARTEMIS (André et al., 2009). These models capture driving dynamics for emission estimation through the classification of traffic situations. Urban traffic situations are classified by the road type, speed limit, and traffic condition (Hausberger et al., 2009; André et al., 2009). In the ARTEMIS, the traffic condition is defined by the ratio of average speed to free-flow speed (André et al., 2009). In the HBEFA, the traffic condition is defined by the level of service (Hausberger et al., 2009). The average emission factor of each traffic situation is obtained from the representative driving cycles. The driving cycles were collected across various combinations of road types, traffic conditions, road gradients, and vehicle types (Hausberger et al., 2009; André et al., 2009). The driving cycles were then clustered based on dynamic characteristics, such as the average speed, percentage of stops, and relative positive acceleration (Knorr et al., 2011).

Some of the uncertainties related to these emission models result from the inaccurate identification of traffic conditions. Since the emission factor during stop-and-go is much bigger than in other traffic situations, emission levels are very sensitive to the identification of stop-and-go situations. The ratio of average speed to free-flow speed itself cannot characterize the traffic conditions well enough, as several different driving profiles could exist at low traffic speed (Montazeri-Gh & Fotouhi, 2011; Kerner et al., 2014). It will lead to big variations in fuel consumption (Schreckenberg et al., 2015). The HBEFA has been integrated with MATsim (Hülsmann et al., 2014). The indicator of traffic conditions showed poor emission estimation performance. Consequently, each link was further divided into a free driving part and a stop-and-go part, and then an emission factor was assigned to each part referenced to the driving cycles in HBEFA (Hülsmann et al., 2014). Although this improves the estimation, there is still a large error at low speed. Some researchers have suggested adding the ratio of density to capacity for classifying traffic conditions (Borge et al., 2012). Moreover, the current traffic situation-based emission models provide emission factors without differentiating between intersection types and without differentiating road parts between intersections. Some studies demonstrated different emission distribution patterns between signalized intersections and roundabouts as a result of different driving behaviors (Salamati et al., 2015). Additionally, the road category and the vehicle-specific driving cycle could be further refined to estimate the emissions better.

As proven by the studies, this type of emission model cannot model link emissions very well, especially in stop-and-go traffic situations. Some studies also examined the potential of assessing urban air quality by integrating traffic situation-based emission models with air quality models (Borge et al., 2012). Since this type of emission model could implicitly represent the impact of traffic conditions, it has been applied to assess traffic demand management (Hülsmann et al., 2014). However, as this type of emission model does not sufficiently consider the influence of speed and acceleration on emissions, it is unsuitable for assessing traffic signal systems and other measures relevant to the driving dynamics.

Mode decomposition emission model: in this type of emission model, the urban driving dynamics are divided into several simplified driving modes. The driving modes consist of decelerating to stop, idling, accelerating from a stop, cruising, and creeping mode (vehicles queuing at a priority junction). The typical emission models are TEE-mode based emission (Negrenti, 1996), Uporal (Matzoros & Van Vliet, 1992), and VT-meso (Rakha et al., 2011). These models distinguish between the signalized intersection, intersection with priority, and roundabout.

For signalized intersections, these emission models consider two driving situations: driving through without a stop and driving with a stop or in a queue. They assume a constant speed when a vehicle drives without stopping. The models differ mainly in the emission factor during the acceleration mode. TEE-mode based emission (Negrenti, 1996) and Uporal (Matzoros & Van Vliet, 1992) assume a constant emission rate in the acceleration mode and do not consider the variability of the emission rate due to the acceleration behavior near the intersection. In the VT-meso model, the emissions in the acceleration mode are the polynomial function of the cruise speed, and the coefficient depends on the level of acceleration rate (Hesham Rakha et al., 2011). Some researchers have proposed another method to estimate emissions on urban networks (Gori, La Spada, et al., 2014). The emission factor of vehicles in a queue and acceleration is differentiated into two traffic conditions: acceleration from the queue to free speed; vehicles cannot reach free-flow speed within one signal cycle (Gori, La Spada, et al., 2014). In the energy-ITS project, the driving cycle has been divided into “short stop” (less than 3km/h for 3 seconds) and “short trip” (over 3km/h for 3 seconds) (Kuwahara et al., 2013).

This type of emission model distinguishes emissions between major driving modes. However, transient emission estimation is not accurate enough. In the case of driving without stop, lack of considering the small speed variations can result in the underestimation of emissions (Barth & Boriboonsomsin, 2012). When frequent accelerations occur, the VT-meso model underestimates NO_x by a range of 10 to 27 percent on the freeway and arterial roads (Rakha et al., 2011). The underestimation could be caused by the oversimplification of driving dynamics and a lack of consideration of other types of speed variations, resulting, for example, from turning movement, conflicting flow, and mixed traffic. The effect of these speed changes is not yet thoroughly studied. The method was tested in an energy ITS project where it performed well in the estimation of fuel consumption on a 5-km trip (Kuwahara et al., 2013). One study categorized the speed profiles according to the number of stops, and each category was assigned one average emission factor (Salamati et al., 2015). This approach can represent the variance of emissions resulting from the number of stops. However, the number of stops cannot fully explain the impact of traffic management and control on emissions (Rakha, Van Aerde, Ahn, & Trani, 2000).

When applying this type of emission model, the distribution of driving modes, queue lengths, and the number of stops need to be obtained. Usually, models of this type are based on the theory of queue formation and dissipation and assumptions about the acceleration rate and cruising speed. However, very few applications are found. Theoretically, this type of emission

model is sensitive to the estimation of operational measures, including demand management and signal control. This type of model structure indicates that emissions can be estimated at street level and that these models can be operational in an urban network. However, their accuracy needs to be improved.

Instantaneous emission model: the emission rate is a function of instantaneous engine states defined by the speed, acceleration, or engine power and engine speed. It is the average result of the representative vehicles of each vehicle category. The model development is based on extensive measurements of vehicle operations, emissions, and fuel consumption across various driving cycles. These emission models can be further divided into the speed-based model, the engine-based model, and the simplified engine-based model.

In the speed-based emission model, the emission rate is dependent on the instantaneous speed and acceleration rate. The typical emission models are VT-Micro (Rakha et al., 2004) and Versit-micro (Ligterink & Lange, 2009). In the VT-Micro, the log-transformed emission rate is a third-order polynomial function of the speed and acceleration rate (Hesham Rakha et al., 2004). In the Versit-micro, the emission rate has a linear relationship with the speed and acceleration rate (Ligterink & Lange, 2009). The emission function differs between deceleration, idling, and acceleration. In the engine-based model, the emission rate or factor is dependent on the engine power/torque and the engine speed. The typical models are VeTESS (Pelkmans et al., 2004), CEME (Barth et al., 2000), and PHEM (Luz & Hausberger, 2011). They contain discreet emission maps which show the measured emission factor at the specific engine power and engine speed. The engine operation variables will be calculated based on the physical engine model. These variables will then be referred to in the emission map and extrapolated. Although transition emissions play a big role, VeTESS could be used only at a quasi-steady state (Boulter et al., 2007). CEME and PHEM cover the transition phase. To reduce the difficulties of calibration and complexities of the models, the engine-based model is simplified in a way that the emission rate is assumed to be dependent only on engine power. Engine power is represented by a function of speed, acceleration, road gradient and vehicle parameters. Examples include the emission model used in the SIDRA INTERSECTION software (Bowyer et al., 1985), Emit (Cappiello et al., 2002), PHEMlight (Krajzewicz, Behrisch, Wagner, Luz, & Krumnow, 2015), the P∆P model (Smit, 2013) and MOVES (Frey et al., 2002). In the P∆P model, the emission rate is a regression function of the engine power and changes in engine power (∆P) (Smit, 2013). In MOVES, the driving dynamics are grouped into operation bins that are defined by the average speed and vehicle engine power, and each operation bin has one average emission factor (Frey et al., 2002).

These emission models are based on different predictors and assumptions and differ in whether they include a catalytic effect, gear shift model, or history effect. Generally, they consider more emission-relevant variables, such as vehicle parameters and driving transient behaviors. Therefore, these emission models could improve the emission estimation. The log-transformed emission models offer better predictions in the case of low emissions than in the case of high emissions (Rakha et al., 2004). CEME tends to overestimate emissions when acceleration begins while underestimating emissions when acceleration ends (Barth et al.,

2000). Zhang and Loannou (2016) used MOVES and CEME to estimate a combination of a variable speed limit and a lane change control. They found that both models show similar results of emission reductions (Zhang & Loannou, 2016). For the PΔP model, the normalized root mean square error of the fuel consumption rate varies between 2–12%, and 3–21% for NO_x (Smit, 2013). To ensure good predictions, Smit (2013) suggested aggregating emissions on a road segment longer than 100m. MOVES tends to overpredict emissions of driving cycles, which emit relatively low emissions (Frey et al., 2002).

One source of the estimation error could be the lack of consideration of the catalytic equipment effect and historical effect. Since the PΔP model does not consider the effect of catalyst efficiency, it cannot reproduce the peak values of NO_x for a petrol SUV of 2006 (Smit, 2013). Thus, to estimate the emissions from modern vehicles resulting from a short trip, the efficiency of catalytic equipment should be considered. The historical effect could also influence emissions, especially the effect of the temperature several seconds before, inertia effect, and the effect of aging after-treatment (Barth et al., 2000). Distortions have not been taken into account in some instantaneous emission models (CEME, MOVES, VeTESS) (Boulter et al., 2007). The speed model and simplified engine model lack consideration of other engine operations such as gear shift behaviors. The engine-based emission model is highly complex and requires many variables of vehicle and engine characteristics. However, only some of the parameters could be calibrated, although some parameters are not sensitive to emissions. Thus, a large degree of uncertainty could result from parameter calibration.

Secondly, this type of emission model requires the measuring of driving speed. One study has found that the emission estimation based on average speed as the input into CEME is less than half of that computed by using speed variations when a big vehicle drives with many accelerations, while 30-40% lower when it drives with fewer speed changes on highways (Turkensteen, 2017). It indicates that the engine emission model needs to include speed fluctuation instead of fixed speed, especially under non-free flow traffic conditions. Some researchers found that when the PHEM is integrated with a traffic simulation model to estimate the emissions on a highway or rural network, there is an onefold difference in emission results between microscopic and mesoscopic simulation models (Behrisch & Erdmann, 2015). PHEM has also been integrated with a microscopic simulation model and a driver dynamics model (So et al., 2018). Some researchers integrated the instantaneous emission model with the macroscopic traffic flow model by transforming the macroscopic traffic variables into traffic volume, average driving speed, and average accelerating rate (Zegeye et al., 2013). The method was applied to the freeway, and the results showed that the average-absolute-relative error of total emissions is less than 10% (Zegeye et al., 2013). The performance needs to be assessed on other network layouts and road segments. For signalized intersections, some researchers derived simplified driving speed profiles from the macroscopic traffic flow model by assuming the constant average acceleration rate and the constant free-flow speed (Jamshidnejad et al., 2017). Its integration with the instantaneous emission model yielded similar results in terms of total emissions on the tested urban road network to those stemming from the integration of the microscopic traffic model with the instantaneous emission model

(Jamshidnejad et al., 2017). However, it is uncertain to what extent this performance can help estimate local emissions on smaller road segments.

Normally the instantaneous emission model is integrated with the microscopic traffic simulation model that forms the microscopic emission estimation framework. To be noted, several studies have discussed the applicability of the microscopic traffic simulation model (da Rocha et al., 2015; Osorio & Nanduri, 2015; da Rocha et al., 2013). It has been addressed that the traffic flow model should be calibrated well for the emission assessment, not only considering traffic performances, but also the speed-acceleration relationship and the desired speed (Hirschmann et al., 2010). The microscopic emission estimation framework cannot adequately estimate emissions per second, while it can be used to estimate a group of vehicles driving short distances (da Rocha et al., 2015). This type of emission model has been widely used to assess various ITS measures, such as vehicle-to-vehicle communications, vehicle-to-infrastructure communications, and adaptive cruising control (Coensel & Botteldooren, 2011; Lüßmann et al., 2014; Stevanovic et al.,2009; Tielert et al., 2010; van Katwijk, 2012; Wang et al., 2014). It could produce a detailed spatial and temporal distribution of emissions and can be integrated with the dispersion model to predict the air quality (Giannouli et al., 2011). Due to the high data and time costs involved in using microscopic traffic simulation models, this type of emission model has rarely been used for big urban networks, especially for real-time applications.

2.3.3 Summary

To assess the impact of ITS measures on emissions, emission models are mostly integrated with traffic flow models. The choice of emission models can be made according to the various needs of assessments, including ITS types, spatial scales, and spatial resolutions. The accuracy of the emission model varies between different road types, congestion levels, spatial resolutions, and types of traffic measures. After a literature review on different emission models, each type of emission models' respective sensitivity to ITS, accuracy, resolution, and operational scale are summarized in Tab. 2.2. It is addressed how the accuracy of an emission model is influenced by its resolution and traffic environment. When a macroscopic average speed-based, or traffic situation-based emission model is used for yearly emission inventory, the error of network emissions could be reduced due to the average effect and size effect. The size of the error reduction is related to the percentage of signalized intersections on a network (Gori, La Spada, et al., 2014).

Generally, the macroscopic emission models are suitable for estimating the total emissions of an urban or regional road network. Based on the length and duration of referenced driving cycles, the traffic situation-based emission model could be applied to estimate the hourly aggregated emissions of several links or a small area, but not for each link. Driving dynamics become more important to estimate link emissions. The mode decomposition emission model further has the potential to estimate link emissions if its performance is improved further. An instantaneous emission model can estimate emissions at smaller segments. It needs to be integrated with a microscopic traffic simulation model, which requires very large data and much

computation time. Consequently, it is unsuitable for real-time assessment. Integrating an instantaneous emission model with a macroscopic or mesoscopic traffic flow model would directly result in a big deviation of estimated emissions. By transforming the macroscopic traffic variables into average acceleration rate and average speed, the integration can estimate emissions close to the result of the microscopic models, but the performance test is limited in the estimation of total emissions on a freeway.

Emission Model	Type of ITS			Accuracy by resolution			Operationality for an urban network
	Traffic demand management	Traffic control	Driving style	Area	Street	Short segment	
Macroscopic emission models (e.g., EMFAC, COPERT, TEE-average speed model)	-	-	-	+	-	-	+
Traffic situation-based emission models (e.g., HBEFA, ARTEMIS)	o	-	-	+	-	-	+
Mode decomposition emission models (e.g., TEE-mode based emission, Uporal, VT-meso)	o	o	-	+	+	-	+
Instantaneous models (VT-micro, Versit-micro, VeTESS, CEME, PHEM, PHEMlight, PΔP, Emit, MOVES)	o	o	o	+	+	+	-

Tab. 2.2 Comparison of emission models for the emission impact assessment of ITS. o: could be – applied in the scenario; -: inaccurate or unsuitable in the scenario; +: relatively accurate and – suitable;

In conclusion, an emission model needs to be developed for the real-time assessment of the impact of ITS on the spatial distribution of emissions. To fulfill this goal, the variables in the emission model should reflect variations in speed. Since the mesoscopic traffic flow model has the potential to assess the traffic flow dynamics of the short distance in real-time, the emission model that uses the traffic flow variables from the mesoscopic traffic flow model can reflect the changes in the distribution of emissions caused by the studied ITS.

2.4 Summary

Road traffic is the dominant anthropogenic source of NO_x, CO, and HCs in urban areas. Vehicle tailpipe emissions are the primary source of road traffic emissions. Emission-influencing factors can be distinguished at different levels of analysis, and factors between these levels are correlated. Signalized intersections are common high-emission areas. Emission levels show spatial heterogeneity near signalized intersections. To identify high-emission areas and estimate the air quality, the detailed spatial distribution of emissions should be studied at the level of the road segment. There exists a lack of studies that properly disaggregate emissions while distinguishing between high and low-emission areas near signalized intersections.

The application of the ITS enables real-time information communication. It makes traffic management more dynamic. The ITS in urban traffic management can influence emissions not only through average speed but also through speed variations. Consequently, a real-time emission impact assessment is required to help choose ITS measures. A traffic flow model and emission model are required for an emission assessment. The traffic flow model provides the input data of the emission model. According to the level of granularity of traffic flow, the traffic flow models can be classified as the macroscopic, mesoscopic, microscopic, and submicroscopic traffic flow models. The problem with submicroscopic and microscopic traffic flow models is that they create high data costs, are time-consuming, and lack in data-quality for calibration and validation. And the macroscopic traffic model lacks accuracy in traffic flow characteristics over short distances and thus lacks accuracy in an emission estimation. In contrast, the mesoscopic traffic model consumes less data and less time than either the microscopic or submicroscopic traffic flow model. Moreover, the mesoscopic traffic model can better simulate the traffic flow dynamics than the macroscopic traffic flow model. Thus, it has a larger potential for assessing the real-time spatial distribution of emissions.

The choice of emission models can be made according to various assessment needs, including ITS types, spatial scales, and spatial resolutions. The accuracy of emission models varies between different road types, congestion levels, spatial resolutions, and types of traffic measures. Instantaneous emission models can estimate emissions at smaller segments. They need to be integrated with microscopic traffic simulation models, which require very large amounts of data and have a much longer computation time. Although the speed of computation could be increased by improving computer processing power, microsimulation requires high quality as well as a large quantity of data for calibration and validation. Thus, methods of data measurement and data processing need to be improved. The mesoscopic traffic flow model has the potential for real-time assessment of traffic flow dynamics over short distances. Moreover, it is less dependent on data. Therefore, for the purpose of this research, a mesoscopic emission model will be developed and will be assessed for its capability in assessing the spatial distribution of emissions.

3. Model development methodology

In this chapter, firstly, the model concept is described. It consists of the resolution, the variables, and the effects on local emissions. The model concept is based on the cause and effect between road traffic and emissions. Subsequently, the chapter explains the basic data, methods for road division, the emission functions, and the design of traffic scenarios.

3.1 Model concept

It is essential to identify hot spots for the design of traffic measures as well as for the air quality assessment. If only average emissions were measured for a long street or corridor, hot spots could be overlooked, or the choice of traffic measures could be based on irrational criteria. To estimate the impact of the ITS in urban traffic management on the spatial distribution of emissions, the basic requirements of the emission model are:

- It is sensitive to traffic management;
- Its implementation can be used for real-time assessment;
- It can distinguish between high and low emission segments;
- It is accurate enough to compare different traffic measures.

Assumptions about the resolution and the model variables have to be made to fulfill these requirements. The concept of the segment division and emission functions are described below.

3.1.1 Segment division

Emission shows spatial heterogeneity between road segments due to the heterogeneity of the traffic environment. The traffic environment can include traffic management and control, infrastructure layout and geometry, traffic volume, fleet composition, and driver behavior. As a result of the interactions of these factors, the traffic flow on each segment shows different dynamic characteristics and a different distribution of driving modes. The emission factor is sensitive to the driving mode of a vehicle. It indicates that when vehicles on a specific short segment have similar driving modes, the vehicles will have similar levels of emissions on this segment. Thus, one way to divide the road is to aggregate the segments which have similar driving modes. Apart from considering the driving mode, the traffic volume and fleet composition should be homogenous, meaning that there exists no diverging or emerging traffic.

Due to the interaction of vehicles near the signalized intersection, the traffic flow is smoother in the middle block with less speed fluctuation, while vehicles decelerate into the queue and then accelerate to a high speed near the stop line. The vehicles accelerate from low or medium speed after crossing the intersection. Emissions are disaggregated into four small segments according to different driving dynamics: midblock (where vehicles mainly cruise), inbound

(where vehicles mainly accelerate), the crossing of the intersection, and outbound (where vehicles accelerate after crossing the intersection) (Fig. 3.1). While crossing the intersection, each traffic stream will be treated separately. The size of each segment can be influenced by traffic management and control. For example, different levels of signal coordination may influence the size of inbound. As an example, the boundary between segments for an isolated signalized intersection is further studied in this study.

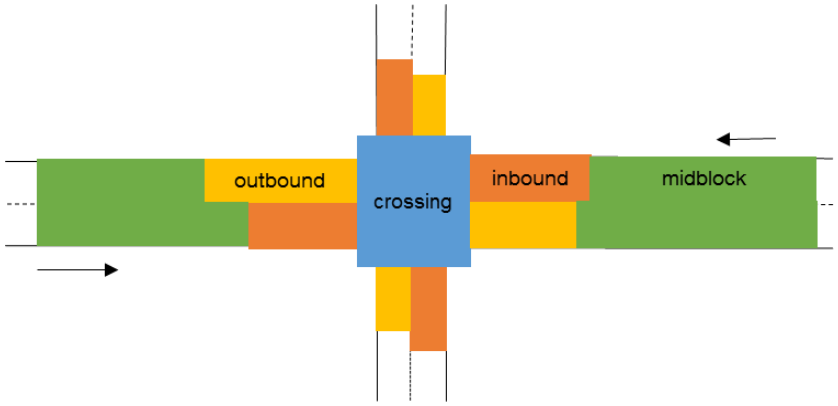

Fig. 3.1 Draft layout of road division

3.1.2 Variables for emission estimation

For the primary goal of contributing to real-time emission impact assessment, two key aspects are of primary concern: the cost of computation time and the accuracy of the difference of emissions between the measures. Emissions measured on each segment for one hour (over several signal cycles) are the total emissions of vehicles that have driven through or driven on the segment. This value is obtained by multiplying the average emission factor with the total traveling distance. The function of the average emission factor should reflect the impact of driving dynamics while the consideration of variables and computing time should allow for real-time estimation.

Based on chapter 2.1.2, traffic variables that can influence emissions are generally classified into three levels: engine dynamics, driving dynamics, and traffic flow dynamics. Emissions can be estimated using the function of kinematic parameters and driving modes. However, they can hardly be obtained from a macroscopic or mesoscopic traffic flow model. For each type of vehicle at each point in time, emissions are directly dependent on the engine dynamics of the vehicle, as reflected by its driving speed and acceleration. The driving dynamics and the engine dynamics are the results of interactions between factors in the traffic system. In one specific traffic environment, similar trajectories consist of a similar combination of driving modes. Emissions have different sensitivity to these driving modes, and driving modes may change with the traffic environment. Hence, emissions could vary as a result of changes in the traffic environment. Since acceleration contributes most to emissions, emission estimation should

consider all possible acceleration events. Speed change within a traffic environment can be caused by traffic control, traffic volume, interaction of different road users, and infrastructure layout. However, it is unknown whether all possible speed changes can have a significant impact on emissions and thus need to be considered in the emission model. Moreover, since local emissions are the result of all vehicles driving through the area, it may be unnecessary to obtain each vehicle's detailed speed files for a local emission estimation. Thus, to estimate emissions on a segment, a method is required that can estimate the average emission factor on the basis of variables at the level of traffic flow dynamics.

At the level of traffic dynamics, parameters could be average speed or queue length, which are vital indicators for traffic efficiency. Although driving dynamics can be reflected to some degree by traffic flow dynamics, queue length, and average speed cannot thoroughly explain the variance of emissions. Thus, some other factors are needed to explain the total variance of emissions. Variables in the traffic system that can impact driving dynamics could be used to explain variance (listed below). Generally, these factors influence the driving mode, acceleration or deceleration rate, duration of each mode, engine power, and engine speed.

- traffic volume: speed variation while going through a green light
- traffic signal control (cycle time, green split, offset): stopping or queueing before the stop line
- distance between adjacent intersections: directly influences platoon dispersion and the signal coordination level, which influences the number of vehicles' stops
- speed limit: the distance of acceleration and deceleration
- conflicting traffic: acceleration, deceleration, and idling due to opposite traffic
- yielding traffic: acceleration, deceleration, and idling due to pedestrians and cyclists
- turning traffic: acceleration and deceleration due to turning movements
- mix traffic: speed of the cars behind the trucks will be slower
- approach type (with or without the turning lane): speed
- lane change: acceleration and deceleration due to lane change
- number of lanes: speed
- width of a lane: speed
- the curvature of a turning lane: vehicles will drive slower and accelerate more slowly when the curvature is sharper
- the slope of the road: engine speed and power
- driving style: acceleration and deceleration rate

In this study, the traffic volume, traffic signal control, speed limit, conflicting traffic, turning traffic, a mix of the cars and trucks, and the presence/absence of a turning lane are analyzed for an isolated signalized intersection. The isolated signalized intersection is defined when signal control does not take into account adjacent signalized intersections (the offset is an irrelevant control variable) (Cascetta, 2001, p.49). When signal coordination between adjacent intersections takes effect, the arrival pattern, which includes early or late arrival and the ratio of vehicle arrival during the green time, needs to be considered additionally.

Due to the power of the simulation, pedestrians, cyclists, lane changing behavior, the curvature, slope, lane width, and the driving style cannot yet be well represented by the microscopic simulation model. Since the goal is to test if these variables can accurately explain emissions, the variables that can best be modeled by microscopic simulations are chosen to be included in the scope of this research. The rest of the variables, including pedestrians, cyclists, lane changing behavior, curvature, slope, lane width, and the driving style, can be studied further once there is a tool that can accurately represent them.

3.1.3 Effect of the variables

Variables interact with each other to influence driving behaviors and emissions. Although these variables can be used as predictors for an emission estimation, their relationship would be highly nonlinear and complex.

To simplify the emission model, the capacity and average speed can be used as composite factors. The capacity is a function of signal control in case of a signalized intersection, gap acceptance in case of a non-signalized intersection, turning ratio, conflicting flow, and truck percentage. The function depends on the type of approach. The capacity is calculated based on the handbook (FGSV, 2015). The average speed is influenced by the capacity, traffic volume, and speed limit. For an isolated signalized intersection, as shown in Fig. 3.2, apart from using the capacity and average speed for variance explanation, the cycle time, turning ratio, conflicting flow, percentage of trucks, traffic volume, and the speed limit are used as additional predictors. As shown in Fig. 3.3, for coordinated signalized intersections, the impact of the signal coordination level on emissions is reflected in the relationship between the ratio of vehicles arriving during green time and emissions. The ratio of vehicles arriving during green time can be estimated by the mesoscopic traffic flow model, which includes a platoon dispersion model. Early or late arrival is a categorical variable. It is measured by the difference between estimated travel time and offset (if the difference is negative, it is early arrival; if positive, it is late arrival) (Fambro et al., 1991). To be addressed, these factors would also be used to estimate the change in the size of each typical segment.

Since the emission factor differs significantly between driving modes (deceleration, acceleration, idling, and cruising), the average emission factor is very sensitive to changes in the distribution of driving modes. These predictors may influence the average emission factor differently. For example, the capacity and volume may influence the number of queued vehicles whose emission factors near the stop line are quite different from that of vehicles outside a queue. The volume may influence the average speed of vehicles that are driving through. The percentage of trucks may influence the emission factor of a similar driving mode. The conflicting traffic may influence the length of the queue and speed near the stop line as well as during the crossing of the intersection. The speed of vehicles leaving the stop line on the turning lane will differ from their speed on a straight-through lane, which influences emissions before the stop line. The ratio of vehicles arriving during the green time will influence the queue length and then the emissions. The function is assumed to be two-term interactive

or quadratic, which includes the interaction between the two variables and the squared terms of each variable.

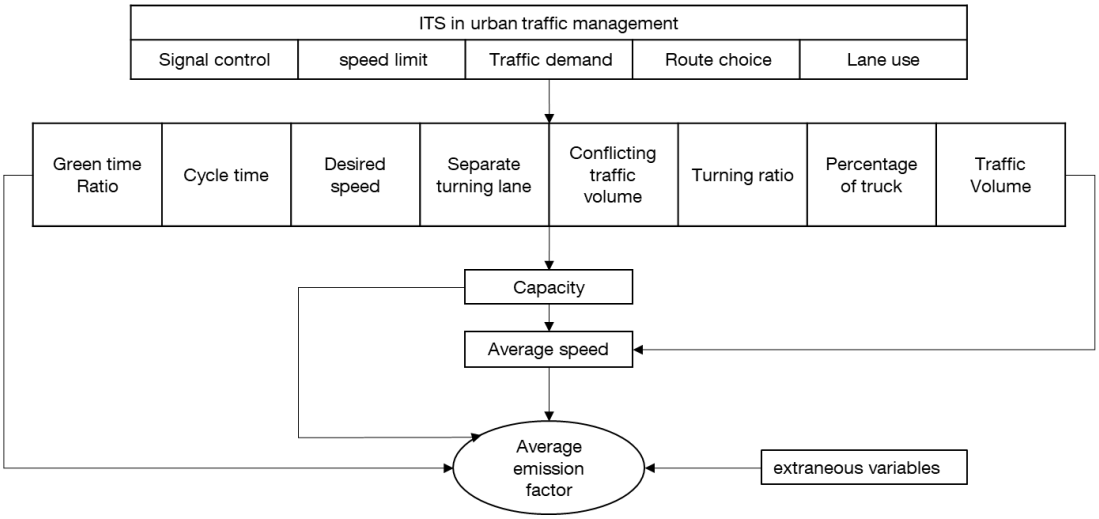

Fig. 3.2 Pathway of the effect on the average emission factor for an isolated intersection

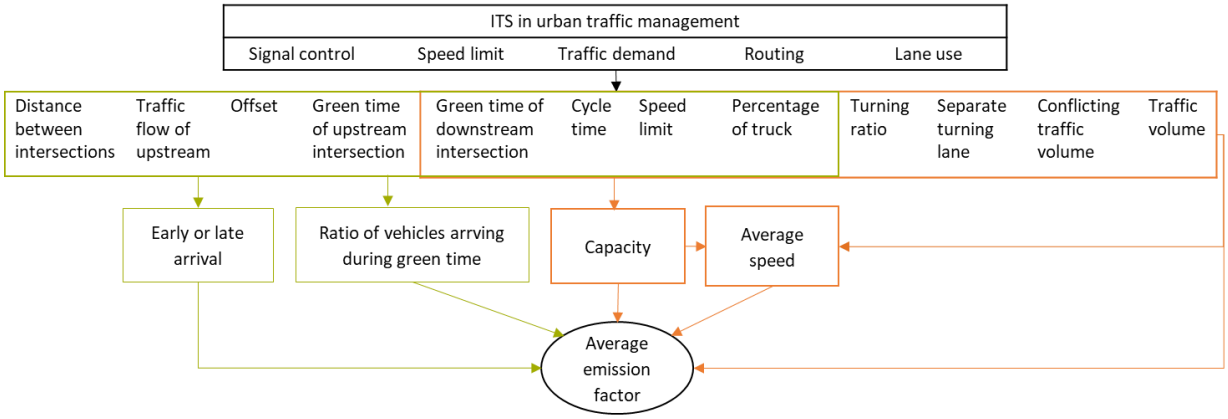

Fig. 3.3 Pathway of the effect on the average emission factor for coordinated intersections. Yellow – indicates the pathway for the isolated signal control intersection. Blue indicates the additional – pathway for coordinated signal control arterials or networks.

Fig. 3.4, Fig. 3.5, Fig. 3.6, and Fig. 3.7 explain how to use the emission model concept to assess typical types of ITS for traffic management and control.

ITS: isolated intersection control
control variables: cycle time, phase, green time ratio

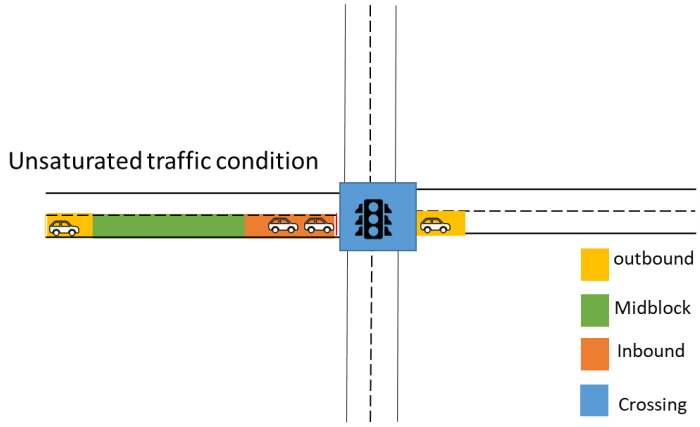

Variables: speed limit**, cycle time, green time ratio,** turning ratio, percentage of trucks, traffic volume, conflicting traffic volume, lane type

⇩

Emission factor= multi-factor regression function(**link capacity, average speed,** turning ratio, percentage of trucks, traffic volume, speed limit, conflicting traffic volume, **cycle time**, lane type)

Fig. 3.4 Illustration of assessing the isolated signal control based on the developed emission –model concept

ITS: coordinated signal control of an arterial street or network
control variables: offset, cycle time, green time ratio

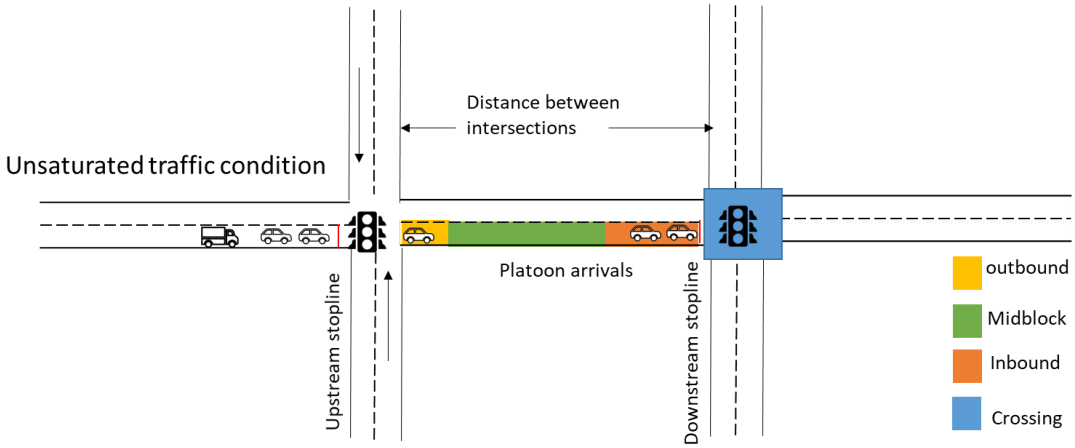

Variables: distance between intersections, speed limit, **offset, cycle time, green time ratio,** turning ratio, percentage of trucks, traffic volume, conflicting traffic volume, lane type

⇩

Emission factor= multi-factor regression function(**ratio of vehicle arrivals during green time, link capacity, average speed,** turning ratio, percentage of trucks, traffic volume, speed limit, conflicting traffic volume, **cycle time**, lane type, **early or late arrivals**)

Fig. 3.5 Illustration of assessing the coordinated signal control based on the developed – emission model concept

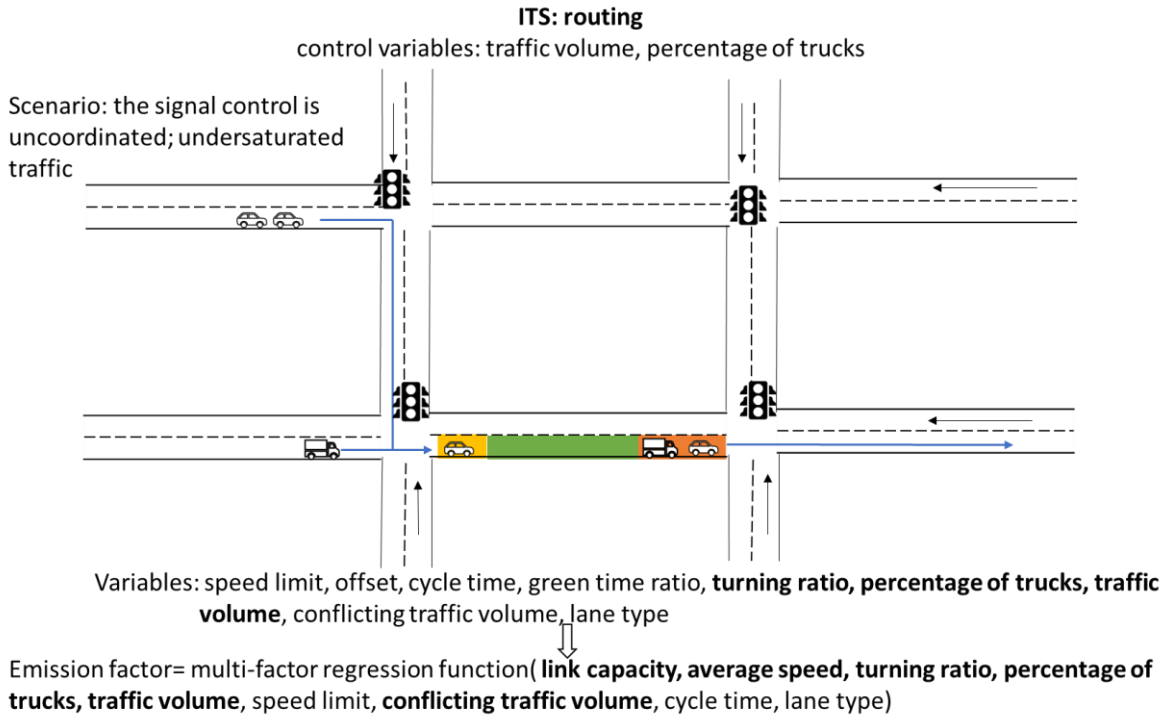

Fig. 3.6 Illustration of assessing the routing effect based on the developed emission model – concept when signals are uncoordinated

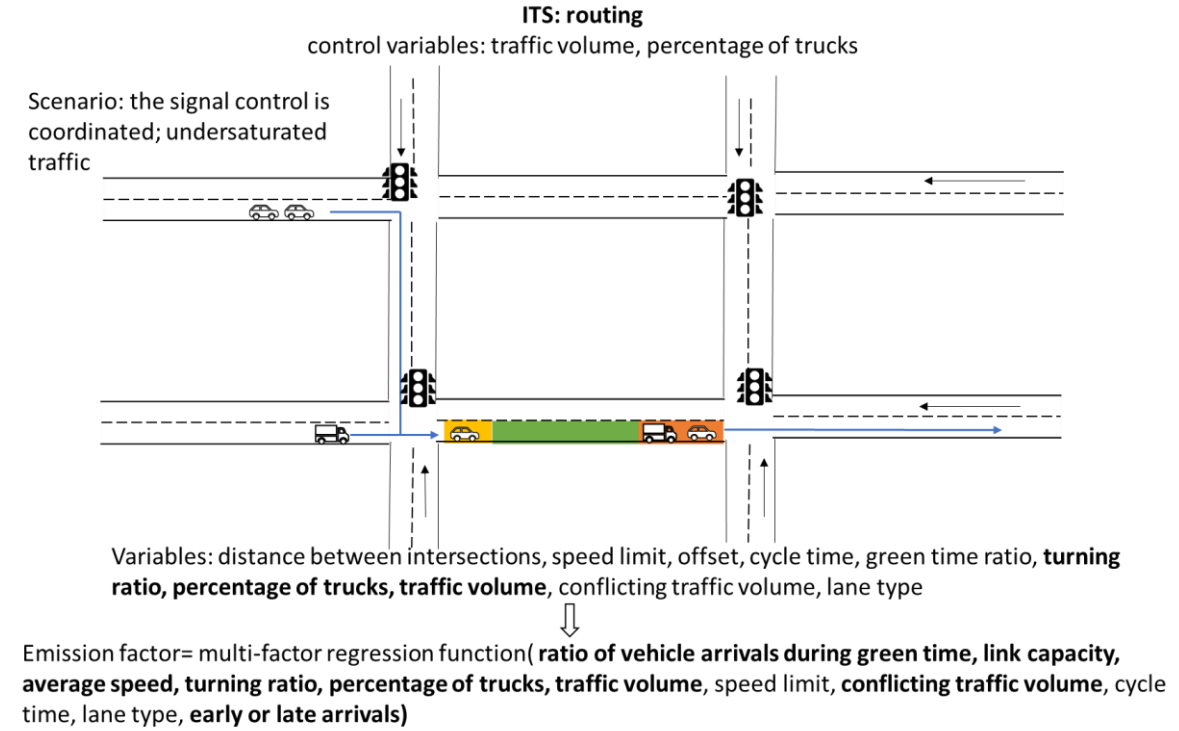

Fig. 3.7 Illustration of assessing the routing effect based on the developed emission model – concept when signals are coordinated

3.2 Basic data

For developing the model, the data needed can be collected from the real world or through modeling. A disadvantage of real-world data is that complete data collection could exceed the research budget. Another limitation is that the scenarios taken into consideration may not have occurred yet. Additionally, real-world data collection tools may be unable to provide trustworthy information since the measurements have errors resulting from the measurement tools and disturbance of the environment. The main methods to measure emissions are tunnel studies, on-board emission measurements (portable emission measurement system), remote sensing, and near-road air quality measurements. The on-board emission measurements are suitable to test the emission factor of an individual vehicle; remote sensing suits more to the instantaneous emission models. In the study by Celikkaya et al. (2019), it was found that the near-road air quality measurements themselves cannot tell what are the causes of high concentrations of air pollutions, since the concentration is a result of a complex interaction between traffic emissions, built environment, and meteorology. The traffic emissions can be estimated by an inverse process, in which an inversed dispersion model is applied to measured air pollutant concentration. However, it is unsuitable for developing an emission model due to the measurement errors of air quality and inaccuracy of the dispersion model. Therefore, instead of real-world measurements, the traffic emissions in each scenario are modeled, and the obtained emissions are used to develop the targeted new mesoscopic emission model.

3.2.1 Emission model

From chapter 2.3.2, it has been concluded that the most detailed emission model is the physics-based emission model. It is based on the engine emission map to estimate emissions. It can capture emissions during the transient process. The two notable models of this type are PHEM and CMEM. PHEM is developed based on European situations, while CMEM is based on American situations. A detailed description of PHEM can be found in the paper by Zallinger et al. (2005). The engine emission map was obtained from transient vehicle tests on roller testbeds. The engine map is a discrete dataset in which the emission rate is determined by the engine speed and engine power. PHEM uses the vehicle longitudinal dynamics model to calculate the effective engine power in 1 Hz resolution. Engine power includes driving resistance and transmission loss. It requires data on the vehicle specifications (such as weight and load of the vehicle), driving cycle, and road longitudinal gradient. Engine speed is calculated based on the gear shift model, tire diameter, final drive, and transmission ratio. The emission rate is then interpolated from the engine map. The average engine emission map is classified by euro class (from EURO 0 to EURO 6) and vehicle category (passenger, light-duty, and heavy-duty vehicle with otto or diesel engine). The vehicle database consists of passenger cars, freight vehicles, light-duty vehicles, articulated vehicle city buses, and coaches. Finally, the parameters are the relevant EU average values. PHEM has, by far, the largest database among detailed vehicle emission models. PHEM has been validated by comparing it to measured emissions from the chassis dynamometer test, onboard measurements, and remote

sensing data (Borken-Kleefeld, 2012; Hausberger, Rodler, Sturm, & Rexeis, 2003; Rexeis, Hausberger, Zallinger, & Kurz, 2007; Soltic & Hausberger, 2004; Zallinger et al., 2005). It can model emissions in diverse driving conditions in which speed, acceleration, longitudinal gradient, vehicle load, and power train differ. PHEM has been applied in various projects and has been used to estimate the impact of different traffic measures, such as vehicle communication (Tielert et al., 2010; Krajzewicz, Heinrich, & Milano, 2013) and signal optimization (Haberl et al., 2014). Additionally, it can help generate the emission map in meters and seconds and be used as an input for the microscopic dispersion model.

3.2.2 Traffic flow model

Based on chapter 2.2.2, the microscopic traffic flow model can model the impact of the variables considered in this research on driving dynamics in sufficient detail. Therefore, the traffic scenario is represented by the microscopic traffic model.

Numerous microscopic traffic flow simulators have been developed, which incorporate car-following and lane-changing behavior. They differ in specific car-following models and lane change models. The most frequently used simulator includes VISSIM, PARAMICS, AIMSUN, and SUMO. The speed profiles generated by the microscopic traffic simulation model can be used as an input in the engine-based emission model. It has been criticized that these simulation models cannot be used to estimate emissions on a second by second basis since they cannot accurately capture second-to-second changes in vehicle dynamics (Song et al., 2013). They have fewer errors in the estimation of emissions of the entire traffic or vehicle platoons at the segment level (da Rocha et al., 2015). The research will focus on traffic emissions at the segment level. Thus, the microscopic traffic flow simulator has the potential to provide the data basis for the model development.

VISSIM is a commercial system developed by a company called PTV AG. The car-following behavior is based on the psycho-physical driver behavior theory and uses the Wiedemann model; and the lane-changing behavior is based on the Sparmann model (M. Fellendorf & Vortisch, 2010). It can accurately reproduce the road infrastructure (complex intersections) and also takes into account vehicle properties and drivers (Maciejewski, 2010). The VISSIM has been widely used for various applications, such as for the analysis of alternative signal control strategies and corridor studies on arterials with signalized and non-signalized intersections. It has been integrated with the detailed emission model to estimate the emissions and the impact of the traffic management and control on emissions (Lv & Zhang, 2012; Kun & Lei, 2007; Zhang & Ioannou, 2016; Hirschmann et al., 2010).

3.2.3 Microscopic emission assessment framework

The integration of VISSIM and PHEM forms the microscopic emission assessment framework. VISSIM provides the inputs that PHEM requires. In PHEM, there exists a mode, called ADVANCE. It provides an interface for traffic models like VISSIM. VISSIM generates the speed

trajectories of individual vehicles in the network, and the data is saved in a file (*.fzp). According to the needs of PHEM, the file should include information about time, x-coordinate, y-coordinate, vehicle number, speed, gradient, vehicle category ID, and street ID. The user should define the fleet composition as an additional input file. According to the composition of the fleet, PHEM should automatically assign every single vehicle with a EURO class and an engine type. PHEM will then separately calculate the emissions of each vehicle per second and save the data in a file (*.mod). The result consists of speed, acceleration, position, engine dynamics, emission rates. Fig. 3.8 shows the integration between VISSIM and PHEM.

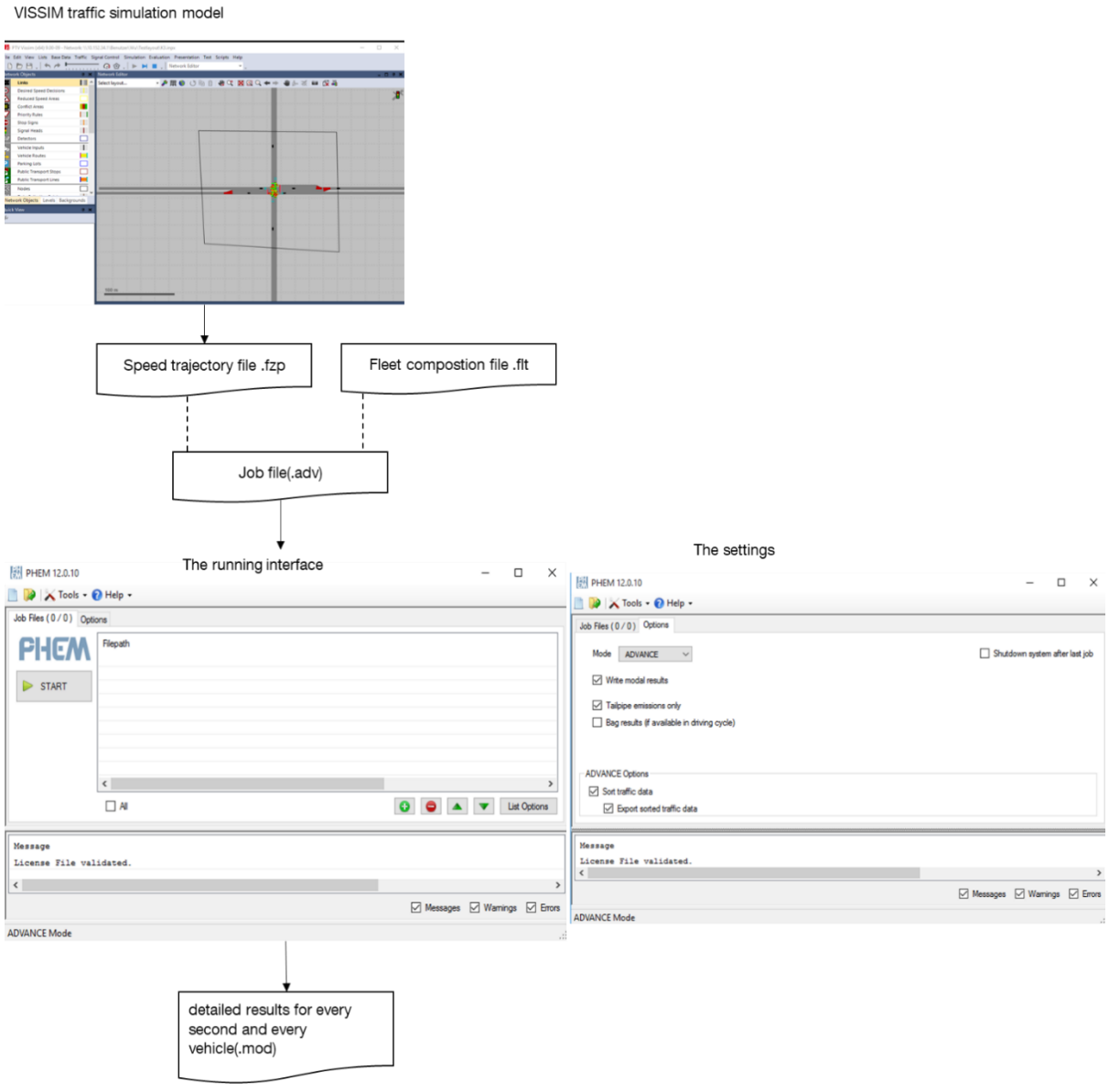

Fig. 3.8 Flow chart of microscopic emission assessment in each traffic scenario

3.3 Modeling methods

Firstly, the road division is studied. Secondly, the emission function for each segment is explored. As Fig. 3.9 shows, the scenarios are designed using the experimental design method and are simulated with VISSIM software. The PHEM model is used to calculate emissions. The spatial data mining method is applied to divide the road into segments, and the regression method is used to generate the emission function.

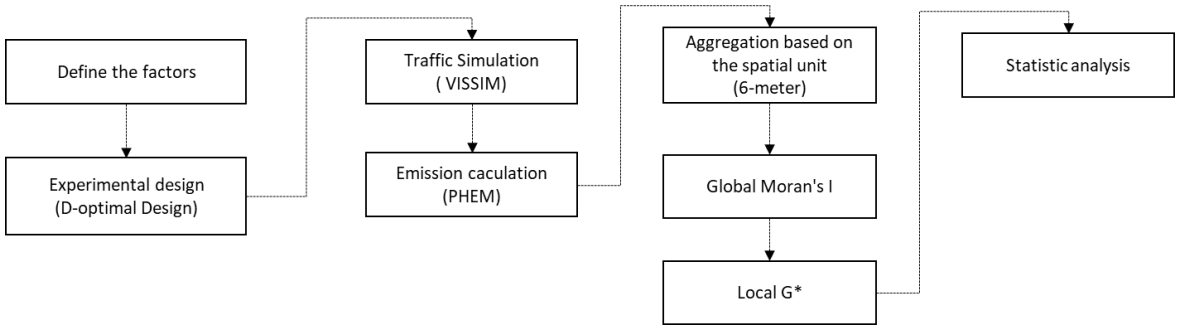

Fig. 3.9 Workflow of the modeling methods

3.3.1 Design of traffic scenarios

The purpose of the experiment is to change the input variables in a system in a way that can help understand the relationship between response and important input variables (Montgomery, 2017, p.2). In order to arrive at relevant conclusions, proper experiment planning is crucial to guarantee that the correct data type is chosen and that the sample size is sufficient (Yale University, n.d.). The statistical design of experiments is “a process of planning the experiment, so that the appropriate data is collected and analyzed by statistical methods” to help yield “valid and objective conclusions” (Montgomery, 2017, p. 11). According to Montgomery (2017), the necessary steps consist of setting the goal and objective of the experiment, selecting and defining the response variable, choosing experimental factors, factor levels, and level ranges, choosing the design method, conducting the experiment, statistical data analysis, drawing conclusions, and making recommendations.

For this study, the goal is to develop proper regression functions to estimate emissions. The response variable is the emission factor of each segment. The essential experimental factors are traffic volume, green ratio, cycle time, truck percentage, speed limit, and lane type. Additional factors are the left-turning ratio, right-turning ratio, as well as conflicting traffic’s traffic volume and truck percentage. The variability resulting from these factors needs to be quantified and extracted to quantify the emission variability resulting from the studied variables. The range of each studied variable is defined on the basis of common urban situations. Experiments cover all possible combinations of these variables. Various levels of service are considered. After considering the two-way interaction and second-order effect, three levels of each variable are chosen. An extraneous variable is a variable that is not of interest to the current study but may influence the response variables and predictors (Colman, 2015, p.224).

In this research, driving behavior constitutes an extraneous variable. Driving behaviors may influence the arrival pattern, capacity, average speed, and emission factor. The randomized assignment of driving behavior parameters to vehicles in the microsimulation model reduces the impact of driving behaviors on the relationship between the targeted predictors and the response variable.

Many design approaches have been developed for fixed factors, including the classical design (e.g., full factorial design and fractional factorial design) and the optimal design. The optimal design constitutes the best option where constraints generated by the classical design, such as limited maximum sample size or an infeasible combination of factors, need to be accommodated (Smucker et al., 2018). Since the computation cost of the classical design is too high when a model includes more than five variables with more than three levels, the optimal design is chosen to generate the design of the experiments. Under the optimal design, a subset of design points is generated from a larger candidate set of design points (NIST, 2013). Design points for the experiments are chosen on the basis of optimality criteria (Montgomery, 2017, p.443). The two major types of optimality criteria are, firstly, the minimization of the variance of the predicted value and, secondly, the variance of parameter estimators. Both optimality criteria can perform differently (Wong, 1994). D-optimality serves to minimize the generalized variance of the parameter estimators (Kiefer & Wolfowitz, 1959). Since the goal of this research is to estimate the parameters accurately, D-optimality is chosen. Equation 1 and Equation 2 are adapted from Atkinson & Donev (1992). According to Atkinson & Donev (1992), the major steps of the D-optimal algorithm are to

(1) define a functional type to describe the relationship between the responsive factor (Y) and the predictors (X).
(2) given the number of experimental runs and the specified function type, generate a candidate set of design points
(3) select the subset of design points from the candidate set, which maximizes the determinant of the X'X matrix.

$$Y = \beta_0 + \beta_1 x_1 + \beta_2 x_2 + \beta_{12} x_1 x_2 + \varepsilon \qquad \text{Equation 1}$$

Where x_1 and x_2 are the major effects of the two factors and $x_1 x_2$ is the interaction term of the two factors. Each factor has two levels represented by 1 and -1.

A four-run design matrix could be

$$X = \begin{bmatrix} 1 & -1 & -1 & 1 \\ 1 & -1 & 1 & -1 \\ 1 & 1 & -1 & -1 \\ 1 & 1 & 1 & 1 \end{bmatrix} \qquad \text{Equation 2}$$

Where the second, third, and fourth columns of X represent the values of x_1, x_2 and $x_1 x_2$, respectively. The first column represents the constant term.

Various computer software programs are widely used to support on experimental designs. The function "cordexch" in Statistics and the Machine Learning Toolbox™ of Matlab is used to generate D-optimal designs. The process of producing optimal design points is iterative. At each step, it exchanges a single element in an initial design matrix X with a new neighboring

element from the candidate set to increase matrix X'X (MathWorks, 2020). The initial design and incremental changes are selected randomly. Besides, there should exist enough data points to ensure precision in the parameter estimation (Minitab Statisticians, n.d.). For this research, the number of experiment runs is set according to the sample size guidelines for regression analysis provided by Minitab Statisticians (n.d.).

3.3.2 Spatial data analysis

Road division in a specific traffic situation serves to separate high-emission areas from low-emission areas. The method can distinguish emission characteristics (average emission level and variance) between these segments in various typical typologies of signalized intersections and traffic situations. For judging the quality of the division method, road segments featuring high emissions should be identified, instead of being concealed in the heterogeneous area; the spatial resolution should not be so detailed that the difference of emissions between segments becomes insignificant; emissions from each segment should be accurately estimated using factors selected for this study.

The exploration of the spatial emission distribution pattern is an issue of spatial data analysis. Exploratory spatial data analysis (ESDA) is “a collection of techniques” to describe spatial properties of data; identify unusual cases; detect spatial patterns in data, and formulate hypotheses about spatial heterogeneity (Haining, 2014, p. 182). Spatial heterogeneity means that the variable displays variation in means, variances, and covariance between locations, which can be generated by the underlying process (A. Getis & Ord, 1996; Haining, 2014, p.186). Heterogeneity can also originate from the spatial unit size identified for measurement (Haining, 2014, p.186). Clusters are one type of major spatial patterns. Clustering will result in the low similarity between classes and high similarity within a class (Tripathy & Hota, 2012). The clustering of areas with a similar emission factor is an issue of cluster detection. There are two major types of cluster detection: one type for the detection of area data and one for point data. Emission data is one type of area data. In the case of area data, the relevant exploratory methods of cluster detection are the Choynowski test, G-statistics, the Besag-Newell test, and the Kulldorff scan test. Previous applications illustrate the strength and weaknesses of each method in terms of power, accuracy, sensitivity, and computational expense (Grubesic et al., 2014).

Spatial autocorrelation constitutes another method of exploratory spatial data analysis. It serves to describe the correlation between the values of a variable, which results from the spatial proximity of these values, and it is quantified by a deviation from the assumption of independent observations (Griffith, 2003). Common techniques are Moran’s I, Geary’s c, and Getis’ G. Local statistics were developed for the signal observation: local Moran’s I, local Geary’s c and local Getis’ Gi (G_i^*) to recognize “hot spots or possible centers of statistically significant clustering” (Getis, 2008, p.307). Local Gi*-statistics can be suitable for the identification of the location of statistically significant hot spots (i.e., connected areas displaying high values) and cold spots (i.e., connected areas displaying low values). The identification of high-emission areas is a question of hot spot analysis.

No study has yet been conducted that uses this method to recognize the spatial pattern of emissions. For this research, it is assumed that there exists a clear boundary between high and low-emission areas. Local G_i*-statistics are chosen to prove the assumption and find the location of the boundary between segments. The local G_i*-statistics obtains a standardized Z-score for each observation in the dataset (Arthur Getis & Ord, 1992). Adapted from Sipos (2017, p.103), equations 3, 4, and 5 show how to calculate the Z-score. The calculated Z-score tells the locations of clusters of high and low values. The p-values indicate statistical significance – the more statistically significant the absolute Z-score, the more intensive the clustering (ERSI, 2018).

When clustering occurs, the neighborhood of the cluster needs to be defined. Commonly used neighbors include contiguity-, distance- and graph-based factors. For this study, a fixed distance is chosen. The emission factor for a spatial unit is analyzed in the context of neighboring emission factors within some specified critical distance. “The distance band that exhibits maximum clustering” is defined as the appropriate distance (ERSI, n.d.). Global Moran's I is used to measure the degree of a cluster (Moran, 1948). In Equation 6, a positive Moran's I indicates the values of the elements are clustered, while a negative one means that values are dispersed.

Global Moran's I and local G_i* are calculated using functions of the “spdep” package in R. Global Moran's I is calculated at several distances, and the distance with the highest Global Moran's I value is used in local G_i* (see the workflow in Fig. 3.4).

$$G_i^* = \frac{\sum_{j=1}^{n} w_{i,j}\, x_j - \bar{X} \sum_{j=1}^{n} w_{i,j}}{S \sqrt{\frac{\left[\left(n \sum_{j=1}^{n} {w_{i,j}}^2 - \left(\sum_{j=1}^{n} w_{i,j} \right) \right)^2 \right]}{n-1}}}$$

Equation 3

$$\bar{X} = \frac{\sum_{j=1}^{n} x_j}{\mathrm{n}}$$

Equation 4

$$S = \sqrt{\frac{\sum_{j=1}^{n} {x_j}^2}{n} - (\bar{X})^2}$$

Equation 5

$$I = \frac{n}{\sum_{i=1}^{n} (x_{i-\bar{X}})^2} \frac{\sum_{i=1}^{n} \sum_{j=1}^{n} w_{i,j}\, (x_{i-\bar{X}})(x_{j-\bar{X}})}{\sum_{i=1}^{n} \sum_{j=1}^{n} w_{i,j}}$$

Equation 6

G_i^* : the Z-score

x_j : the value of element j

$w_{i,j}$: the spatial weight between element i and j

n : the total number of elements

I : the value of Moran's I index

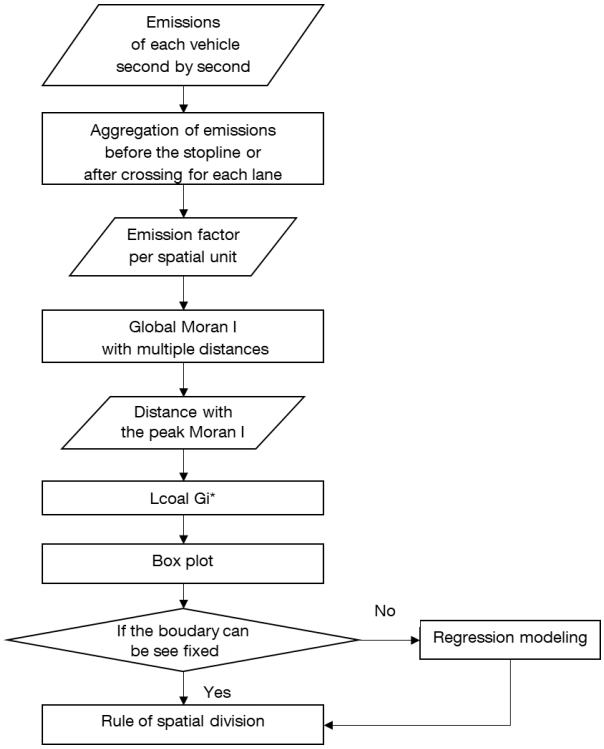

Fig. 3.10 Flow chart of the boundary division

3.3.3 Regression method

This section aims to mathematically describe the relationship between predictors and the emission factor per segment. The elimination of not statistically significant variables was attempted to find the right relationship. Many possible models were considered to achieve a Goldilocks balance with the number of predictors. The specification of the regression models rests on an iterative process (see Fig. 3.11). Firstly, the model needs to be specified by choosing the predictors and function type. Initially, typical linear models are tested: a first-order linear model, the first order with a two-way interaction model, and stepwise linear regression. The variables firstly considered are those to describe the traffic on the studied lane. Subsequently, the parameters for each model are estimated. Due to the uncertainties involved with the traffic simulation model and the emission model, the obtained emission and traffic data has a certain error in each scenario.

Moreover, noise is generated from the environment. It is assumed that the error is normally distributed. An estimator is used to attempt to approximate the unknown parameters. OLS (Ordinary least squares) is used in this study. The models are then evaluated and compared. If some of the models are accurate enough, these models are chosen for the application. Otherwise, models are improved by adding or removing terms, transforming the response variable, or by testing higher-order models. Variables on the adjacent lane or conflicting traffic are added to test if they can improve the emission estimation. The following factors are expected to lead to an accurate estimation of the relationship.

Multicollinearity exists when there is a high correlation between predictors. It tends to inflate the variance of estimated coefficients and may lead to a wrong effect sign. VIF (Variance inflation factors) in Equation 7 and Equation 8 indicate how severe the multicollinearity is in the model. Equation 7 is adapted from the on-line course material (Pardoe et al., 2020). If VIF is 1, the predictor and the remaining predictors have no correlations; if VIF is bigger than 4, it indicates that further investigation is needed; if VIF is bigger than 10, it indicates that correction is required (Pardoe et al., 2020).

$$VIF_i = \frac{1}{1 - R_k^2}$$ Equation 7

$$R^2 = 1 - \frac{\sum_{i=1}^{i=n}(y_i - \hat{y_i})^2}{\sum_{i=1}^{i=n}(y_i - \bar{y})^2}$$ Equation 8

R_k^2 : the coefficient of determination of the linear regression function (the predictor k serves as a linear function of the rest predictors).
y_i: i_{th} observed data
$\hat{y_i}$: i_{th} predicted value
$\overline{y_i}$: the mean of the observed data

Performance evaluation: after fitting the model, it is checked whether the coefficient signs and effect magnitudes align with the theory. The prediction slice plot helps to judge if the coefficient signs and effect size are reasonable (Minitab Blog Editor, 2019). The 10-fold cross-validation method is chosen to examine the predictive accuracy of the fitted model. Following this method, the dataset is partitioned into ten sets. For each set, the model is then trained to use the out-of-fold observations and is assessed using the in-fold data. Lastly, the average test errors of all folds are calculated. The F-test is used to check if the model fits the data better than a model without predictors. The adjusted R^2 is used to evaluate the explanatory power of the regression model. The RMSE (root mean square error) is an indicator to measure the error of a regression function. The standardized residual plot is checked. It can help answer if the residuals are approximately normally distributed as assumed in this regression method and if a variable, a higher-order term, or interaction between terms, is missing. The residuals should be scattered roughly symmetrically around 0. When the models have similar adjusted $R^{2,}$ and RMSE and the residuals are roughly symmetrically distributed, simpler models would be chosen for application.

$$R^2_{adjusted} = 1 - \frac{(1-R^2)(n-1)}{n-p-1}$$ Equation 9

$R^2_{adjusted}$: the coefficient of determination of the linear regression equation
n : the number of the sample size
p : the number of predictors.

$$RMSE = \sqrt{\frac{\sum_{i=1}^{n}(y_i - \hat{y}_i)^2}{n}} \qquad \text{Equation 10}$$

y_i : i_{th} observed data
$\hat{y}_i$: i_{th} predicted value
n : the total number of data points.

When a term is removed: whether a predictor variable should be included in the final regression model is based on the consideration of two factors: statistical significance and a hierarchical model. Statistical significance is examined by conducting a t-test. Because the lower-order term indicates the basic information about the shape of the relationship and the higher-order term refines it, the lower-order term would likely remain kept in the regression function if the higher-order term is statistically significant and there are also not too many statistically significant terms (Minitab Blog Editor, 2016).

The regression-related algorithms and processes are implemented with Matlab. The regression Learner App in Matlab is used to train, validate, and tune the regression models.

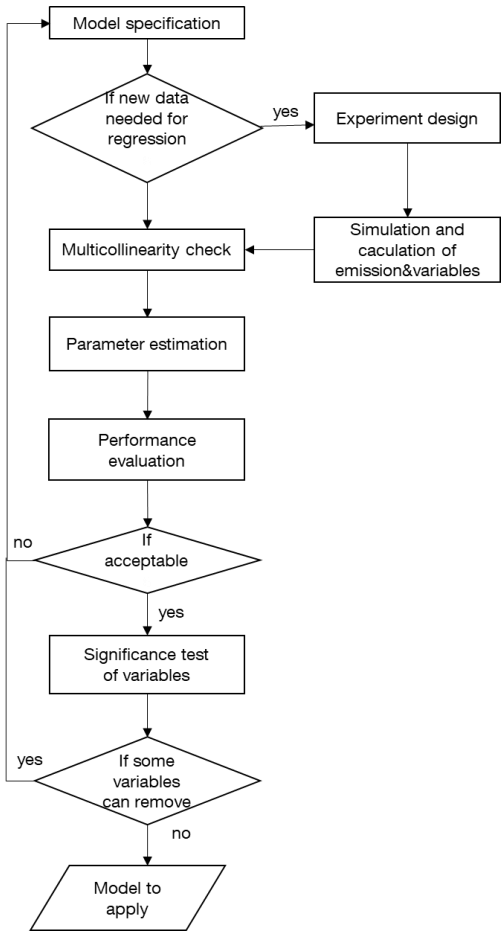

Fig. 3.11 Steps of regression modeling

3.4 Modeling

The model development methodology is applied to two types of road approaches of an isolated signalized intersection, which are used as examples to examine the feasibility of the model. The methodology reveals how the lane should be divided into smaller segments before the stop line and after crossing the intersection. For each lane, the spatial division method is applied to explore the boundary between high and low upstream emission areas. At the intersection, each crossing lane is regarded as one segment. By conducting variance studies of the boundaries, the rule for each type of lane is defined. For each segment, its hourly traffic volume (q), truck percentage, turning ratio, cycle time (C), capacity (c), speed limit (V), average speed ($\bar{v}$), opposite traffic volume, and truck percentage of opposite traffic are used as predictors for regression modeling. Following the regression modeling steps, the regression model is selected for the test. The main and interaction effect of each selected model is described and explained.

3.4.1 Scenarios

In this section, the scenarios to which the model development methodology is applied are described. The description includes the layout of the signalized intersection, the values of the variables, and the simulation settings.

Scenario description

Two major types of approaches are studied, one is a straight lane with right and left-turning lanes, another is one lane with straight-through traffic and turning traffic. These two approaches are designed on an isolated signalized intersection. It is a realistic virtual intersection. The intersection for the model development is in Fig. 3.12. The east approach has one straight lane with left- and right-turning lanes. The left-turning lane is around 60 meters long, and the right-turning lane is 48 meters long. The south approach consists of one lane with a mix of straight-through traffic and turning traffic. The left-turning traffic from the east faces conflicting traffic from the west. The traffic light is Fixed time signal control. The inter-green time has a duration of 7 seconds. The signal settings for the left-turning, right-turning, and straight-through traffic are the same on the east approach. The east approach and south approach are the study area for emission modeling. The east and south approaches are separately studied since they have opposite signal phases, which means that their signal phases are not permitted to run simultaneously by the signal controller.

The variables and their levels for each lane on the east approach are listed in Tab. 3.1. Variables include hourly traffic volume of straight-through traffic (q_s), left-turning hourly traffic volume per hour (q_l), right-turning hourly traffic volume (q_r), conflicting hourly traffic volume(q_c), truck percentage of straight-through traffic (truck_s), truck percentage of left-turning traffic (truck_l), truck percentage of right-turning traffic (truck _r), truck percentage of conflicting traffic (truck_c), speed limit (V) and green ratio. The C is set to be 60 seconds. The

truck percentage of each direction is the ratio of hourly truck volume divided by the hourly traffic volume of each direction.

On the south inflow, the left-turning traffic is set as 0. The right-turning ratio (a_r), q, truck percentage of each direction, C, and V are varied (Tab. 3.2).

The quadratic effect and interaction effect are assumed. Thus each variable should have at least three levels. The levels of C, green ratio, and V are set according to common real-world values. The range of the truck percentage is based on an urban situation. The middle point is set at the second level so that the points are more homogeneously distributed. For the east approach, the levels of traffic volume are set while ensuring that the queue length on the turning lane is no longer than the length of the turning lane. For the south approach, the levels of traffic volume and turning ratio are set to cover the various volume to capacity ratios. By applying the D-optimal method to each approach, the scenarios for each approach are obtained.

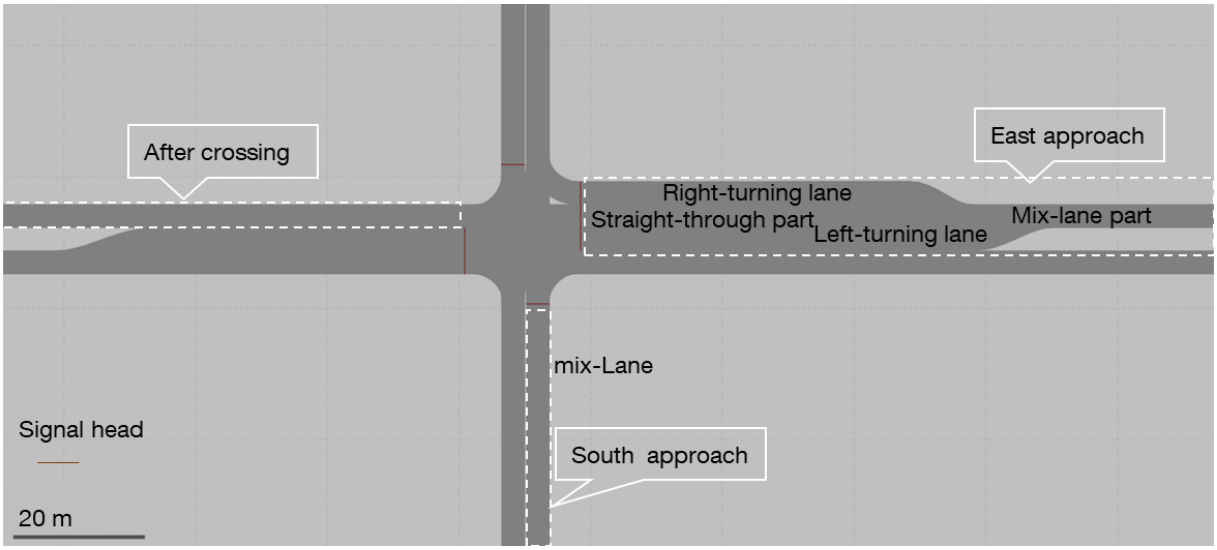

Fig. 3.12 Intersection in VISSIM for model development

Green ratio	truck_l	truck_r	truck_s	truck_c	q_l [veh/h]	q_r [veh/h]	q_s [veh/h]	q_c [veh/h]	V [km/h]
[0,3, 0.4, 0.5]	[0, 0.025, 0.05]	[0, 0.025, 0.05]	[0, 0.025, 0.05]	[0, 0.025, 0.05]	[120, 180, 240]	[120, 180, 240]	[120, 180, 240]	[0, 67, 134]	[30, 40, 50]

Tab. 3.1 The variables and levels on the east approach

C [s]	Green ratio	a_r	q [veh/h]	truck _r	truck _s	V [km/h]
[60, 90, 120]	[0,3, 0.4, 0.5]	[0.1, 0.5, 0.9]	[500, 600, 700]	[0, 0.025, 0.05]	[0, 0.025, 0.05]	[30, 40, 50]

Tab. 3.2 Variables and levels on the south approach

Scenario simulation

These scenarios are simulated in VISSIM 9.00. The composition of vehicle classes is based on statistics from 2010, which are provided in PHEM. The gear-shift model embedded in PHEM is used. Driving behaviors are set at the default values in VISSIM, which represents regular driving. VISSIM allows the user to select a time step between 0.1 and 1.0 seconds. The time resolution should be at least 3hz to obtain realistic trajectories (Hirschmann et al., 2010). Setting the time step at 0.1 seconds can help obtain a more realistic speed trajectory (Fellendorf & Vortisch, 2001). Therefore, the simulation resolution is set at 10-time steps per second of the simulation.

The number of runs: microsimulation takes into account the stochastics of the traffic flow, and the results depend on the random number seed of each run. To have a statistically valid value for the emission factor, more simulation runs with different random number seeds are required. The minimum number of runs can be calculated by Equation 11 (Dowling et al., 2004; FGSV, 2006; Hoffmann, 2014).

$$n = \frac{t(\alpha, n-1)^2 s^2}{C^2}$$ Equation 11

n: the minimum number of runs
$t(\alpha, n-1)^2$: the value based on the student-t distribution
s: standard deviation
C: the desired confidence interval

A confidence interval is the range of values within which the true mean value may fall. The initial confidence interval can be calculated by Equation 12 (Hoffmann, 2014, p. 95).

$$2 * 1.96 * \frac{s}{\sqrt{n}} \qquad \text{Equation 12}$$

A confidence level is a probability that the true mean will fall within the confidence interval. 95% is picked as the level of confidence.

The ten simulation runs are performed to estimate the initial standard deviation of the emission factor of NO_x on each six-meter segment. It shows that if ten is assumed to be the minimum number of simulations required, then the confidence interval reached is smaller than the one calculated by equation 12. Therefore, each scenario is simulated ten times.

3.4.2 Spatial division

The basic spatial unit is defined as six-meter since it is the average distance between passenger cars in a queue. The average emission factor (EF) of all simulation runs per scenario is used for the spatial division algorithms. The result of each lane is described below. The boxplot of the Z-score at each spatial unit helps to identify the variance and mean of the Z-score. The top line of the rectangle indicates the third quartile. The horizontal line in the rectangle is the median. The bottom line of the rectangle indicates the first quartile. The horizontal line above the rectangle is the maximum value. The line below the rectangle indicates the minimum value. The relative vertical spacing between labels reflects the proportionality of the values of the variable.

East approach

Before applying the spatial division method, changes in fleet composition and traffic volume on a lane need to be considered. On the straight-through lane, some vehicles change the lane to enter the turning lane. The lane changing leads to changes in traffic volume and fleet composition. Thus, the straight-through lane is divided into two parts. One part consists only of straight-through traffic, which starts at the stop line to 48 meters away from the stop line. The remaining road section features mixed traffic and includes vehicles switching to the turning lane.

On the left turning lane, high emissions occur near the stop line, while cold spots are detected on the remaining parts of the lane (Fig. 3.13). There is no apparent relationship between the queue length and the size of high-emission areas. For all situations, the area within 12 meters from the stop line features a significantly high emission factor. In most cases, high emissions are located within 18 meters from the stop line and only in a few cases up to 24 meters from the stop line. Therefore, the division point between high and low-emission areas is chosen to be 18 meters from the stop line.

On the right turning lane, significantly high-emission areas exist within 12 meters from the stop line, while high-emission areas in most cases exist up to 18 meters from the stop line (Fig. 3.14). The boundary between high and low-emission areas on the right turning lane is set at 18 meters from the stop line. The locations of high emissions on the straight-through lane are like the ones on the right-turning lane (Fig. 3.15). Therefore, the boundary between high and low-emission areas on the straight-through lane is also at 18 meters from the stop line.

It is possible to further distinguish between hot and cold spots on the section before the turning lane, where turning traffic and straight-going traffic mix. There is a relatively high-emission area near the lane changing section compared to the section above (Fig. 3.16). Compared to the emission factor near the stop line, the emission factors of these spots are quite low. It is similar to the average emission factor of the rest of the queue as well as of the section before the queue. Thus, the section before the turning lane is treated as one segment.

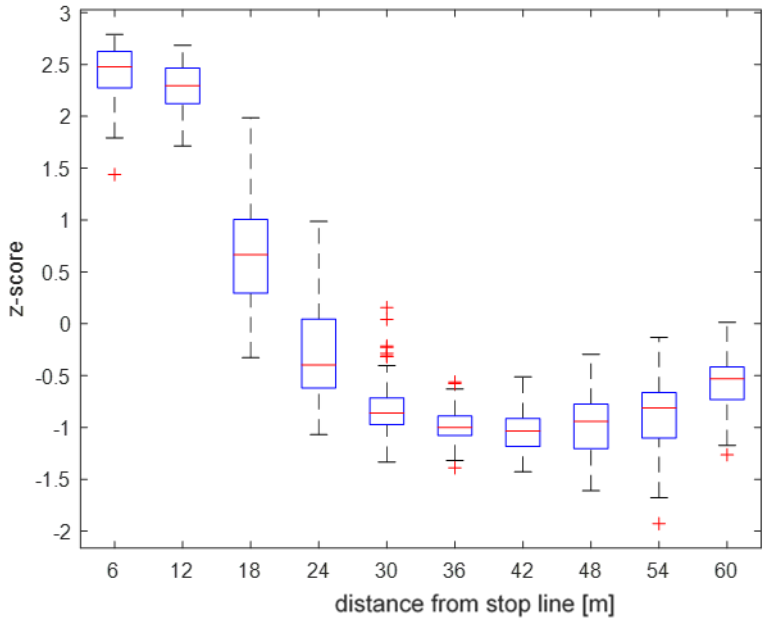

Fig. 3.13 Z-score of the left-turning lane

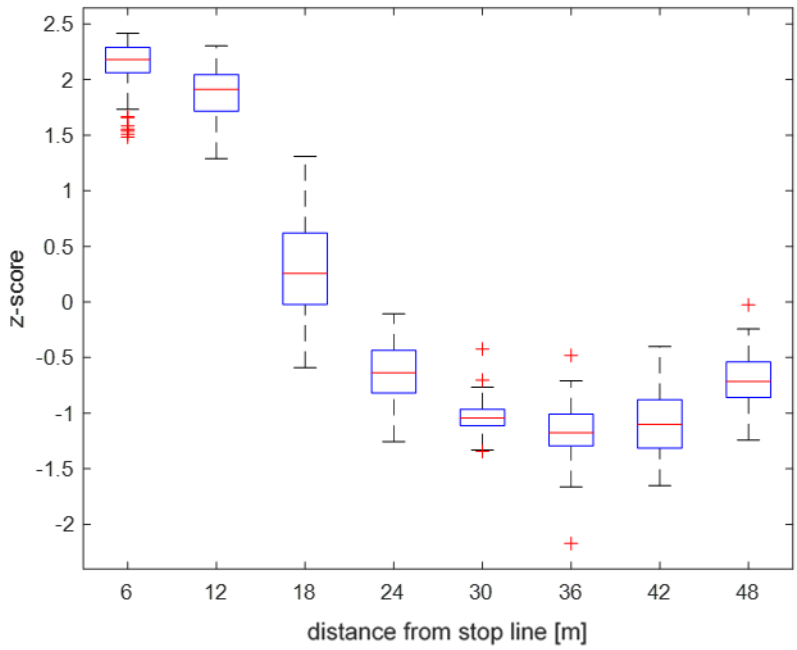

Fig. 3.14 Z-score of the right-turning lane

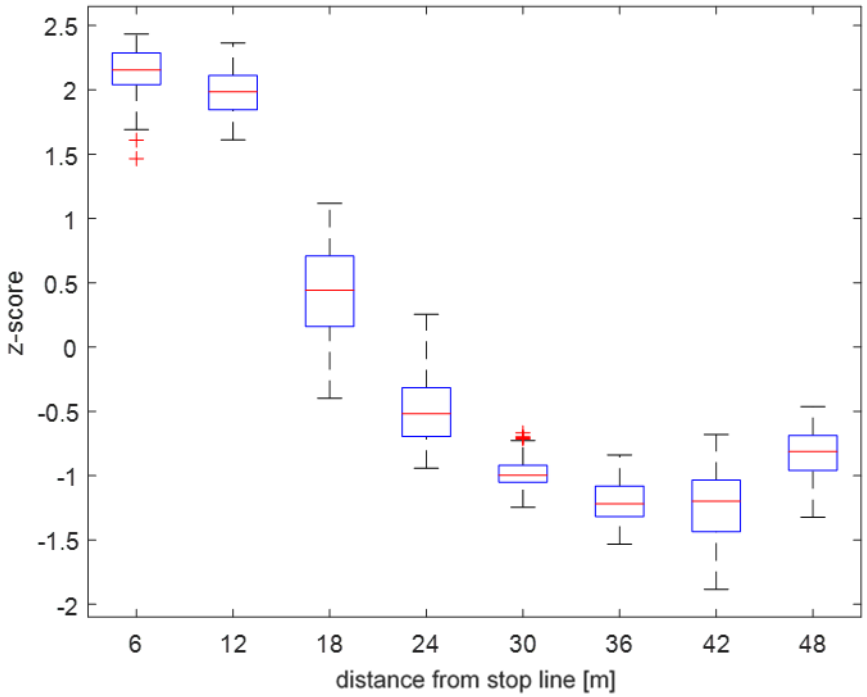

Fig. 3.15 Z-score of the straight-through lane

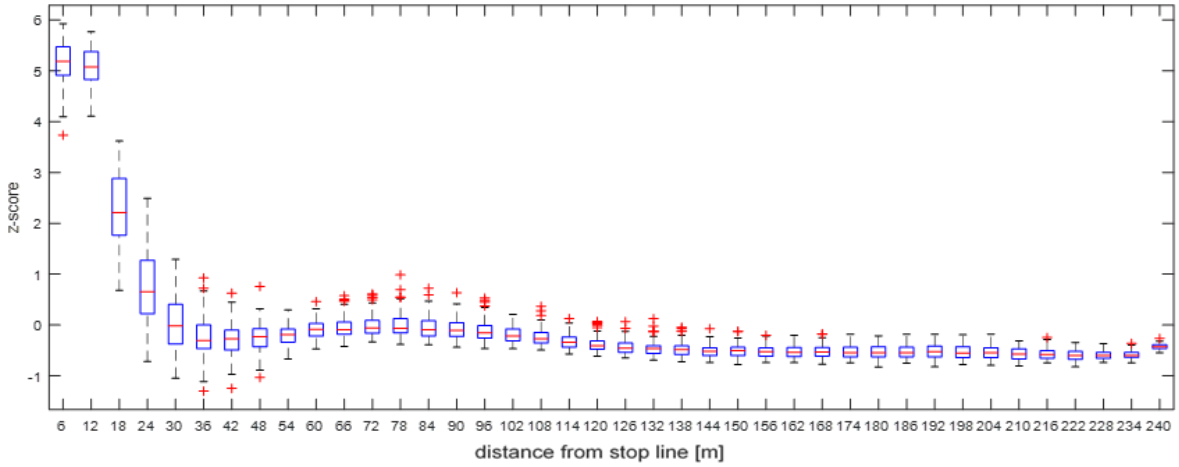

Fig. 3.16 Z-score of the lane with the straight-through and turning traffic

South approach

The segment of the south approach investigated has a length of 120 meters. When the queue length is shorter than 120 meters, the size of the high-emission area ranges from 36 to 72 meters (Fig. 3.17). The stepwise regression method is applied to the estimation of the size of the hot spot (distance from the stop line) using the a_r, C, c, q, truck percentage, and V. The significant variables and the coefficients are listed in Tab. 3.3. The R-squared is 0.8, and the adjusted R-squared is 0.77. Since all the VIF values are below 10, the assumption of no serious multicollinearity is met. The scatterplot of the standardized residual on standardized predicted values does not funnel out or curve. Thus, the assumptions of linearity and homoscedasticity are met as well. It is found that the truck percentage is not a statistically significant predictor. The a_r, q, and c have positive relations to the size of the hot spot while C and V have negative relationships. For the cases where the queue is longer than 120 meters, the investigation should be enlarged to cover the entire length of the queue.

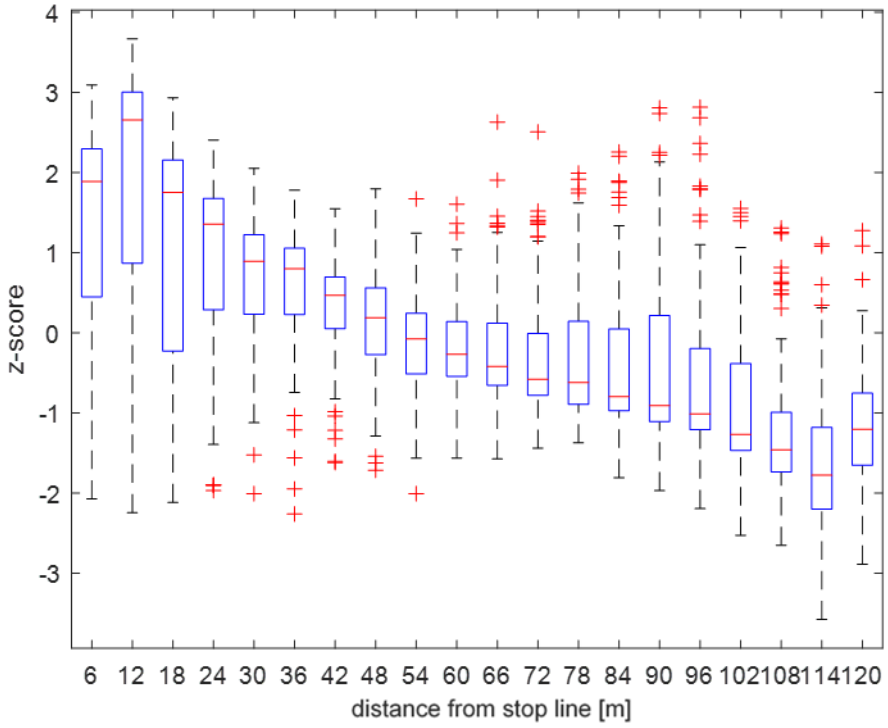

Fig. 3.17 Z-score of the lane with straight-through and right-turning traffic

Variables	Coefficients	P-value
Intercept	5.371	<0.001
a_r	1.763	<0.001
C	0.037	<0.001
c	-0.005	<0.001
q	0.009	<0.001
V	-0.056	<0.05

Tab. 3.3 Regression result for hotspot size of a lane with right-turning and straight-through traffic

After crossing

The downstream road segment consists of right-turning traffic in the north, straight-through traffic in the east, and left-turning traffic in the south. When the V is 30 km/h, the area within 12 meters after the crossing is a hot spot in all studied cases (Fig. 3.18). When the V is 40 km/h, the area within 18 meters after the crossing is a significant hot spot in all scenarios (Fig. 3.19). Less than 25% of cases are hot spots at the segment 30 meters away from the stop line.

When the V is 50 km/h, the area within 18 meters after the crossing is a significant hot spot in all scenarios as well (Fig. 3.20). However, more than 75% of cases are hot spots at the segment 30 meters away from the stop line.

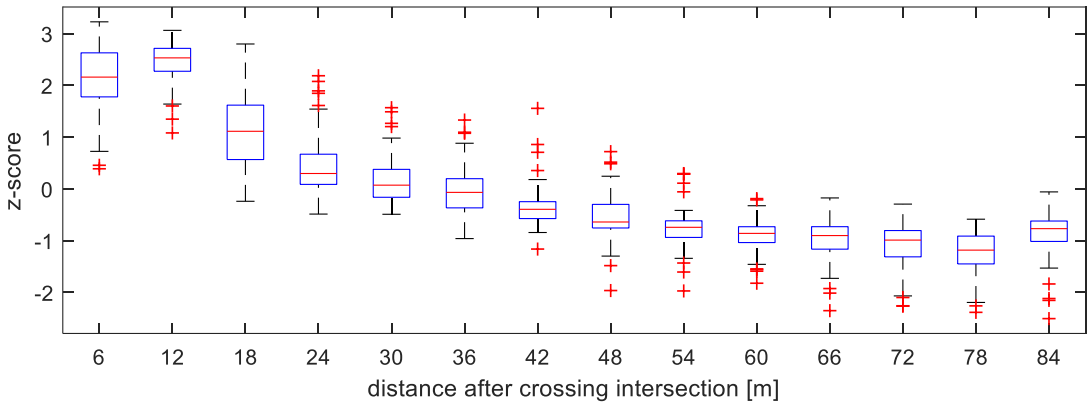

Fig. 3.18 Z-score after crossing the intersection when the speed limit is 30 km/h

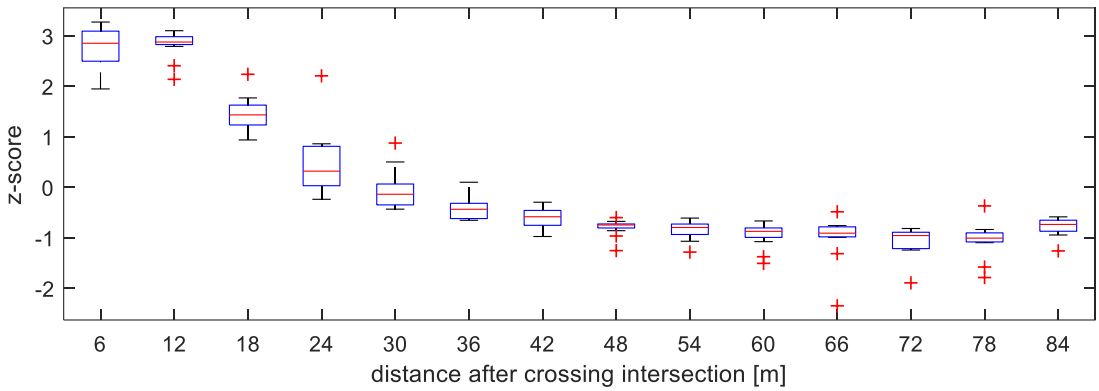

Fig. 3.19 Z-score after crossing the intersection when the speed limit is 40 km/h

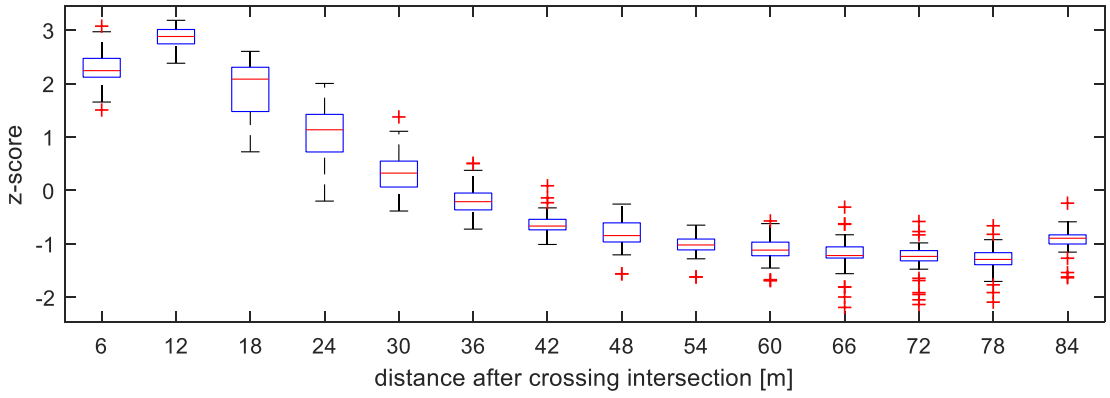

Fig. 3.20 Z-score after crossing the intersection when the speed limit is 50 km/h

Discussion

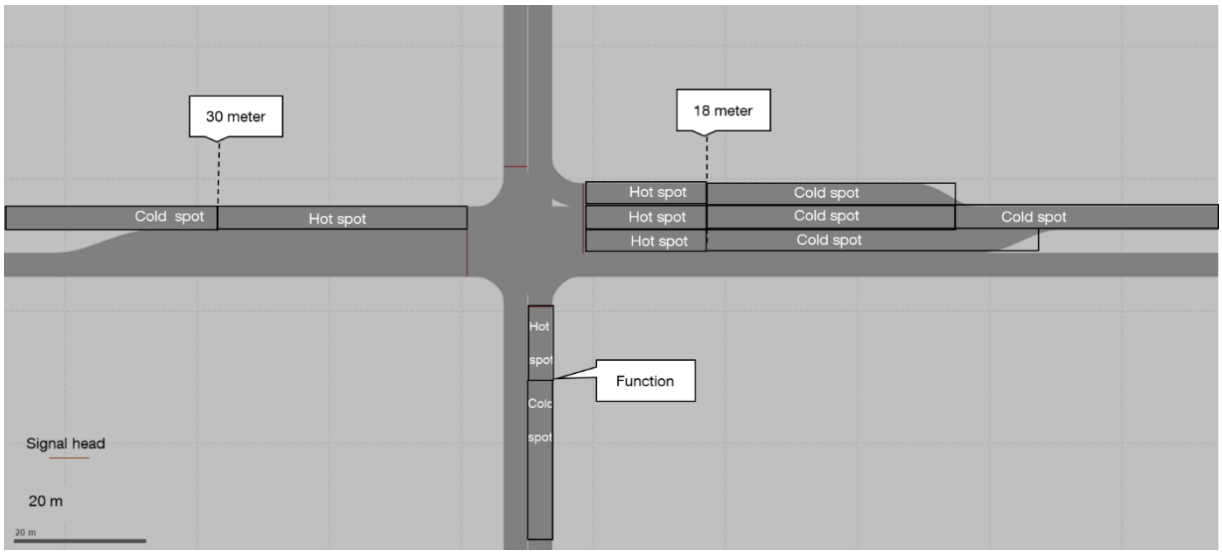

Fig. 3.21 Boundary between the hot and cold spot

The spatial division of each lane is shown in Fig. 3.21. The spatial pattern and the size of the high-emission area can be explained by the distribution of driving modes. The driving modes can be categorized as acceleration, deceleration, idling, and cruising. The emission factor during acceleration is the highest, while deceleration has the lowest emission factor. High-emission areas are located near the stop line, where significant accelerations occur. The area with the remaining section of the queue and before entering the queue has relatively low emissions since the major driving dynamics in this section consist of a mix of small accelerations at low speeds and decelerations, which have low emission factors.

For the east approach, the size of the high-emission area remains relatively constant in various traffic scenarios. The reason for this could be that while vehicles may switch lanes to enter the turning lane, these vehicles would decelerate or drive at a relatively slow speed. In this case, the average emission factor could be much lower than in the area near the stop line, where significant accelerations occur. For segments in which vehicles drive in different directions, the average emission factor on each segment does not differ significantly, because vehicles standing in queue accelerate only to low speeds on these sections while simultaneously interacting with lane switching vehicles.

For the south approach, the result shows that the truck percentage is not a statistically significant predictor to predict the size of the high-emission area. The right-turning ratio, traffic volume, and capacity have positive relations to the size of the hot spot, while cycle time and speed limit have negative relationships. When there is more right-turning traffic, the speed of vehicles leaving the stop line is lower. The slower speed results in a lower emission factor near the stop line. The cluster of relatively high-emission areas could, therefore, include smaller segments. When there is more traffic, there are more vehicles that queue during the red time and at the beginning of the green time. Therefore, areas in which acceleration occurs are more

extended, and the high-emission area is enlarged. When capacity is higher due to a higher green ratio, the percentage of vehicles that drive through without queueing is bigger. It reduces the difference in the average emission factor between segments, which results in enlarging the area of relatively high emissions. When the speed limit is higher, the distance of decelerating is longer. It leads to an increase in the size of the low-emission area. When the cycle time is longer, more vehicles may queue at the beginning of green time. Consequently, the percentage of vehicles in the acceleration mode near the stop line is significantly increased, which increases the size of the emission factor. Therefore, the cluster of high emission factors is relatively close to the stop line. It can be concluded that the size of the relatively high-emission area is not only dependent on queue length. Instead, its variance can be better estimated using the function of the turning ratio, traffic volume, capacity, cycle time, and speed limit.

On the downstream road, the average emission factor is higher after crossing the intersection than further downstream. It can be explained by the fact that vehicles may accelerate beyond the speed limit. There exists a trend that when the speed limit is higher, the size of the relatively high-emission area is larger. It is probably because vehicles need to drive a longer distance to reach the speed limit. When the speed limit is low, such as around 30 km/h, the area that is further away from the intersection features a hot spot. *S*ince the average emission factor is not significantly high, these areas are aggregated with surrounding low-emission areas as one cold spot. The boundary between high and low-emission areas on the downstream road is set at 30 meters after crossing the intersection.

3.4.3 Emission function

Based on the rules described in the previous chapter, four major types of segments are defined: the upper section of the lane, the segment near the stop line, the crossing, and the section after crossing the intersection. Each type of segment is further distinguished by lane type: straight-through lane, right-turning lane, left-turning lane, or mix-traffic lane. For each segment, the emission function needs to be examined. The optimized emission functions for the segments near the stop lines are described below. The emission functions for the rest of the segments can be found in Appendix.

Near stop line of the left-turning lane (Fig. 3.22)

- A bigger truck percentage can result in a higher emission factor of NO_x, and the effect size will be smaller when there exist stronger conflicting flow and bigger capacity. The emission factor of a truck is much higher than that of a passenger car during acceleration. When more vehicles stand in a queue, emissions differ more strongly between different truck percentages. When there exists stronger conflicting flow, the speed to which vehicles accelerate is decreased, which leads to a smaller difference in emissions between trucks and passenger cars.

- Capacity has a negative relation with the emission factor. Its absolute effect size is increased in the case of more trucks, bigger traffic volume, and larger conflicting volume.

- Traffic volume has a positive relationship with the emission factor, and the effect size is smaller when capacity is higher.

- Conflicting traffic volume has a negative relation with the emission factor. On the one hand, conflicting traffic causes a vehicle queueing before the stop line to accelerate to a lower speed. On the other hand, conflicting traffic causes vehicles without stopping to decelerate. The absolute effect size of the conflicting traffic volume is increased if the capacity and truck percentage are higher. If capacity is high, fewer vehicles will queue. They decelerate more strongly when facing the increased conflicting flow. This leads to lower emission factors. Moreover, the emission factors of trucks are more sensitive to their driving modes. Thus, a bigger truck percentage can lead to a bigger drop in the average emission factor when the vehicle fleet faces conflicting traffic.

- The speed limit has a negative relation with the emission factor. Vehicles decelerate more strongly in case of high driving speed, which can result in fewer emissions. The absolute size of the effect is larger in the case of a higher percentage of trucks.

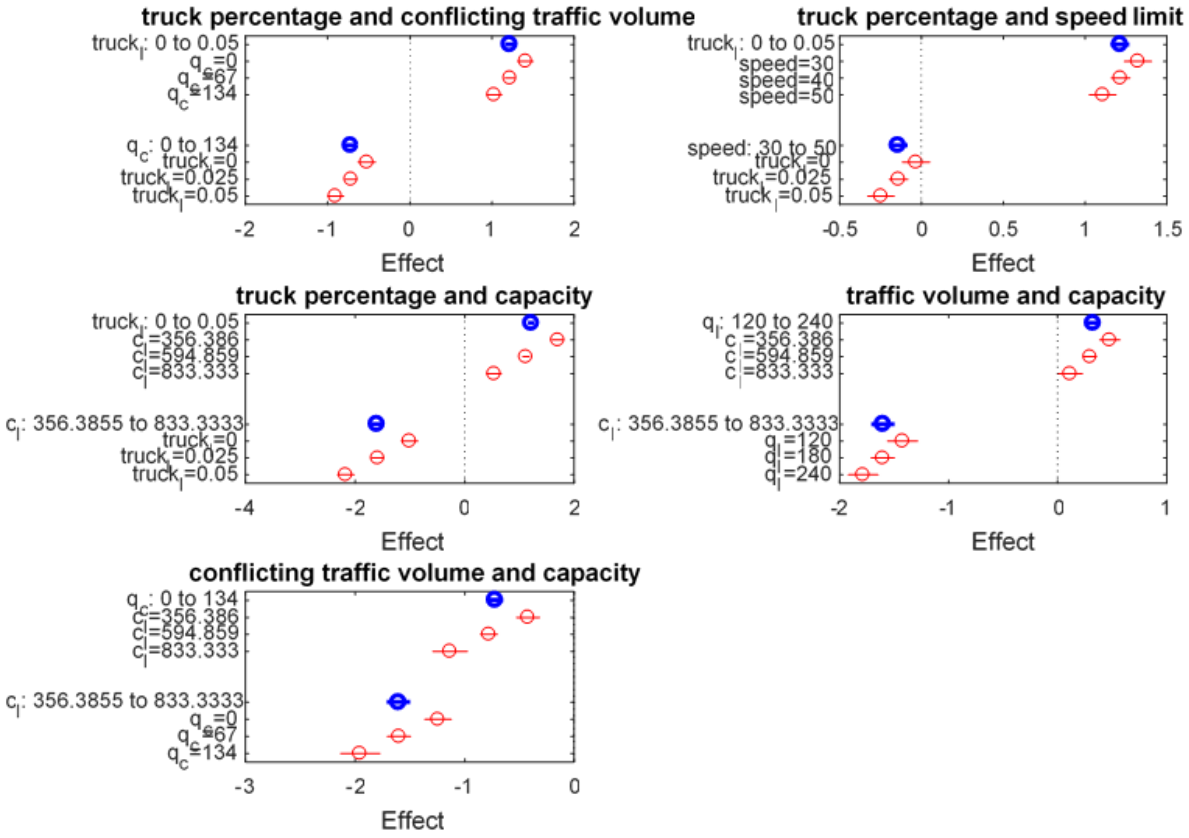

Fig. 3.22 Interaction effect near the stop line of the left-turning lane

Near the stop line on the straight-through lane

In Fig. 3.23, the interaction effects are shown.

- The truck percentage has a positive relation to the emission factor of NO_x. The effect size gets bigger when there is less traffic, bigger capacity, or lower average speed.
- The traffic volume has a positive relation to the emission factor of NO_x. The effect size gets bigger at a lower truck percentage, lower capacity, and higher average speed.
- With higher capacity, the emission factor of NO_x gets lower. The absolute effect size gets smaller with a higher truck percentage, less traffic, and a higher average speed.
- With a higher average speed, the emission factor of NO_x gets lower. The absolute effect size gets bigger when there is a higher truck percentage, less traffic, and lower capacity.

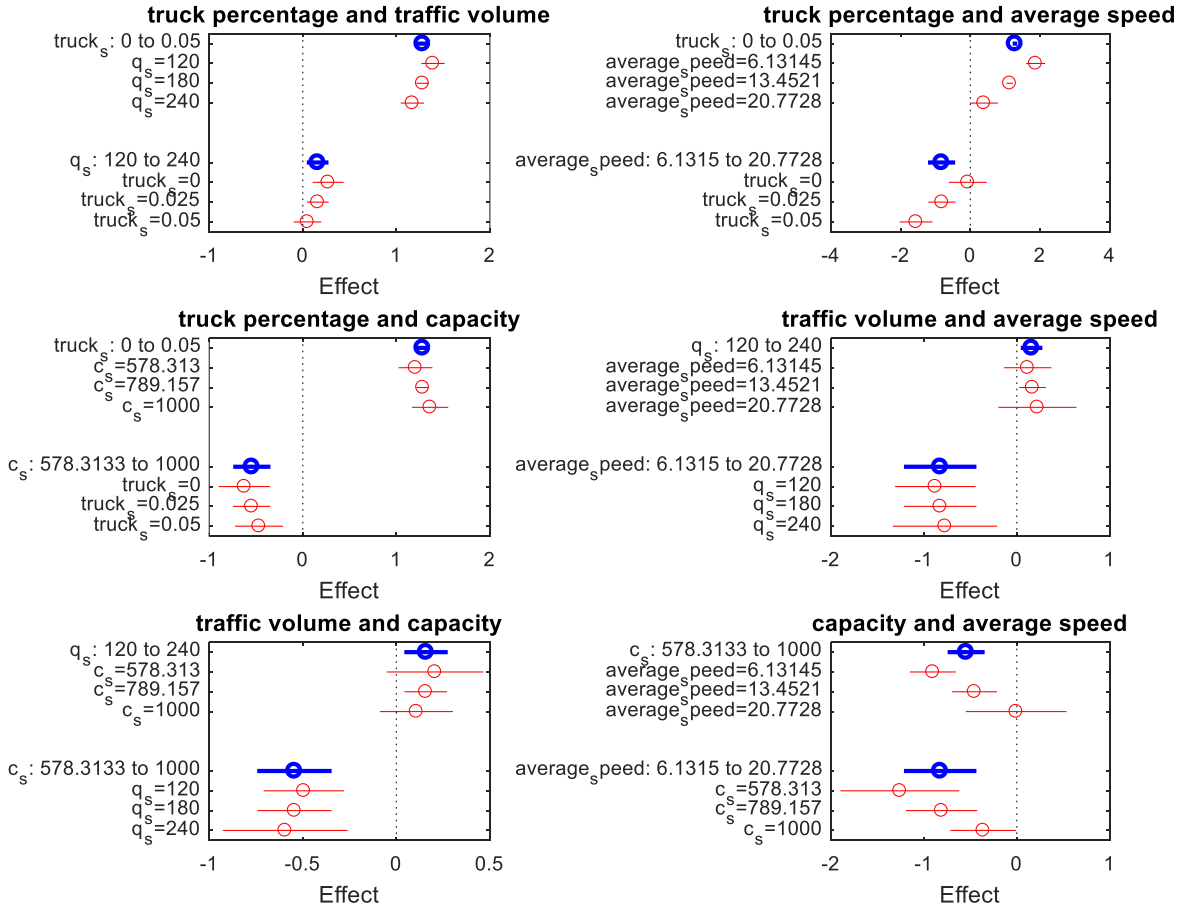

Fig. 3.23 Interaction effect near the stop line on the straight-through lane

Near the stop line on the mix-traffic lane

For the west approach with one lane, the right-turning ratio, traffic volume, truck percentage of right-turning traffic and straight-through traffic, capacity, cycle time, speed limit, and average speed are used as predictors. The multicollinearity test shows that there exists no obvious multicollinearity. The stepwise model is selected. The result is displayed in Fig. 3.24:

- The right-turning ratio has a negative relationship with the emission factor of NO_x. The absolute effect size increases with more trucks from either straight-through traffic or right-turning traffic and with higher capacity, while it decreases at a higher speed limit.
- The truck percentage has a positive effect on the emission factor of NO_x. The effect size of the truck percentage in each direction is bigger when the ratio of the traffic volume in the corresponding direction is bigger.
- Capacity has a negative relation to the emission factor of NO_x. The absolute effect size of capacity on average emission factor decreases when the truck percentage of the right-turning traffic increases.
- Speed limit has a positive relation to the emission factor of NO_x when the right-turning ratio is smaller. The relationship turns negative when most traffic is right-turning.
- Average speed and cycle time have negative effects on the emission factor of NO_x.

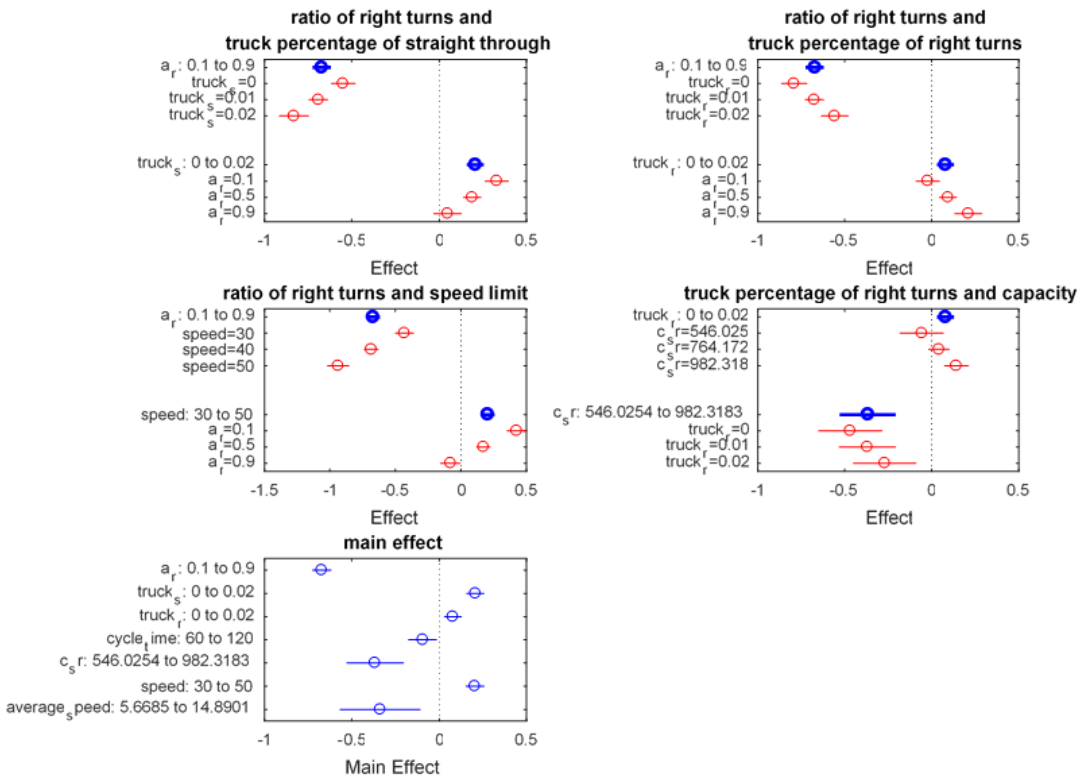

Fig. 3.24 Effect near the stop line on the lane with straight-through and right-turning traffic

3.5 Summary

The model development methodology is applied to two types of road approaches, namely one approach consisting of the straight-through lane, the right-turning lane, and the left-turning lane; another approach consisting of the lane with straight-through and right-turning traffic.

The spatial pattern and the size of the high-emission areas can be explained by the distribution of driving modes. High-emission areas are located near the stop line, where major accelerations occur. The area with the remaining part of the queue and before entering the queue has relatively low emissions since major driving dynamics in this area consist of a mix of small accelerations at lower speeds and decelerations. The size of the high-emission area on the separate lane remains relatively constant in various traffic scenarios. For the lane with the straight-through and right-turning traffic, the truck percentage is not a statistically significant predictor to estimate the size of the high-emission areas. The right-turning ratio, traffic volume, and capacity all have positive relations to the size of the hot spot, while cycle time and speed limit have a negative relation with the size of the hot spot. It is concluded that the size of the relatively high-emission area is not only dependent on queue length. Instead, it is suggested that its variance can be better estimated by using the function of the turning ratio, traffic volume, capacity, cycle time, and speed limit. On the road segment, after crossing the intersection, the average emission factor of NO_x (EF_NO_x) is higher in the area near the intersection than further downstream. The boundary between high and low-emission areas downstream is found at 30 meters after crossing the intersection.

The emission function is developed for each type of segment and summarized in Tab. 3.5. Lane type explains the differences between emission functions. The predictors interact with each other to influence the average emission factor. The effect signs of the factors depend on the segment type. The effect signs are explained by changes in driving modes.

Segment	Regression function
hot spot_sr	'EF_NO$_x$~1 +C +$\bar{v}$ + a_r*truck_s + a_r*truck_r + a_r*V + truck_r*c_sr'
cold spot_sr	'EF_NO$_x$~1 + truck_s + C + c_sr + a_r*truck_r + a_r*q_total + a_r*$\bar{v}$ '
hot spot_s	'EF_NO$_x$~1 + truck_s*q_s + truck_s*c_s + truck_s*$\bar{v}$ + q_s*c_s + q_s*$\bar{v}$ + c_s*$\bar{v}$'
cold spot_s	'log(EF_NO$_x$)~1 + truck_s + q_s + V + c_s'
hot spot_l	'EF_NO$_x$~1 + truck_l*q_c + truck_l*V + truck_l*c_l + q_l*c_l + q_c*c_l'
cold spot_l	'EF_NO$_x$~1 + truck_l*q_l + truck_l*V + truck_l*c_l + q_l*q_c + q_l*c_l + q_c*c_l'

cold spot_slr	'EF_NO_x~1 + truck_l*truck_s + truck_l*q_s + truck_l*q_l + truck_l*q_r + truck_l*V + truck_s*truck_r + truck_s*q_s + truck_s*q_l + truck_s*q_r + truck_s*V + truck_r*q_s + truck_r*q_l + truck_r*q_r + truck_r*V + q_s*q_l + q_s*q_r + q_l*q_r + q_l*$\bar{v}$ + q_r*$\bar{v}$'
crossing_s_sr	'EF_NO_x~1 + a_s + truck_s + c_sr + V + C*q_total'
crossing_s_s	'EF_NO_x~1 + truck_s*V + truck_s*c_s + q_s*V + V*c_s'
hot spot_after crossing	'EF_NO_x~1 + truck_es + truck_sl*c_e + truck_sl*q_sl + truck_sl*q_nr + truck_nr*q_es + truck_nr*V + C*$\bar{v}$ + C*q_sl + q_es*V + q_es*$\bar{v}$ + V*$\bar{v}$+ V*q_sl + V*q_nr + c_e*$\bar{v}$ + c_e*q_nr + q_sl*q_nr'

Tab. 3.5 Emission function of each segment

4. Model test

The goal of the study is to develop an emission model that is comparable to the microscopic emission estimation framework. The model is used to compare traffic measures in terms of emission impact. Accordingly, the level of emission change resulting from each traffic measure should be accurately estimated. Rerouting is a traffic management strategy to reduce traffic congestions. As an example, the effect of rerouting on NO_x is tested to assess the performance of the developed model. The test scenario refers to the application of the emission model concept for assessing the routing effect drafted in Fig. 3.6. Two scenarios are created, namely a basic scenario, and a rerouting scenario. In each scenario, the estimated emission factor of NO_x by the development model is compared with the results of PHEM and HBEFA. The absolute changes of the emission factors of NO_x after rerouting are compared between these models to study the sensitivity of each model to rerouting.

4.1 Methods to test

The rules of the spatial division of different lane types and the emission function for each segment are tested. The result of the spatial division is compared with the result from the Local G* method. The estimated emission factor is compared with the result of PHEM and HBEFA. The models are evaluated at various spatial resolutions, namely the segment-level, the lane-level, the approach-level, and the stream-level. The division of segments is carried out according to the spatial division rules in Fig. 3.21. The lane-level refers to each lane before the stop line. The approach-level includes all lanes on which vehicles drive in the same direction to arrive at the stop line. The stream-level includes all lanes running in one direction, from upstream to downstream.

HBEFA is developed based on PHEM (Hausberger et al., 2009). HBEFA is a typical traffic situation-based emission model. The traffic situation is defined by the combination of road type, speed limit, and level of service. The level of service is defined by average speed. In each traffic situation, the average emission factor is assigned for each type of vehicle category. It is based on fleet composition for the years 1990-2030 in different countries, including Germany, Austria, Switzerland, Sweden, Norway, and France. HBEFA 3.3 is the newest version released in 2017. It includes an update of NO_x emissions of newer diesel passenger cars, especially updates of hot emission factors of NO_x of diesel passenger cars of the types Euro-4, Euro-5, and Euro-6 based on new measurements from laboratories, real-world measurements as well as remote sensing data. The detailed description can be found in the reports (Hausberger et al., 2009; Keller, Hausberger, Matzer, Wüthrich, & Notter, 2017). HBEFA is commonly used to estimate street-level emissions.

4.2 Test scenario

The intersection of interest is intersection 3 (Fig. 4.1). The tested intersection has four arms (Fig. 4.2). The east approach consists of three types of lanes: one lane with straight–through and right-turning traffic (sr), straight-through lane(s), and a left-turning lane (l). The cycle length of the signal is 90 seconds, and the speed limit is set at 30 km/h. The setting for each test lane is summarized in Tab. 4.1. The left-turning lane in the east has a length of approximately 60 meters. The investigated length of each lane before the stop line is the same as the length for the model developed in the previous chapter. In the rerouting scenario seen in Tab. 4.2, half of the traffic driving from the east approach of intersection 1 to the west approach of intersection 4 by crossing intersection 3, is rerouted onto lane 1.

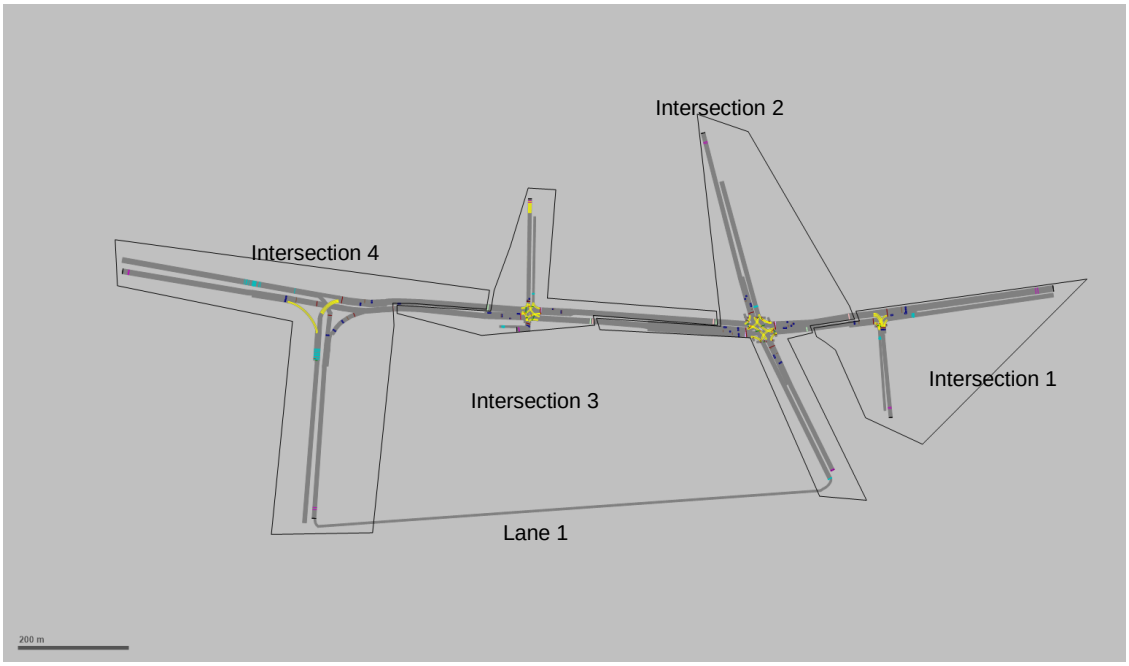

Fig. 4.1 Road network

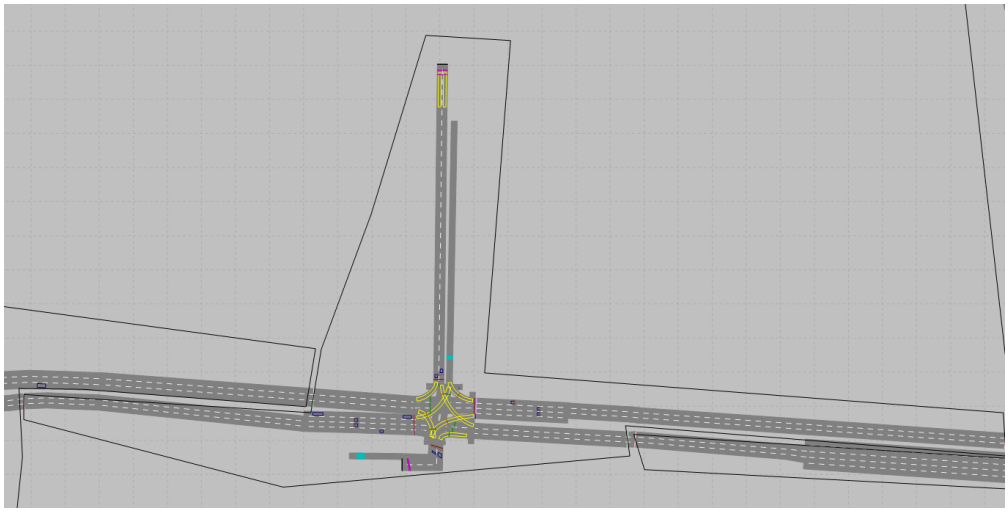

Fig. 4.2 Intersection 3 which is to be evaluated

lane	C [s]	green ratio	q [km/h]	turning ratio	truck percentage of turning traffic	truck percentage of straight-through traffic
east_sr	90	0.36	419	0.11	0.02	0.05
east_s	90	0.36	539	0.00	0.00	0.08
east_l	90	0.53	42	1.00	0.00	0.00
north_r	90	0.18	53	1.00	0.02	0.00

Tab. 4.1 Setting of each lane in the basic scenario

4.3 Test results

This subchapter describes the results of the predicted boundaries between the high-emission and the low-emission areas, and the estimated average emission factors in the basic as well as the rerouting scenarios. The predicted boundary is compared with the result from the Local G* method. The performance of the developed model for the average emission factor is evaluated by comparing it with PHEM and HBEFA. Changes in the average emission factor due to rerouting are compared between the developed model and PHEM and HBEFA.

4.3.1 The boundary between high- and low-emission area

The results of spatial division are summarized in Tab. 4.3. Before crossing the stop line on the lane with straight-through and right-turning traffic, the predicted high-emission area has the same size as the area identified by the local G_i* method (see in Fig. 4.3). The predicted high-

emission areas on the straight-through lane and after crossing the intersection fall within the area estimated by the local G_i*. In Fig. 4.4, the Z-score is slightly higher than 0 on the segment around 18-24 meters away from the stop line. It can be concluded that the predicted model can identify the significant high-emission area on the straight-through lane. The predicted high-emission area is smaller than that resulting from the Local G_i*. The predicted high-emission area on the left-turning lane covers the same area as the local G_i*. As Fig. 4.5 shows, the significant high-emission area of the left-turning lane is between 6 and 12 meters away from the stop line. The area closest to the stop line shows lower emissions than the remaining area of the segment. It could be explained by the slower acceleration due to conflicting traffic flow from the opposite direction.

Fig. 4.3 shows that the size of the high-emission area is smaller in the rerouting scenario on the lane with straight-through traffic and right turns. Since the straight-through traffic is less, there is less traffic that accelerates. Consequently, the size of the high-emission area is smaller.

Fig. 4.4 shows that there is no change in the size of the high-emission area on the straight-through lane in the rerouting scenario. However, the Z-score is slightly lower in the high-emission area, while it is slightly higher in the low-emission area. The lower traffic volume in the rerouting scenario makes fewer vehicles in the queue. Thus, the acceleration-related emissions are lower. Since there are fewer vehicles that decelerate in the low-emission area, the emissions are higher.

Fig. 4.5 shows that the positive Z-score is slightly higher in the rerouting scenario on the left-turning lane. Vehicles drive at slower speeds before the stop line. The average emission factor of NO_x is bigger at a higher speed. Left-turning vehicles drive at a higher speed due to the reduction in straight-through traffic, leading to a slightly higher average emission factor.

Fig. 4.6 shows that the high-emission area after the crossing is smaller due to the rerouting. It is because traffic volume is smaller in the rerouting scenario, allowing vehicles to accelerate faster to reach the speed limit.

To summarize, the developed model can accurately estimate the location of the high-emission area on the lane with mixed straight-through and right-turning traffic, as well as on the straight-through lane. It overestimates the size of the high-emission area on the left-turning lane, while it underestimates the size of the high-emission area after crossing the intersection. A dynamic prediction model is developed to estimate the size of high-emission areas for both lanes.

Lane	Basic scenario		Rerouting scenario	
	Local G_i* [m]	Predicted [m]	Local G_i* [m]	Predicted [m]
sr	48	48	42	42

s	24	18	24	18
l	12	18	12	18
After crossing	54	30	48	30

Tab. 4.3 Boundaries between hot and cold spots

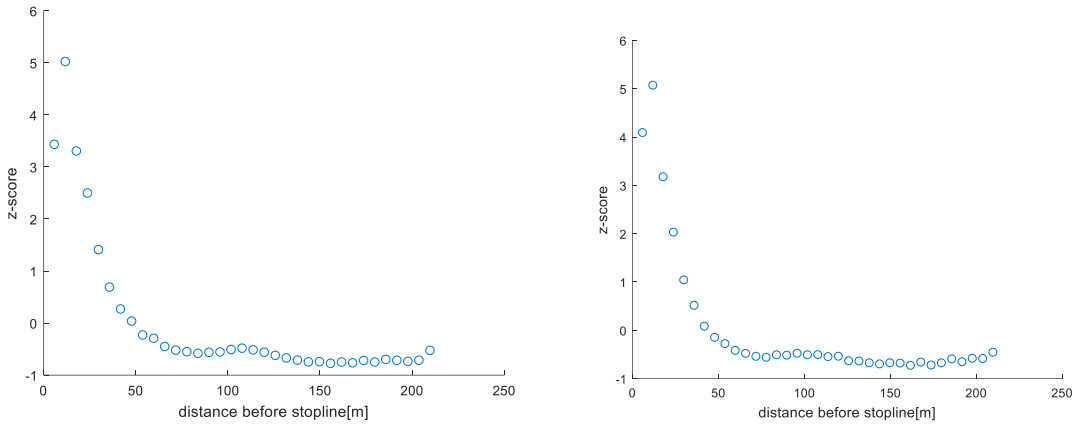

Fig. 4.3 Results of the local G_i^* for the lane with both straight-through and right-turning traffic in the – basic scenario (left) and in the rerouting scenario (right)

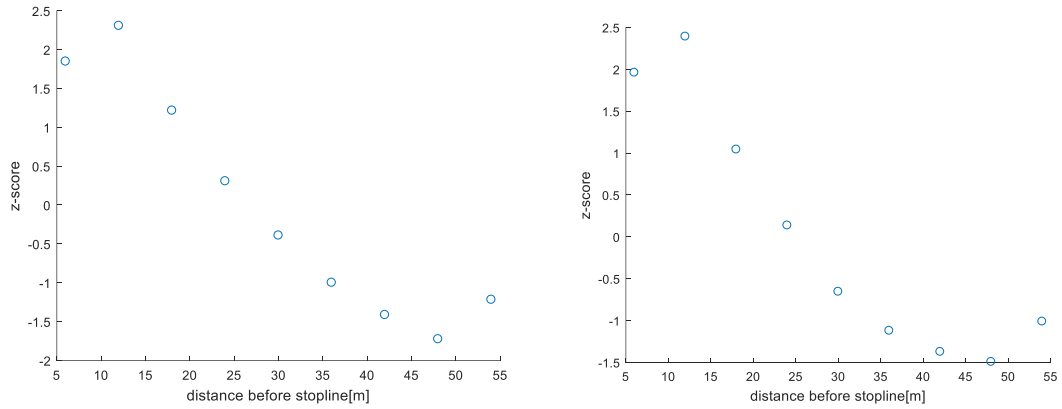

Fig. 4.4 Results of the local G_i^* for the straight-through lane in the basic scenario (left) and the – rerouting scenario (right)

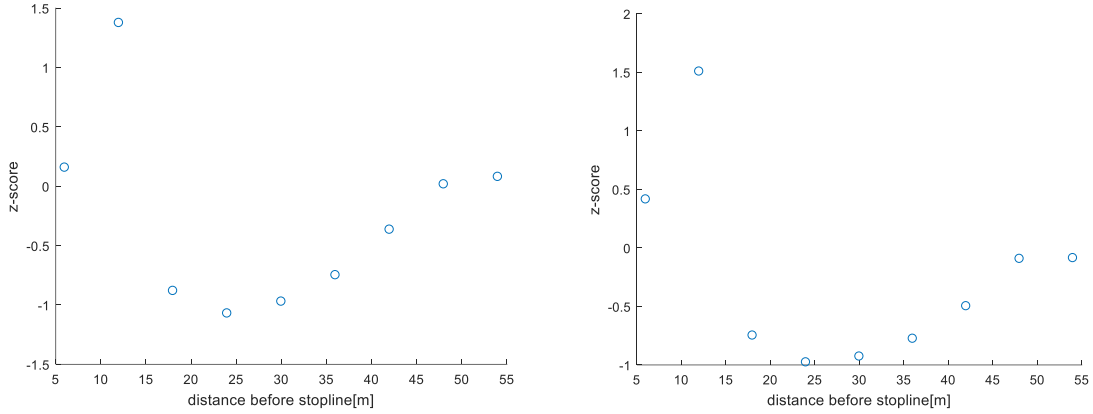

Fig. 4.5 Results of the local G_i^* for the left-turning lane in the basic scenario (left) and the rerouting – scenario (right)

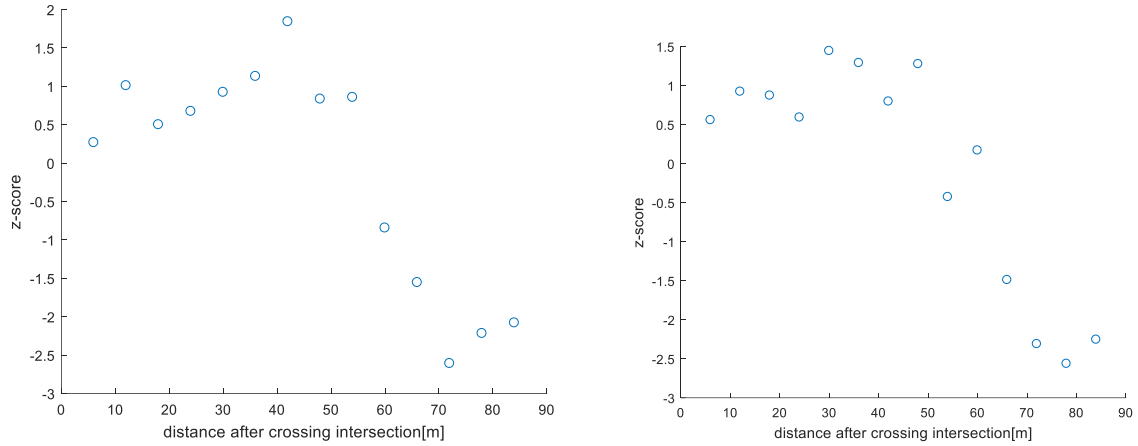

Fig. 4.6 Results of the local G_i^* for the lanes after crossing the intersection in the basic scenario (left) – and the rerouting scenario (right)

4.3.2 The emission factor of NO_x

The PE (percentage error) indicates the difference between the emission factor of NO_x predicted by the developed model or HBEFA and the one predicted by PHEM. The comparisons are made at different spatial resolutions.

$$\mathrm{PE} = \frac{\left| EF_{NOx_{PHEM}} - EF_{NOx_{Predicted}} \right|}{EF_{NOx_{PHEM}}}$$

Equation 13

$EF_{NOx_{PHEM}}$ is the average emission factor of NO_x estimated by PHEM.

$EF_{NOx_{Predicted}}$ is the average emission factor of NO_x by the developed model in the research or by HBEFA.

Segment-level

Fig. 4.7, and Fig. 4.8 show the PE at the segment-level. For the hot spot on each lane, the PE of the emission factor of NO_x predicted by the developed model is below 30%, while the PE of HEBFA is above 50%. At the hot spots on the lane with straight-through and right-turning traffic, the straight-through lane as well as at the after-crossing lane, the emission factor of NO_x is overestimated by between 10% and 18% by the developed model, while the emission factor of NO_x of the hot spot on the left–turning lane is nearly 30% underestimated. The high deviation on the left-turning lane may be attributed to the radius of the crossing. Since the left-turning lane has a bigger turning radius than the intersection for model development, the speed near the stop line is higher. Higher speed can result in a higher emission factor of NO_x. HBEFA underestimates emission factors of NO_x at hot spots on all lanes.

At the cold spots on the lane with the straight-through and right-turning traffic as well as on the straight-through lane, the emission factors of NO_x predicted by the developed model are 13-36% bigger than that predicted by PHEM. The difference could be due to lane switching between these lanes. Some vehicles may switch lanes only when approaching the stop line. The emissions of these vehicles are then only partly emitted on each of these lanes. The emission function in Tab. 3.5 shows that traffic volume has a positive effect on the average emission factor. As a result, the average emission factor is overestimated. The prediction of HBEFA is 12-16% bigger than that of PHEM on the lane with the straight-through and right-turning traffic, while it is 17-30% smaller on the straight-through lane.

For the cold spots on the left-turning lane and the section with both straight-through and left-turning traffic, the emission factors of NO_x predicted by the developed model are 7-33% smaller than that predicted by PHEM. The underestimations of the emission factors of NO_x on segments with straight-through and left-turning traffic can be due to the same reason as the overestimation on the adjacent lanes. The underestimations of the emission factors of NO_x on the left-turning lanes may also be caused by the size of the turning radius. The prediction by HBEFA on the left-turn lane is 11-25% smaller than that by PHEM, while it is 24% higher on the section with both straight-through and left-turning traffic. These differences can be explained by the fact that HBEFA does not consider acceleration occurring at the cold spots of the left-turning lane and does not take into account deceleration on the upper section.

For the straight-crossing traffic from the lane with both straight-through and right-turning traffic as well as from the straight-through lane, the developed model leads to highly overestimated values. It could be due to the length of the crossing section. Since the length of the crossing is bigger than that of the intersection chosen for model development, the average speed at the crossing is higher. While crossing, the acceleration rate is relatively low, and the average emission factor decreases as the average speed increases. It indicates that average speed or crossing length can be added to the emission function. The HBEFA underestimates NO_x by 34% compared to PHEM for traffic from the straight-through lane. The underestimation may be linked to the fact that HBEFA does not sufficiently account for the acceleration effect.

It can be concluded that the developed model performs better for all the hot spots, the upper section featuring both straight-through and left-turning traffic and for the section after crossing, while HBEFA performs better for cold spots on the left-turning lane, for the lane with both straight-through and right-turn traffic, and the lane with straight-crossing traffic from both straight-through and right-turning traffic.

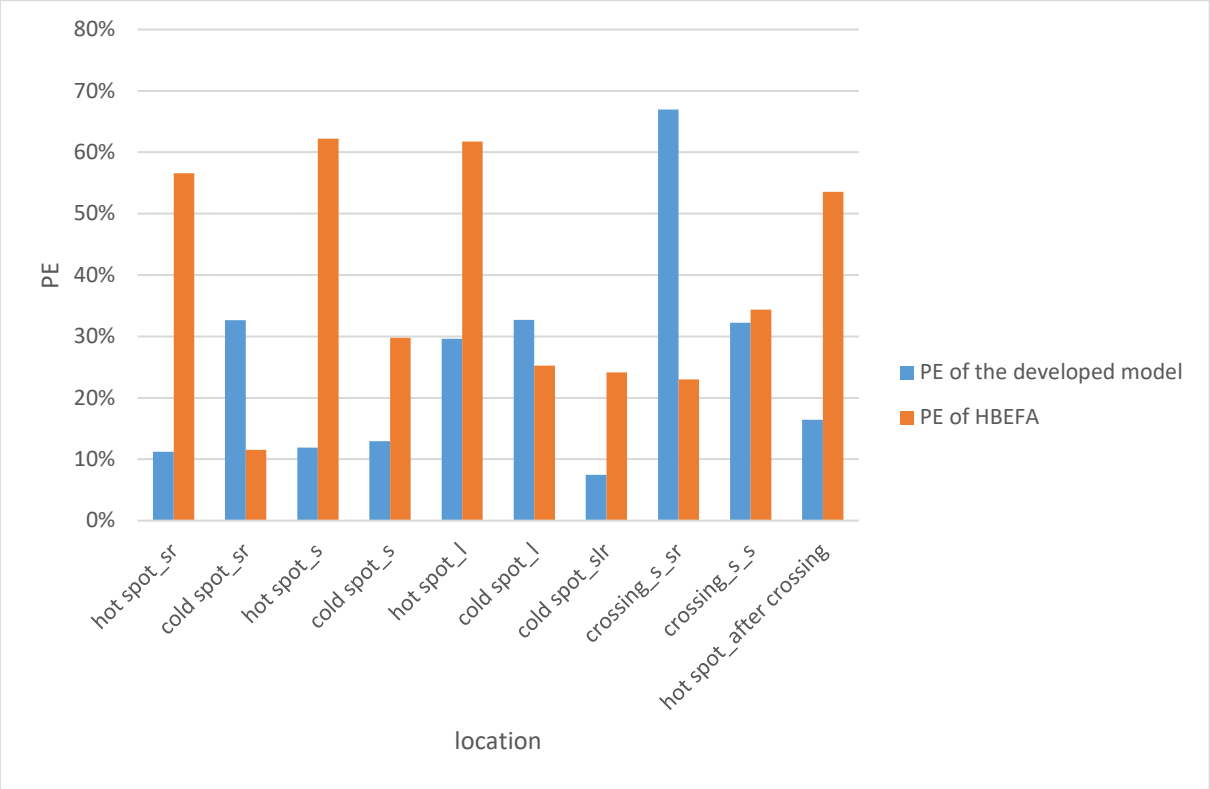

Fig. 4.7 PE of the developed model and HBEFA compared to PHEM in the basic scenario

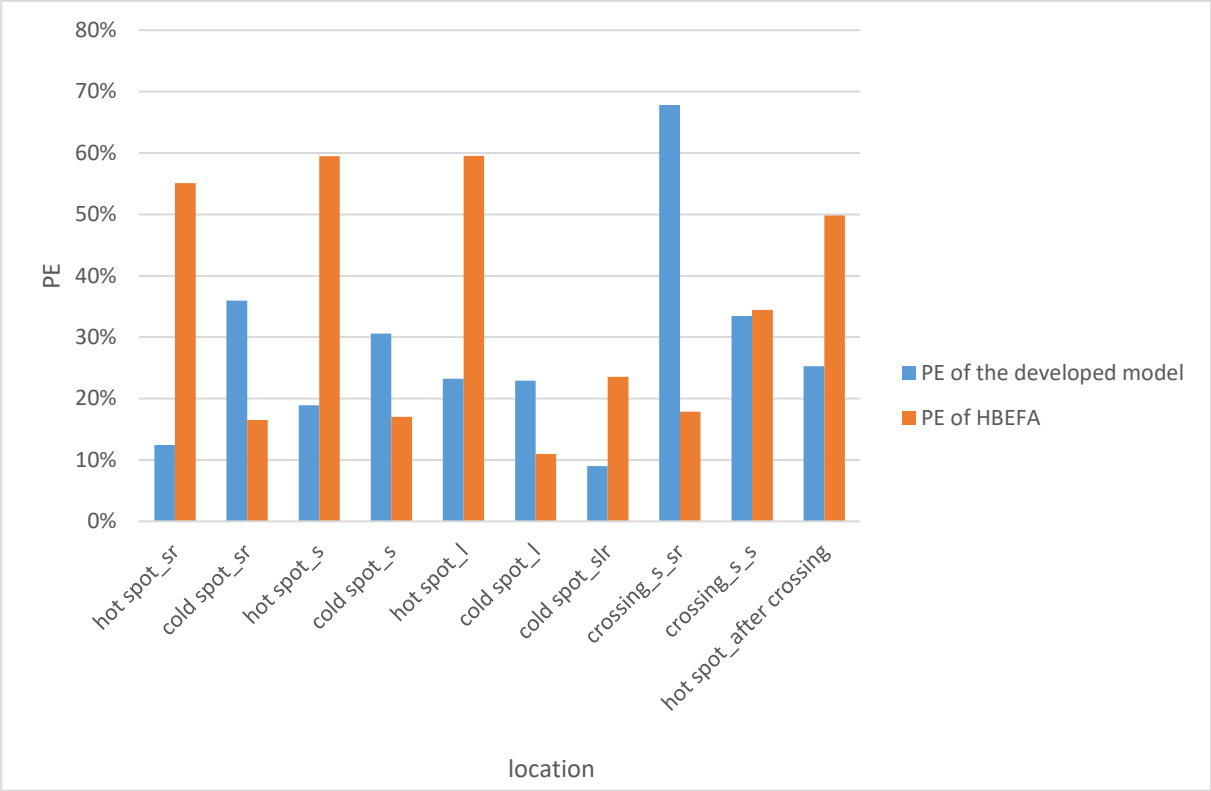

Fig. 4.8 PE of the developed model and HBEFA compared to PHEM in the rerouting scenario

Lane-, approach- and stream-level

Fig. 4.9, and Fig. 4.10 show the PE of the emission factor of NO_x for the aggregated segment. Before the stop line of the lane with the straight-through and the left-turning traffic, and the lane with both straight-through and right-turning traffic, the emission factors of NO_x estimated by the developed model are 0.5-19% bigger than that predicted by PHEM, while 6%-34% lower than that predicted by HBEFA. Before the stop line of the left-turning lane, the emission factors of NO_x estimated by the developed model are 21-30% lower than that estimated by PHEM and 31-41% lower than that by HBEFA. For the east approach, the PE of the developed model is less than 3%, while the PE of HBEFA ranges from 16% to 21%. The estimations of the developed model are 40% higher than that by PHEM for the straight crossing from the east approach, while HBEFA estimates 31-32% lower than by PHEM. For the stream from east to west, which includes traffic from the east approach, the straight-crossing lane, and the hot spot after crossing, the estimations by the developed model were 13-17% higher than those by PHEM while 16-17% lower than results by HBEFA.

Except for the straight-crossing lane, the emission factor of NO_x estimated by the developed model is much closer to that estimated by PHEM than that predicted by HBEFA, both at lane-level and approach-level. The developed model overestimates stream emissions mainly because of the error in the estimation for the straight-crossing lane. HBEFA underestimates

stream emissions since it underestimates the emissions from hot spots. The developed model and HBEFA have a similar absolute value of differences from PHEM in stream emissions.

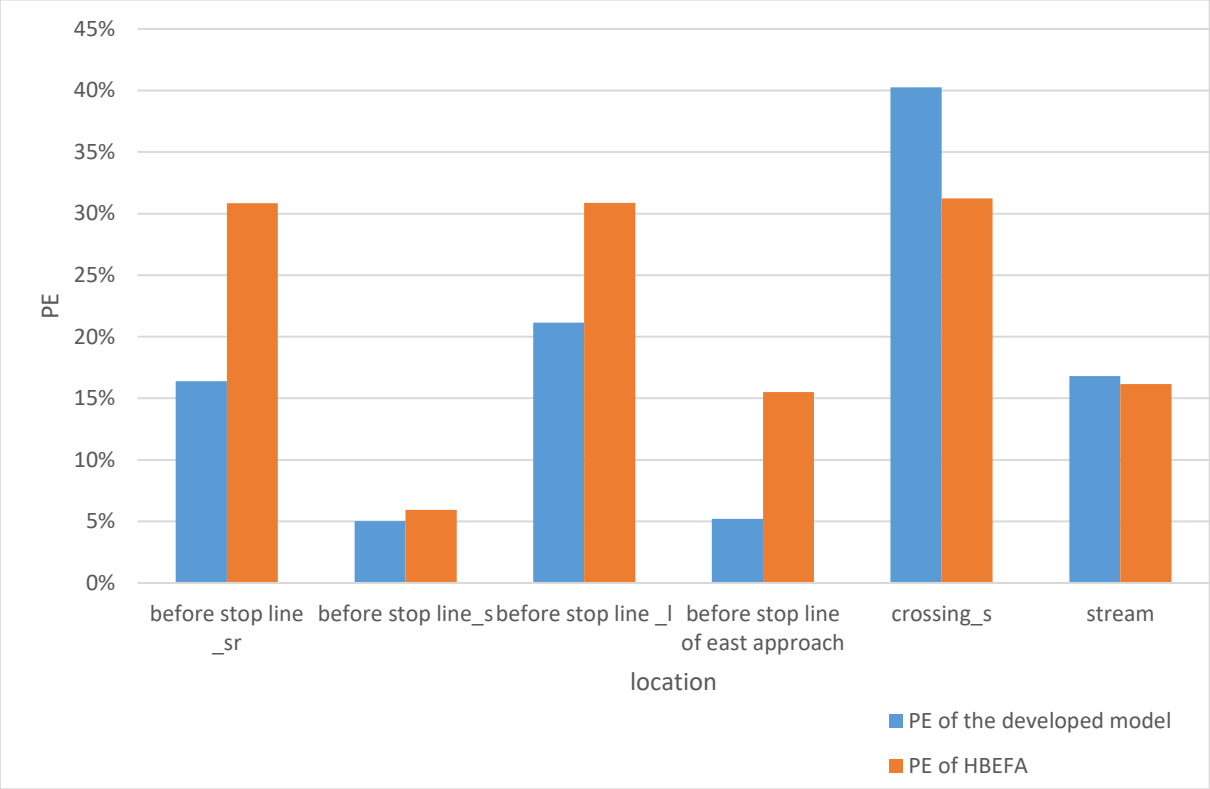

Fig. 4.9 PE of the developed model and HBEFA compared to PHEM for aggregated segments in – the basic scenario

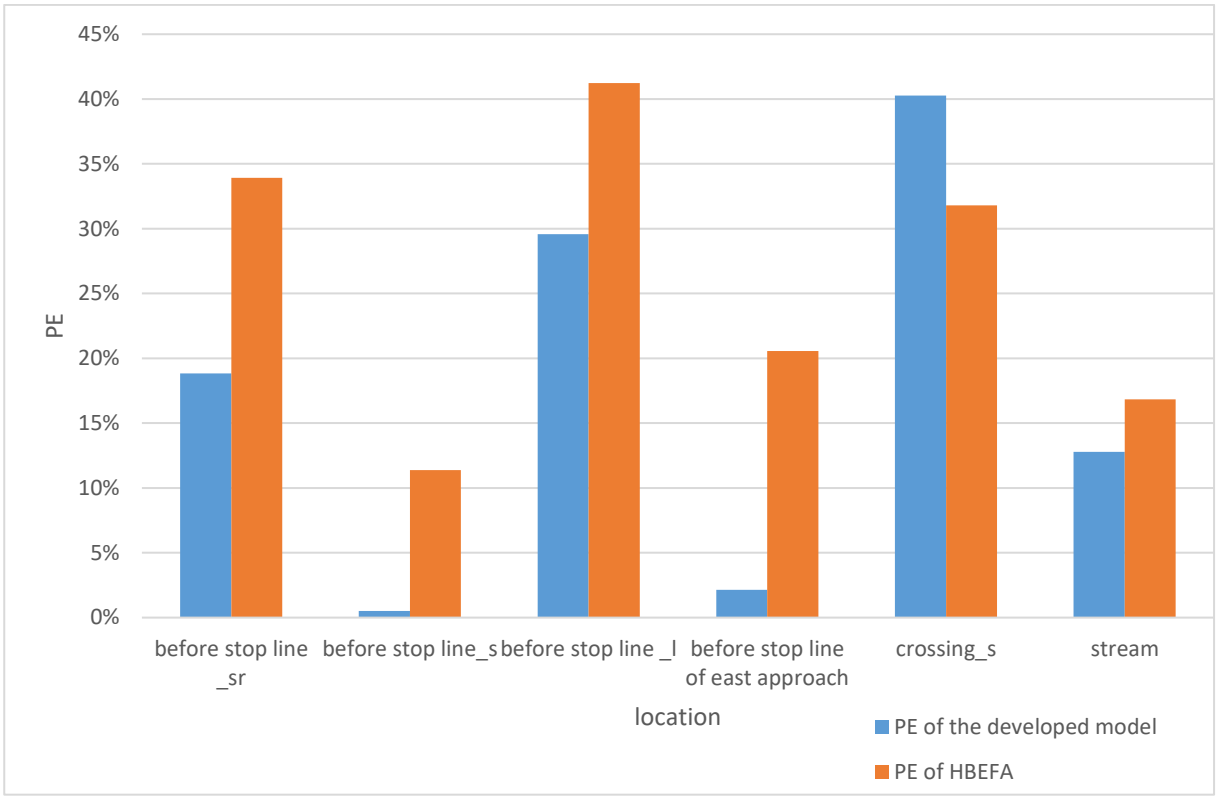

Fig. 4.10 PE of the developed model and HBEFA compared to PHEM for aggregated segments in – the rerouting scenario

The routing effects

After rerouting, the NO_x factors are decreased in all studied segments. Fig. 4.11 shows the changes in the emission factor of NO_x on each segment estimated by PHEM, the developed model, and HBEFA. The estimated changes by the developed model on the segments of the lane with straight-through and right-turning traffic, as well as on the straight-crossing from the straight-through lane, are nearly the same as the ones estimated by PHEM. The developed model is less sensitive to rerouting than PHEM on the segments of the straight-through lane, the left-turning lane, and after crossing. For the straight-crossing from the lane with straight-through and right-turning traffic, and the upper section with straight-through and left-turning traffic, the changes estimated by the developed model are higher than those predicted by PHEM. At the segment-level, HBEFA is much less sensitive to rerouting than PHEM. The developed model performs much better than HBEFA for estimating changes in the emission factors of NO_x on all the studied segments.

Fig. 4.12 shows the estimated changes in the emission factors of NO_x due to rerouting on aggregated segments. On the lane with straight-through and right-turning traffic, the change estimated by the developed model is higher than that predicted by PHEM, while on the straight-through lane with a short left-turning lane, the change estimated by the developed model is lower than that estimated by PHEM. For the east approach, the changes estimated by the developed model are lower, while they are higher on the straight-crossing lane. In the cases

above, HBEFA yields smaller estimated changes than PHEM. The estimation of emission changes by HBEFA is more accurate at the stream-level than at the lane- and approach-level. At the lane- and approach-level, the developed model can much more accurately estimate changes in the emission factors of NO_x than either PHEM or HBEFA. At the stream-level, HBEFA performs slightly better. HEBFA underestimates the changes by 10% while the developed emission model underestimates the changes by 14%.

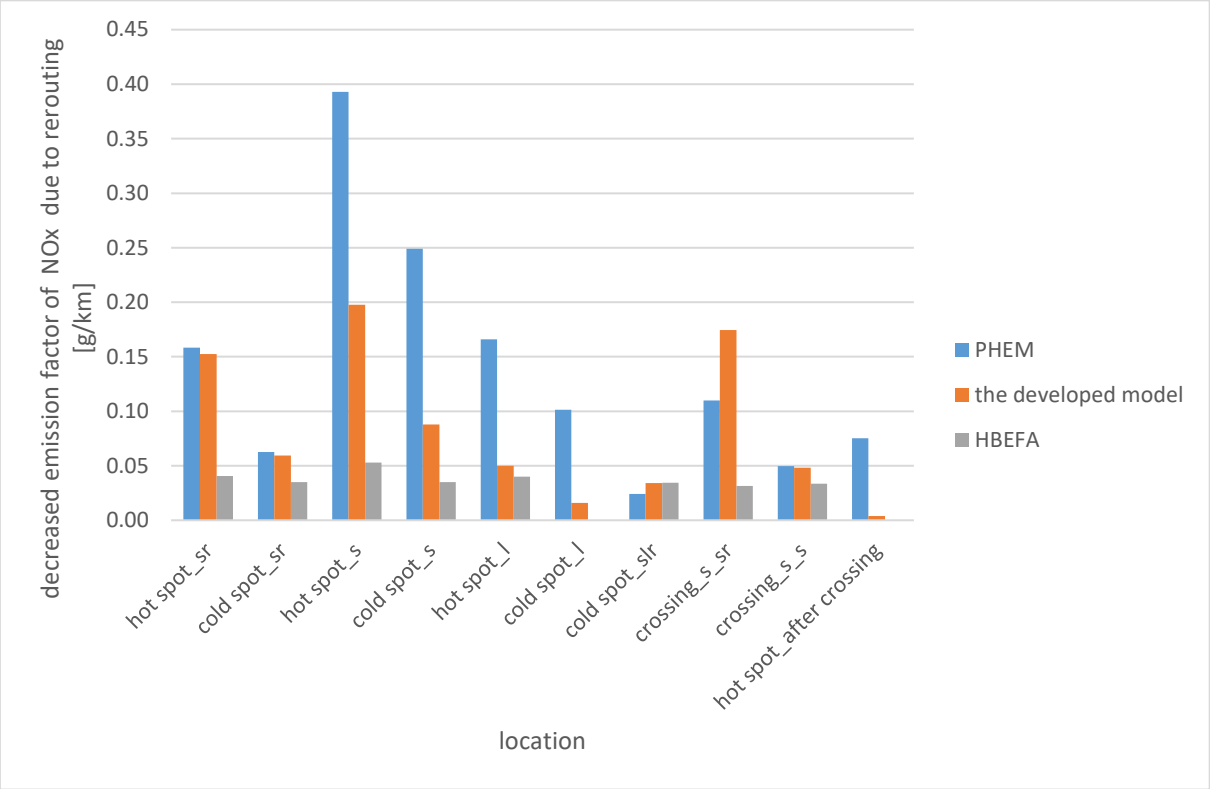

Fig. 4.11 Prediction of the emission changes due to rerouting for each segment

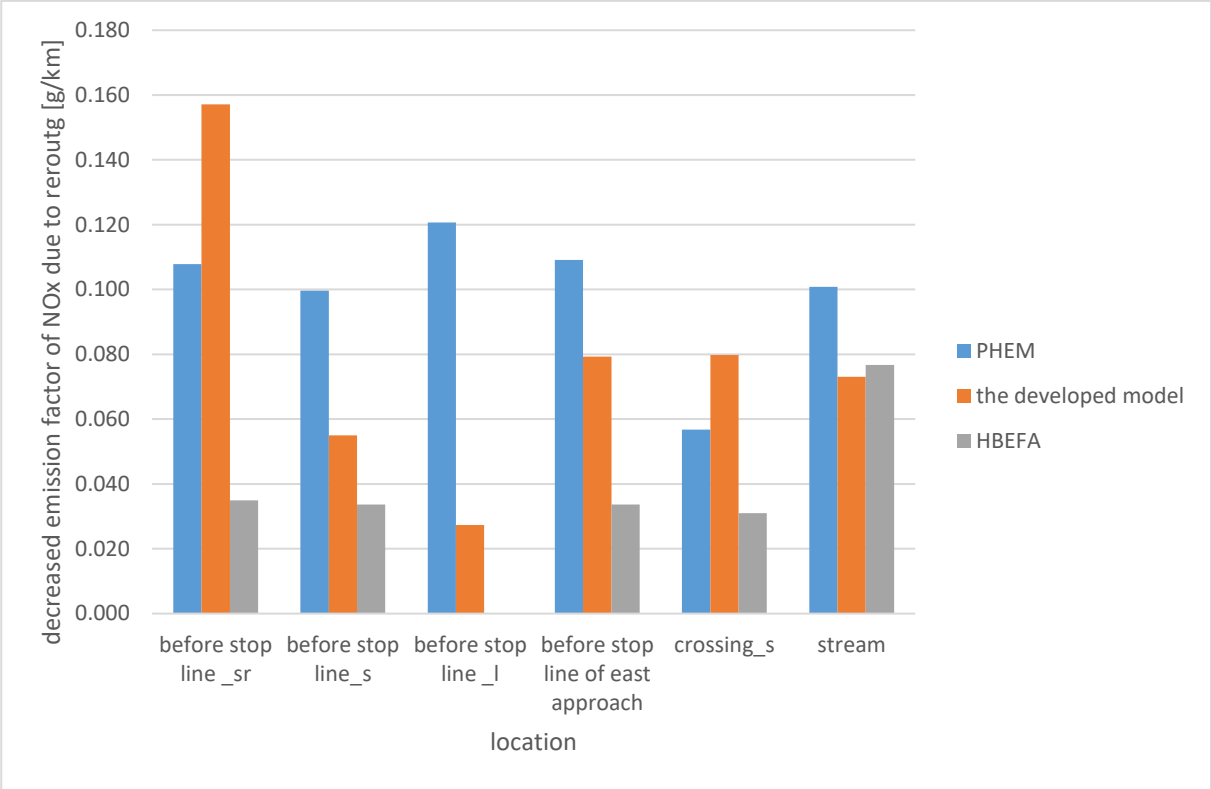

Fig. 4.12 Prediction of the emission changes due to rerouting for aggregated segments

4.4 Summary

The results show that the developed model can identify emission hot spots on each type of lane. The HBEFA emission model underestimates the emissions of hot spots. It leads to the underestimation of emissions at the lane-, approach-, and stream-level. The developed emission model performs much better than HBEFA in the estimation of emissions from hot spots, lanes before the stop line, and at the approach-level. The performance of the developed model closely resembles that of PHEM at the approach-level. The developed model and HBEFA have similar absolute differences in stream emissions compared to PHEM. The developed emission model yields much better performance on the estimation of the rerouting effect than HBEFA at the segment-, lane- and approach-level. HBEFA produces slightly better estimates of stream emissions than the developed model. Although the developed emission model is sensitive to the rerouting effect, the accuracy of emission estimations at the segment- and lane-level needs to be improved. The results indicate that the accuracy of the estimation of traffic volume on a road segment is essential to obtain a reasonable estimation of segment or lane emissions, especially for multi-lanes where drivers switch between lanes. The emission function for left-turning traffic can be further refined by accounting for the turning radius. For increasing the model's accuracy in estimating emissions crossing an intersection, the intersection geometry is suggested to be considered by adding geometry or average speed as additional predictors. To further improve the estimation of the segment's size after crossing, it

is suggested to develop a regression function instead of a fixed size. These improvements would also help close the gap to PHEM in the estimation of changes in stream emissions.

5. Application to estimate the immissions

Air pollutants emitted from vehicles will disperse to other places. A literature review conducted by Ahmad et al. (2005) summarized the factors influencing the dispersion in urban street canyons and intersections based on existing wind tunnel studies. These factors include turbulence caused by moving traffic, building geometry (such as aspect ratio and roof shape), street dimension, and approaching wind directions (Ahmad et al., 2005). Humans, especially pedestrians and cyclists on or near roads, are exposed to immissions (ambient air pollutions). Street canyons are streets lined by buildings on both sides. Air pollutants concentrate mostly within street canyons, as proven by measurements conducted in European cities (European Environment Agency (EEA), 2015; M. Rzeszutek & Szulecka, 2016; Mateusz Rzeszutek et al., 2019). Thus, estimating the exposure of humans to pollutants and improving air quality in street canyons are essential steps for protecting human health. The emission results from the developed mesoscopic traffic emission model need to be integrated into a dispersion model to evaluate how the ITS can influence the immissions.

Many dispersion models have been developed to represent the dispersion process. Vardoulakis et al. (2003) listed common dispersion models and suggested using a semi-empirical model for traffic planning and CFD for identifying specific locations on a street where air quality needs to be monitored. The authors also addressed the importance of accuracy of inputs like emission factors and the importance of validation of dispersion models (Vardoulakis et al., 2003). Lateb et al. (2016) further summarized the advantages and limitations of different types of dispersion models. The main types of dispersion models suitable for street canyons are semi-empirical models and computational fluid dynamics (CFD) models.

Semi-empirical models are parameterized models based on Gaussian dispersion. They are widely used to model dispersion in urban street canyons because they involve fewer costs of data and calculation. Since empirical parameters are typically based on measurements in a particular street canyon, new validations need to be carried out for other street canyons, which feature different geometry and dispersion conditions (Murena et al., 2009). Commonly used semi-empirical models include SIRANE, OSPM, and CALINE4. They operate at the street-level.

SIRANE treats each street segment as a rectangular street canyon and an intersection as a node (Soulhac et al., 2012; Wang et al., 2016). OSPM cannot model the dispersion at intersections, and Caline is mostly applied on highways (Wang et al., 2016). OSPM was used to model the average monthly and hourly emissions of black carbon in street canyons, and the average emission rates on the streets were calculated based on an emission inventory and vehicle activity data (Brasseur et al., 2015). It showed good results in the case of a stable boundary layer (Brasseur et al., 2015). It was concluded that the impact of vehicle speed

should be considered in high traffic density because the emission factor and the turbulence effect are higher at low vehicle speed during rush hours (Brasseur et al., 2015). A study comparing SIRANE, OSPM, and CALINE4 showed that SIRANE could better capture the effect of street canyon configuration (height of buildings, gradient, and presence/absence of a park) than either OSPM or Caline4 (Wang et al., 2016). The estimated average link emission factor or link emissions by MOVES were used as inputs of dispersion models (Wang et al., 2016). The difference between the simulated and measured results shows that these models can estimate the average near-road concentrations in different situations, but are inappropriate to capture the effects of varied meteorological and traffic conditions (Wang et al., 2016).

The CFD models represent the detailed dispersion process in a complex urban built environment. They can model the high-resolution dispersion (in meters) within a street canyon. However, they are unsuitable for modeling dispersions for an urban network due to the long computation time involved (Fu et al., 2020). Thus, the CFD model has been used to set the parameters of the semi-empirical models (Grylls et al., 2019). FLUENT is one of the more common CFD models. It has been used to estimate roadside ambient air quality near an intersection and was integrated with PTV VISSIM and an instantaneous emission model to take into account the turbulence caused by vehicle movement. It concluded that the inclusion of the turbulence effect could help identify high concentrations of emissions that cyclists and pedestrians are exposed to (Woodward et al., 2019). It was found that the measured and CFD modeled concentrations of NO_x at signalized intersections were higher than the concentrations between intersections (Kwak et al., 2018). Other typical CFD models are Reynolds-averaged Navier-Stokes (RANS) models and Large-Eddy Simulation (LES) models. One study compared the RANS model and the LES model (Tominaga & Stathopoulos, 2011). The results of the study show that the LES model produced a better distribution of concentrations within street canyons and proved that LES could model the turbulence diffusion within street canyons more accurately. The comparison between the CFD LES model (uDALES) and SIRANE shows although the use of average concentration derived from SIRANE can lead to an underestimation of exposure levels for pedestrians, a linear correction factor can solve this problem (Grylls et al., 2019).

Since the assessment of ITS is conducted on an urban scale, semi-empirical dispersion models are suitable to be integrated with the developed emission model to assess ITS. Lin and Ge (2006) used the cell-transmission traffic model to consider the spatial heterogeneity of traffic emissions into the dispersion model, and its results showed higher concentrations of CO than the results based on link emissions. The study indicates that information on the detailed spatial distribution of emissions is required to estimate the concentrations of near-road air pollutants. Therefore, the developed emission model is assumed to be better suited for capturing the spatial variations of the concentrations of air pollutants along roads and intersections and for identifying high exposure levels. The SIRANE model led to satisfactory results in European cities. Therefore, it is chosen to explain how the mesoscopic emission model is integrated with a dispersion model to estimate the changes in near-road air quality resulting from ITS. SIRANE was developed at the Ecole Centrale de Lyon, and a detailed

description can be found in the study of Lionel Soulhac et al. (2011). The integration between the developed emission model and SIRANE is shown in Fig. 5.1.

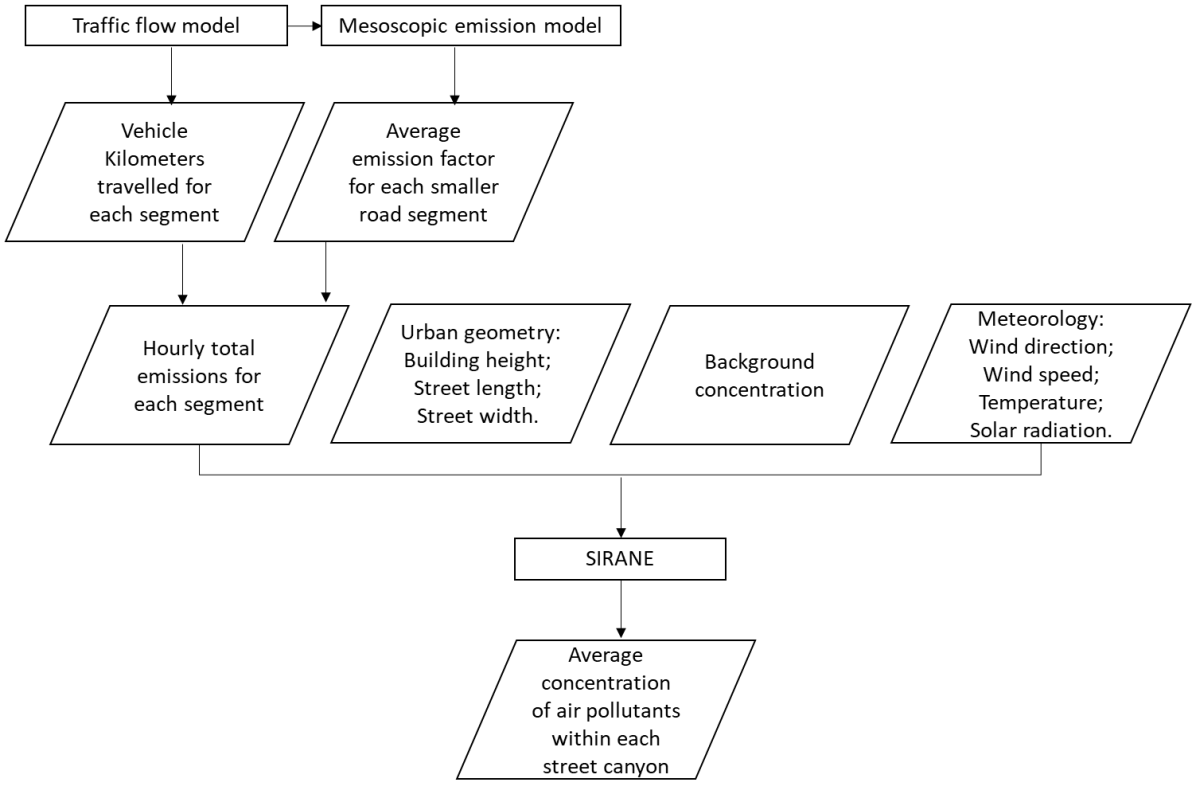

Fig. 5.1 Integration between the developed emission model and the dispersion model

6. Conclusions and outlook

This chapter begins by summarizing the research objectives, research questions, methodology, and findings. Subsequently, the contributions, transferability, and limitations of the model concept as well as the model development methodology, are discussed. The chapter ends with recommendations for further research.

Summary

Road traffic emissions are the dominant sources of air pollutions in the city, including NO_x, PM, CO, and HCs. As these pollutants can harm human health, road traffic emission and air quality have attracted much attention from the public and the government. Emissions are heterogeneously distributed on the road network due to the variance in local traffic and infrastructure. Intersections and near intersections are hot spots of emission. Urban road traffic management can influence the amount and spatial distribution of emissions. It is necessary to conduct an emission impact assessment to help design and choose relevant traffic management measures for emission reduction. ITS with the help of information and communication technology can make traffic management more dynamic. Consequently, a real-time emission assessment is required to choose the most suitable ITS measures. Furthermore,

the detailed spatial distribution of emissions is one of the necessary inputs for a detailed air quality map and exposure analysis.

Existing emission assessment does not distinguish between emission hot spots and cold spots. It gives no information if and to what extent emission levels at hot spots fluctuate and what factors may contribute to these changes. In this study, the division of a road into several segments near a signalized intersection is explored to distinguish between high- and low-emission areas effectively. It is achieved through the application of the spatial data analysis method, which helps with the identification of hot spots. The local G* method is one common way to discern cluster structures with high and low features. It is applied in each traffic scenario to obtain the boundary between the high and low-emission areas. Through a statistical and variance study, rules for the road division are specified. Generally, the road is divided into four parts: the upper section of the lane where small speed variation can occur, the segment near the stop line where significant accelerations occur, the crossing, and the section after crossing the intersection where vehicles accelerate further. Lane types of the section before the stop line include a lane with only straight-through traffic, a right-turning lane, a left-turning lane, and a lane with traffic in different directions. The types of crossing lanes include a left-turning lane, a right-turning lane, and a straight crossing lane. The emission of each road segment is estimated separately.

A mesoscopic emission model is developed to enable real-time emission impact assessment. The model assumes that emissions can be estimated with the help of a regression function, including traffic variables, which can be obtained through a macroscopic or mesoscopic traffic model. Variables included in the function are speed limit, average speed, the cycle time of the traffic signal in the case of signal-controlled intersections, capacity, traffic volume, truck percentage, turning ratio, conflicting traffic volume, and conflicting traffic's truck percentage. The D-optimal design, one of the experimental design methods, is applied for designing the traffic scenarios. The scenarios are simulated by the high-resolution microscopic traffic simulation model VISSIM. The emissions in each scenario are estimated by the physical emission model PHEM.

The methodology is applied to a 4-arm signalized intersection. Two approaches are studied: one approach that consists of a left-turning lane, a straight-through lane, and a right turning lane; another that consists of a lane with both right-turning and straight-through traffic. The results of the local G* show that on the approach with three separate lanes, high-emission areas on each lane are generally located within 18 meters from the stop line. The size of the hot-emission area on the lane with mixing straight-through and right-turning traffic is dynamic. A regression function is developed to estimate its size. The boundary between relatively high- and low-emission areas downstream is located 30 meters after the crossing of the intersection.

To develop the emission model, linear, interactive, and stepwise regression models are tested. The multicollinearity among the predictors, residual distribution, and sign of the effect of each term is checked. The regression model, which is theoretically meaningful and meets the

regression assumptions with a good (adjusted) R-squared value, is chosen for the test. The results of the model development show that a regression function with sufficiently accurate performance has been developed for each road segment.

The developed emission model is tested on another intersection of a small road network. The tested results show that the rules can identify the high-emission area before the stop line on the lane of straight-through and right-turning traffic as well as the straight-through lane. It overestimates the size of the high-emission area on the left-turning lane, while it underestimates the size after crossing the intersection. A dynamic prediction model can be developed to refine the estimated results of these lanes.

The developed model is compared with the traffic situation-based emission model HBEFA and PHEM. The percentage difference compared to PHEM acts as a performance indicator to evaluate the developed emission model by the research and HBEFA. The comparisons are made at different spatial resolutions. The test results show that the developed model generally performs better for all hot spots, while HBEFA performs better for cold spots. For the crossing, the developed model lacks predictivity, which could be due to no consideration of the length of the crossing lane. In most cases, estimations of emission factors of NO_x by the developed model are far closer to those by PHEM than those by HBEFA at the lane- and approach-level. HBEFA and the developed model perform similarly well when estimating stream emissions, while HEBFA tends to underestimate, and the developed model tends to overestimate emissions. It is tested whether the developed model can estimate the rerouting effect. For the estimation of the impact of rerouting on the emission factor of NO_x, the developed model performs better than HBEFA at the segment-, lane-, approach-level, while the results of HBEFA at the stream-level are slightly better than those from the developed model. The developed model can be improved by considering lane changes at midblock, the turning radius of turning traffic, the length of the crossing lane, and a regression function for the accurate size of the segment after crossing.

The study introduced how to estimate urban near-road air quality by integrating the developed emission model and a proper dispersion model. Since the measurements are hardly representative enough for assessing the accuracy of the developed emission model, the research did not conduct a comparison between measured and modeled air quality.

Transferability and limitations

Apart from the signalized four-way intersection, the emission model concept can be applied to other types of intersections and control: T/Y-intersection, roundabouts, stop sign-controlled intersections, yield sign-controlled intersections, and uncontrolled intersections. Although the type of control and number of streams may differ, vehicles will experience similar driving dynamics at all types of intersections: driving at a low variation of speed on midblock; either decelerating and coming to a full stop before the intersection and then accelerating to leave the lane or driving without significant decelerations and accelerations; driving to cross the intersection; accelerating after crossing. Thus, the street is divided into four segments: an

upper section (midblock), a section near the stop line (inbound), the section crossing the intersection, and the section after crossing (outbound). The spatial data analysis used in this study can be applied to find out how the boundaries between these segments vary in different situations. The emission factor can be a function of the traffic volume, fleet composition, capacity, volume, and fleet composition of the conflicting traffic, speed limit, average speed, cycle time in the case of a signalized intersection, and distance between intersections.

For a non-signalized roundabout, the road can equally be divided into four segments: an inbound section where vehicles decelerate to enter the circulating lane, the circulating section, the outbound section where vehicles exit the circulating lane and drive downstream, and a midblock section where vehicles usually drive downstream at a relatively constant speed. The emission factor of each segment can be a function of traffic variables, infrastructure layout, and infrastructure geometry. Variables can include traffic volume, speed limit, capacity, average speed, the diameter of the roundabout, entry deflection angle, number of approaches, grade, and spacing between roundabouts. For a signalized roundabout, the cycle time can be an additional predictor. The modeling methodology developed by the research can be applied to find out the boundaries between these segments in various situations and the regression function for each segment to estimate the average emission factor.

The developed emission model concept can be also applied to ramps. Ramp metering is a signalized control on a ramp when vehicles on the ramp enter the main lane. The ramp can be divided into three parts: the segment where vehicles arrive on the ramp; the segment where vehicles stop before the stop line; and the segment where vehicles leave the stop line and accelerate to enter the ramp. At a signalized ramp, the boundary between the first and second segments is estimated to be the same as the boundary on a straight lane. The emission functions for the first two parts are also found to be the same as those for a straight lane at a signalized intersection. Besides, the length of each segment needs to be considered to estimate the emission factor of the third segment. It is because a study has found that the length of a segment can influence the acceleration rate: a shorter segment will lead to faster acceleration (G. Yang & Tian, 2019). The main lane would be divided into three segments: an upstream section before connecting with the ramp, the segment where vehicles enter the main lane, and a downstream section after the ramp. On the second segment, upstream vehicles on the main lane may switch lanes or decelerate due to encountering vehicles entering the ramp. The size of the segment is assumed to depend on the average speed on the main lane. For the upstream and downstream segments, the emission factors depend on the average speed, speed limit, and fleet composition. For the interaction segment, the average emission factor is assumed to be a function of the number of lanes, average speed, speed limit, traffic volume on the main lane, traffic volume on the ramp, the capacity of the ramp, fleet composition, and grade. The spatial cluster method can be applied to identify the exact boundaries between segments. For a ramp without metering, the method is similar to that applied to ramp metering. The main difference is that the ramp can be divided into two parts. Moreover, for a highway interchange, the curvature of the road is an additional predictor of the emission factor.

In this study, drivers are assumed to comply with lane markings and traffic controls. In the real world, drivers may disobey these regulations and, for example, engage in unsafe lane changes, cross lane boundaries, use prohibited lanes (such as HOV lanes), cross red lights, or exceed the speed limit. These factors may disturb the traffic flow, resulting in traffic accidents and generate additional accelerations and decelerations. No studies have been found to quantify the impact of the compliance level of these traffic regulations on road traffic emissions. In the case of a high level of disobedience, the significance of its impact on emissions should be studied.

The study investigated unsaturated traffic conditions (i.e., the traffic volume was assumed to be lower than the intersection capacity at each signal cycle). When traffic demand exceeds capacity (oversaturation), some vehicles may queue for a longer duration than one signal cycle, resulting in a longer queue. In the case of severe oversaturation, queue length may exceed the length of the lane and extend into the upstream intersection. It would raise the risk of gridlock as the queue would block the adjacent lane. Under oversaturated traffic conditions, vehicles may experience periods of stop-and-go driving. There will be no road segment on which vehicles can drive with cruising speed. As a consequence, the spatial heterogeneity of emissions from saturated traffic will differ from the heterogeneity of unsaturated traffic, and new ways for road division into smaller road segments would have to be researched. Meanwhile, it has to be investigated whether there exists a proper regression function of traffic flow variables, intersection layout, lane geometry, and traffic control to estimate emissions for each road segment.

In this study, driving scenarios considered include turning, yielding, stopping, and queueing due to signal control, speed changes due to the traffic density and truck percentage, and overtaking. Driving behaviors consist of steering, braking, accelerating, and gear shifting. These behaviors are influenced by the traffic environment and also a driver's individual characteristics (such as age, gender, education, emotion, and driving experience). The behaviors influence engine power and engine speed and, therefore, emissions. Since the goal of the research is to assess the ITS for traffic management and control, the driving behaviors of different drivers are not described in detail in the models. Instead, the distribution of each parameter that describes driver behaviors is used in the microscopic simulation model, and the gear shift model is included in PHEM. ADAS, or automatic driving, can change the driving behaviors of a specific vehicle with a specific driver. Existing studies have found that the deployment of ADAS or autonomous vehicles on roads can reduce road emissions by smoothing traffic flow (e.g., Stern et al., 2019). Although the impact of traffic flow characteristics on emissions is included in the developed emission model through predictors of average speed and capacity, the question remains if the developed emission model can fully capture the emission changes due to ADAS and autonomous driving.

Emissions from trucks and cars are considered in the research. With new energy vehicles entering the market, their tailpipe emissions need to be considered for roadside air quality. Hybrid electric vehicles, one type of new energy vehicle, can emit tailpipe emissions. Driving

strategies for electric motors and combustion engines, charging strategies, driving conditions (vehicle load and speed), electric mileage, and ambient temperature can influence the emissions of plug-in hybrid electric vehicles (Ehrenberger et al., 2020). To make the developed emission model applicable to scenarios with hybrid electric vehicles, the average emission factors of hybrid electric vehicles have to be categorized. When a specific type of hybrid electric vehicles with a particular drivetrain and efficiency technology is driving under the status of a vehicle using an electric motor and combustion engine in certain traffic conditions, its emissions can be estimated based on real-world measurement, laboratory testing, or with the help of an emission model like PHEM. The average emission factor of this type of hybrid vehicles can be developed for the respective traffic condition and the use pattern of the electric motor and combustion engine. Subsequently, a database of emission factors can be established for hybrid electric vehicles. When applying the developed emission modeling concept to scenarios with hybrid electric vehicles, the emission factor can be adjusted by adding hybrid electric vehicle emissions. Meanwhile, a methodology needs to be developed to estimate and predict the hybrid modes of hybrid electric vehicles.

When applying this model concept and methodology to other countries, additional variables need to be researched to see how they affect the emission factors and spatial distribution of emissions. Examples of additional variables are a large volume of pedestrians, shared lane use with motorbikes, and a high number of overtaking in China; a high volume of motorcycles in India; and differences in the compliance to traffic control and lane markings. Since driver behaviors vary in different countries, driving styles need to be localized to develop an emission model.

In order to evaluate the impact of ITS on segment-level emissions, further research is needed to improve the developed emission model. The solutions can be an accurate estimation of traffic volume on each segment or lane, consideration of the turning radius and the length of the crossing lane, and a regression function for the accurate size of the segment after crossing.

Conclusions and contributions

The developed mesoscopic emission model is based on the segmentation of road links to distinguish high and low emissions. The spatial data mining method (Local G*) is used to distinguish high- and low-emission areas near an intersection. The estimation of emissions of each segment is related to traffic conditions and traffic composition. These variables can be obtained through macroscopic traffic models, mesoscopic traffic models, or measurements by roadside or in-vehicle (mobile) equipment. The regression function is developed based on the integration of a microscopic traffic simulation model (VISSIM) and a detailed physical emission model (PHEM). The measurements of air quality are biased and influenced by many other variables like weather, local climate, local buildings, and trees. Real-world data collection cannot account for all representative scenarios and cannot fulfill the requirements of a variance study. The microscopic method can instead simulate a wide range of scenarios and is under control. Moreover, it can well estimate the emissions of a group of vehicles. Thus, the

microscopic methodology is suitable to develop the relationship between the average emission factor and the predictors. The model concept is developed to compare the emission impacts of different ITS measures, including isolated and coordinated signal control, ramp metering, variable speed limit, as well as routing and traffic demand management. It considers various pathways through which these ITS measures can influence traffic emissions. Although the developed emission model cannot produce absolute emissions nor immissions, the developed emission model can be used to compare the impacts of different ITS measures for urban traffic management and control on the spatial distribution of emissions on the urban road network. The developed emission model can be further integrated with a dispersion model to estimate the immissions and to assess exposure levels.

Compared with the microscopic emission assessment framework, the developed model concept consumes less time and data. It performs better than the traffic situation-based emission model HBEFA for emission estimations and emission impact assessments of the ITS at the segment-, lane-, and approach-level. The HBEFA and the developed model reach relatively similar estimations on the absolute difference of stream emissions from PHEM. The developed emission model can be further improved by adding the impact of intersection geometry on emissions. A better estimation of traffic volume on each segment can improve the estimation of segment emissions as well. It is also suggested that a dynamic prediction model can help refine the estimation of the segment's size after crossing an intersection and, therefore, the emission estimation.

Outlook

Future research can investigate the following topics. Firstly, the emission model concept and modeling methodology can be applied to other types of intersections (three-way intersections, highway with ramps, stop/yield sign-controlled intersections, uncontrolled intersections, and roundabouts). Secondly, the emission model can be further extended to cover other vehicle types like hybrid vehicles based on the modeling of the use pattern of electric motors and combustion engines. Thirdly, further research can study the spatial heterogeneity of emissions in oversaturated traffic conditions and check if the model concept is suited to oversaturated traffic conditions. Fourthly, it is necessary to investigate whether the developed emission model can fully capture the emission changes due to ADAS and autonomous driving. Fifthly, when applying this model concept and methodology to other countries, localized driving behaviors (driving style, overtaking, compliance to traffic control and regulations), differences in traffic composition (e.g., the higher percentage of motorbikes in China or motorcycles in India), and mixed lane use need to be considered. Sixthly, the effect of pedestrians, cyclists, public transportation, road slope, intersection size, radius of curvature, and road width should also be investigated with the help of a more refined traffic flow model. Lastly, the estimations of the segment size and emission factor after crossing an intersection need to be improved.

References

Aguiléra, V., & Tordeux, A. (2011). Integration of a speed-dependent emission model in dynamic traffic assignment: A large-scale application to the Paris metropolitan area. *Procedia - Social and Behavioral Sciences*, *20*, 475–484. https://doi.org/10.1016/j.sbspro.2011.08.054

Ahmad, K., Khare, M., & Chaudhry, K. K. (2005). Wind tunnel simulation studies on dispersion at urban street canyons and intersections - A review. *Journal of Wind Engineering and Industrial Aerodynamics*, *93*(9), 697–717. https://doi.org/10.1016/j.jweia.2005.04.002

Andersen, J., & Sutcliffe, S. (2000). Intelligent Transport Systems (ITS) - An Overview. *IFAC Proceedings Volumes*, *33*(18), 99–106. https://doi.org/10.1016/s1474-6670(17)37129-x

André, M., Keller, M., Sjödin, Å., & Gadrat, M. (2009). The Artemis European tools for estimating the transport pollutant emissions. *Proceedings of the 18th International Emission Inventories Conference*, *1*, 10. http://www.epa.gov/ttn/chief/conference/ei18/session6/andre.pdf%5Cnhttp://publications.jrc.ec.europa.eu/repository/handle/JRC51277

Arthur Getis. (2008). A History of the Concept of Spatial Autocorrelation: A Geographer's Perspective. *Geographical Analysis*, *40*(3), 297–309. http://dx.doi.org/10.1111/j.1538-4632.2008.00727.x

Atkinson, A., & Donev, A. (1992). *Optimum Experimental Designs*. Oxford University Press.

Avetisyan, H. G., Miller-Hooks, E., Melanta, S., & Qi, B. (2014). Effects of vehicle technologies, traffic volume changes, incidents, and work zones on greenhouse gas emissions production. *Transportation Research Part D: Transport and Environment*, *26*, 10–19. https://doi.org/10.1016/j.trd.2013.10.005

Barth, M., & Boriboonsomsin, K. (2012). *ECO-ITS : Intelligent Transportation System Applications to Improve Environmental Performance*.

Barth, M. J., An, F., Younglove, T., Scora, G., Levine, C., Ross, M., & Wenzel, T. (2000). *Development of a Comprehensive Modal Emissions Model.Final report project 25–11* (Issue April).

Beevers, S. D., & Carslaw, D. C. (2005). The impact of congestion charging on vehicle emissions in London. *Atmospheric Environment*, *39*(1), 1–5. https://doi.org/10.1016/j.atmosenv.2004.10.001

Behrisch, M., & Erdmann, J. (2015). Comparing emission and traffic flow models of different categories. *2015 International Conference on Models and Technologies for Intelligent Transportation Systems, MT-ITS, 2015*, 164–168. https://doi.org/10.1109/MTITS.2015.7223252

Bie, Y., Liu, Z., Ma, D., & Wang, D. (2013). Calibration of platoon dispersion parameter considering the impact of the number of lanes. *Journal of Transportation Engineering*, *139*(2), 200–207. https://doi.org/10.1061/(ASCE)TE.1943-5436.0000443

Borge, R., de Miguel, I., de la Paz, D., Lumbreras, J., Pérez, J., & Rodríguez, E. (2012). Comparison of road traffic emission models in Madrid (Spain). *Atmospheric Environment*, *62*(X), 461–471. https://doi.org/10.1016/j.atmosenv.2012.08.073

Borge, R., Narros, A., Artíñano, B., Yagüe, C., Gómez-Moreno, F. J., de la Paz, D., Román-Cascón, C., Díaz, E., Maqueda, G., Sastre, M., Quaassdorff, C., Dimitroulopoulou, C., & Vardoulakis, S. (2016). Assessment of microscale spatio-temporal variation of air pollution at an urban hotspot in Madrid (Spain) through an extensive field campaign. *Atmospheric Environment*, *140*, 432–445. https://doi.org/10.1016/j.atmosenv.2016.06.020

Boriboonsomsin, K., & Barth, M. (2008). Impacts of freeway high-occupancy vehicle lane configuration on vehicle emissions. *Transportation Research Part D: Transport and Environment*, *13*(2), 112–125. https://doi.org/10.1016/j.trd.2008.01.001

Borken-Kleefeld, J. (2012). Remote sensing for identifying high emitters and validating emission models. In *Conference presentation, ERMES 2012 Plenary Meeting, 27-28 September 2012*.

Boulter, P. G., McCrae, I. S., & Barlow, T. J. (2007). *A review of instantaneous emission models for road vehicles*.

Bowyer, D. P., Akcelik, R., & Biggs, D. C. (1985). Guide To Fuel Consumption Analyses for Urban Traffic Management. In *Australian Road Research Research Report* (Issue 32). http://trid.trb.org/view.aspx?id=281980

Brasseur, O., Declerck, P., Heene, B., & Vanderstraeten, P. (2015). Modelling black carbon concentrations in two busy street canyons in Brussels using CANSBC. *Atmospheric Environment*, *101*, 72–81. https://doi.org/10.1016/j.atmosenv.2014.10.049

Brilon, W. (2005). Roundabouts : A State of the Art in Germany. *National Roundabout Conference: 2005 Proceedings*, 15.

Ca. (2015). *EMFAC2014 - Technical Documentation: Vol. III*.

Cantarella, G., Watling, D., De Luca, S., & Pace, R. D. (2019). Appendix B traffic flow theory. In *Dynamics and Stochasticity in Transportation Systems: Tools for Transportation Network Modelling* (p. 357). Elsevier. https://doi.org/https://doi.org/10.1016/C2017-0-01089-3

Cappiello, A., Chabini, I., Nam, E. K., Lue, A., & Abou Zeid, M. (2002). A statistical model of vehicle emissions and fuel consumption. *Proceedings. The IEEE 5th International Conference on Intelligent Transportation Systems*, *September*, 801–809. https://doi.org/10.1109/ITSC.2002.1041322

Cascetta, E. (2001). Transportation Supply Models. In *Transportation Systems Engineering: Theory and Methods* (p. 710). Springer US. https://doi.org/10.1007/978-1-4757-6873-2

Celikkaya, N., Fullerton, M., & Fullerton, B. (2019). Use of Low-Cost Air Quality Monitoring Devices for Assessment of Road Transport Related Emissions. *Transportation Research Procedia*, *41*, 762–781. https://doi.org/10.1016/j.trpro.2019.09.125

Choudhary, A., & Gokhale, S. (2019). On-road measurements and modelling of vehicular emissions during traffic interruption and congestion events in an urban traffic corridor.

Atmospheric Pollution Research, *10*(2), 480–492. https://doi.org/10.1016/j.apr.2018.09.008

Christopher Frey, H., Rouphail, N. M., & Zhai, H. (2006). Speed- And facility-specific emission estimates for on-road light-duty vehicles on the basis of real-world speed profiles. *Transportation Research Record*, *1987*, 128–137. https://doi.org/10.3141/1987-14

Coensel, Bert De, & Botteldooren, D. (2011). Traffic signal coordination : a measure to reduce the environmental impact of urban road traffic ? *40th International Congress and Exposition on Noise Control Engineering (Inter-Noise-2011)*, *5*, 4218–4223.

Cohen, S., Christoforou, Z., & Seidowsky, R. (2014). Assessing the impact of speed limit changes on urban motorways: A simulation study in Lille, France. *Transportation Research Procedia*, *3*(July), 915–924. https://doi.org/10.1016/j.trpro.2014.10.071

Colman, A. M. (2015). *A dictionary of psychology* (4 edition). Oxford University Press. https://doi.org/10.1093/acref/9780199657681.001.0001

Consortium, A. (2013). *classification of ITS*.

d'Orey, P. M., & Ferreira, M. (2014). ITS for Sustainable Mobility: A Survey on Applications and Impact Assessment Tools. *IEEE Transactions on Intelligent Transportation Systems*, *15*(2), 477–493. https://doi.org/10.1109/TITS.2013.2287257

da Rocha, T. V., Leclercq, L., Montanino, M., Parzani, C., Punzo, V., Ciuffo, B., & Villegas, D. (2015). Does traffic-related calibration of car-following models provide accurate estimations of vehicle emissions ? *Transportation Research Part D: Transport and Environment*, *34*, 267–280. https://doi.org/10.1016/j.trd.2014.11.006

De Coensel, B., Can, A., Degraeuwe, B., De Vlieger, I., & Botteldooren, D. (2012). Effects of traffic signal coordination on noise and air pollutant emissions. *Environmental Modelling and Software*, *35*, 74–83. https://doi.org/10.1016/j.envsoft.2012.02.009

Delavarrafiee, M., & Frey, H. C. (2018). Real-world fuel use and gaseous emission rates for flex fuel vehicles operated on E85 versus gasoline. *Journal of the Air and Waste Management Association*, *68*(3), 235–254. https://doi.org/10.1080/10962247.2017.1405097

Ding, Y. (2000). *Quantifying the Impact of Traffic-Related and Driver-Related Factors on Vehicle Fuel*. Virginia Polytechnic Institute and State University.

Dowling, R., Skabardonis, A., & Alexiadis, V. (2004). *Traffic Analysis Toolbox Volume III : Guidelines for Applying Traffic Microsimulation Modeling Software: Vol. III*.

Du, J., Li, Q., & Qiao, F. (2018). Impact of Different Ramp Metering Strategies on Vehicle Emissions along Freeway Segments. *Journal of Transport & Health*, *9*, S38. https://doi.org/10.1016/j.jth.2018.05.020

Ehrenberger, S. I., Konrad, M., & Philipps, F. (2020). Pollutant emissions analysis of three plug-in hybrid electric vehicles using different modes of operation and driving conditions. *Atmospheric Environment*, *234*(September 2019), 117612. https://doi.org/10.1016/j.atmosenv.2020.117612

Elefteriadou, L. (2014). *An Introduction to Traffic Flow Theory* (Vol. 84). New York: Springer. https://doi.org/10.2307/3006702

Ellenberg, M., & Bedeaux, J. F. (1999). Calming waves for safety: a time to rethink green waves? *Traffic Technology International*, 55–58.

Environmental Protection Agency. (1993). *Federal Test Procedure Review Project: Preliminary Technical Report*.

Erdmann, J. (2014). Lane-Changing Model in SUMO. *SUMO2014 Modeling Mobility with Open Data*, 77–88.

ERSI. (n.d.). *Best practices for selecting a fixed distance band value*. https://pro.arcgis.com/en/pro-app/tool-reference/spatial-statistics/choosingdistanceband.htm

ERSI. (2018). How Hot Spot Analysis (Getis-Ord Gi*) works. *ArcGIS Pro Tool Reference*. https://pro.arcgis.com/en/pro-app/tool-reference/spatial-statistics/h-how-hot-spot-analysis-getis-ord-gi-spatial-stati.htm

European Environment Agency (EEA). (2015). Air quality in Europe — 2015 report. In *Report* (Issue 5). https://doi.org/10.2800/62459

Fambro, D. B., Chang, E., & Messer, C. J. (1991). *Effects of the Quality of Traffic Signal Progression on Delay*. http://onlinepubs.trb.org/Onlinepubs/nchrp/nchrp_rpt_339.pdf

Fellendorf, M., & Vortisch, P. M. (2010). Microscopic traffic flow simulator VISSIM. In *Fundamentals of traffic simulation* (pp. 63–93). Springer.

Fellendorf, Martin, & Vortisch, P. (2001). Validation of the microscopic traffic flow model VISSIM in different real-world situations. *Proceedings of the 80th Annual Meeting of the Transportation Research Board Compendium of Papers*, *January 2001*, 1–9. http://trid.trb.org/view.aspx?id=689890

Feng, Y., Yu, C., & Liu, H. X. (2018). Spatiotemporal intersection control in a connected and automated vehicle environment. *Transportation Research Part C*, *89*, 364–383. https://doi.org/10.1016/j.trc.2018.02.001

Fernandes, P., Coelho, M. C., & Rouphail, N. M. (2017). Assessing the impact of closely-spaced intersections on traffic operations and pollutant emissions on a corridor level. *Transportation Research Part D: Transport and Environment*, *54*, 304–320. https://doi.org/10.1016/j.trd.2017.05.016

Fernandes, P, Salamati, K., Rouphail, N. M., & Coelho, M. C. (2015). Identification of emission hotspots in roundabouts corridors. *Transportation Research Part D*, *37*, 48–64. https://doi.org/10.1016/j.trd.2015.04.026

Fernandes, Paulo, & Coelho, M. C. (2017). Pedestrian and Cyclists Impacts on vehicular Capacity and Emissions at different Turbo-roundabouts layouts. *Transportation Research Procedia*, *27*, 452–459. https://doi.org/10.1016/j.trpro.2017.12.003

FGSV. (2006). *Hinweise yur mikroskopische Verkehrsflussimulation. Grundlagen und Anwendung*.

FGSV. (2015). *HBS - Handbuch für die Bemessung von Straßenverkehrsanlagen*.

Fontes, T., Fernandes, P., Rodrigues, H., Bandeira, J. M., Pereira, S. R., Khattak, A. J., & Coelho, M. C. (2014). Are HOV/eco-lanes a sustainable option to reducing emissions in a medium-sized European city? *Transportation Research Part A: Policy and Practice*, *63*, 93–106. https://doi.org/10.1016/j.tra.2014.03.002

Freedman, R. (1984). Road traffic emission mapping. *Environmental Pollution. Series B, Chemical and Physical*, *7*(3), 159–177. https://doi.org/10.1016/0143-148X(84)90046-6

Frey, H., Unal, A., Chen, J., Li, S., & Xuan, C. (2002). Methodology for developing modal emission rates for EPA's multi-scale motor vehicle & equipment emission system. In *State University for US EPA, Ann Arbor, MI* (Issue October). http://www.epa.gov/otaq/models/ngm/r02027.pdf%5Cnhttp://scholar.google.com/scholar?hl=en&btnG=Search&q=intitle:Methodology+for+Developing+Modal+Emission+Rates+for+EPA+?+s+Multi-Scale+Motor+Vehicle+and+Equipment#0%5Cnhttp://scholar.google.com/scholar?hl=en&btn

Fritzsche, H. T. (1994). A Model for Traffic Simulation. In *Traffic Engineering and Control* (pp. 317–321).

Fu, X., Xiang, S., Liu, Y., Liu, J., Yu, J., Mauzerall, D. L., & Tao, S. (2020). High-resolution simulation of local traffic-related NOx dispersion and distribution in a complex urban terrain. *Environmental Pollution*, *263*(x), 114390. https://doi.org/10.1016/j.envpol.2020.114390

Gastaldi, M., Meneguzzer, C., Giancristofaro, R. A., Gecchele, G., Lucia, L. Della, & Prati, M. V. (2017). On-road measurement of CO2 vehicle emissions under alternative forms of intersection control. *Transportation Research Procedia*, *27*, 476–483. https://doi.org/10.1016/j.trpro.2017.12.048

Getis, A., & Ord, J. K. (1996). Local spatial statistics: An overview. In P. Longley & M. Batty (Eds.), *Spatial Analysis: Modeling in A GIS Environment* (pp. 261–277). John Wiley & Sons.

Getis, Arthur, & Ord, J. K. (1992). The Analysis of Spatial Association by use of distance statistics. *Geographical Analysis*, *24*(3), 189–206. https://doi.org/10.1111/j.1538-4632.1992.tb00261.x

Giannouli, M., Kalognomou, E.-A., Mellios, G., Moussiopoulos, N., Samaras, Z., & Fiala, J. (2011). Impact of European emission control strategies on urban and local air quality. *Atmospheric Environment*, *45*(27), 4753–4762. https://doi.org/10.1016/j.atmosenv.2010.03.016

Gipps, P. G. (1981). A behavioural car-following model for computer simulation. *Transportation Research Part B: Methodological*, *15*(2), 105–111. https://doi.org/10.1016/0191-2615(81)90037-0

Gipps, P. G. (1986). A model for the structure of lane-changing decisions. *Transportation Research Part B*, *20*(5), 403–414. https://doi.org/10.1016/0191-2615(86)90012-3

Gkatzoflias, D., Kouridis, C., Ntziachristos, L., & Samaras, Z. (2007). Copert 4. Computer Program to calculate emissions from road transport. In *European Environment Agency*.

Goel, A., & Kumar, P. (2014). A review of fundamental drivers governing the emissions, dispersion and exposure to vehicle-emitted nanoparticles at signalised traffic intersections. *Atmospheric Environment*, *97*, 316–331. https://doi.org/10.1016/j.atmosenv.2014.08.037

Goel, A., & Kumar, P. (2016). Vertical and horizontal variability in airborne nanoparticles and their exposure around signalised traffic intersections. *Environmental Pollution*, *214*, 54–69. https://doi.org/10.1016/j.envpol.2016.03.033

Gori, S., La Spada, S., Mannini, L., & Nigro, M. (2014). A new methodological framework for within-day dynamic estimation of pollutant emissions in a large congested urban network. *European Journal of Transport and Infrastructure Research*, *14*(3), 268–289.

Gori, S., Spada, S. La, Mannini, L., & Nigro, M. (2014). *A new methodological framework for within-day dynamic estimation of pollutant emissions in a large congested urban network*. *14*(14), 268–289.

Griffith, D. . (2003). *Spatial Autocorrelation and Spatial Filtering: Gaining Understanding through Theory and Scientific Visualization*. Springer-Verlag Berlin.

Grote, M., Williams, I., Preston, J., & Kemp, S. (2016). Including congestion effects in urban road traffic CO_2 emissions modelling: Do Local Government Authorities have the right options? *Transportation Research Part D: Transport and Environment*, *43*, 95–106. https://doi.org/10.1016/j.trd.2015.12.010

Grubesic, T. H., Wei, R., Murray, A. T., Grubesic, T. H., Wei, R., & Murray, A. T. (2014). Spatial Clustering Overview and Comparison : Accuracy, Sensitivity, and Computational Expense. *Annals of the Association of American Geographers*, *104*(6), 1134–1156. https://doi.org/10.1080/00045608.2014.958389

Grumert, E. F., Tapani, A., & Ma, X. (2018). Characteristics of variable speed limit systems. *European Transport Research Review*, *10*(2), 1–12. https://doi.org/10.1186/s12544-018-0294-8

Grumert, E., Ma, X., & Tapani, A. (2015). Analysis of a cooperative variable speed limit system using microscopic traffic simulation. *Transportation Research Part C: Emerging Technologies*, *52*, 173–186. https://doi.org/10.1016/j.trc.2014.11.004

Grylls, T., Le Cornec, C. M. A., Salizzoni, P., Soulhac, L., Stettler, M. E. J., & van Reeuwijk, M. (2019). Evaluation of an operational air quality model using large-eddy simulation. *Atmospheric Environment: X*, *3*, 100041. https://doi.org/10.1016/j.aeaoa.2019.100041

Guo, R., & Zhang, Y. (2014). Exploration of correlation between environmental factors and mobility at signalized intersections. *Transportation Research Part D: Transport and Environment*, *32*, 24–34. https://doi.org/10.1016/j.trd.2014.05.011

Haberl, M., Fellendorf, M., Luz, R., & Hausberger, S. (2014). Integrating an Emission Minimizing Extension in an Adaptive Signal-Control Optimization Algorithm. *International Transport and Air Pollution Conference (TAP)*, 1–5.

Haining, R. (2014). *Spatial Data Analysis : Theory and Practice*. Cambridge University Press.

Hall, D. L., Anderson, D. C., Martin, C. R., Ren, X., Salawitch, R. J., He, H., Canty, T. P., Hains, J. C., & Dickerson, R. R. (2020). Using near-road observations of CO, NOy, and CO2 to investigate emissions from vehicles: Evidence for an impact of ambient temperature and specific humidity. *Atmospheric Environment*, 117558. https://doi.org/10.1016/j.atmosenv.2020.117558

Hallmark, S. L., Guensler, R., & Fomunung, I. (2002). Characterizing on-road variables that affect passenger vehicle modal operation. *Transportation Research Part D: Transport and Environment*, *7*(2), 81–98. https://doi.org/10.1016/S1361-9209(01)00012-8

Hausberger, S, Rexeis, M., Zallinger, M., & Luz, R. (2009). Emission Factors from the Model PHEM for the HBEFA Version 3. In *University of Technology, Graz*.

Hausberger, Stefan, Rodler, J., Sturm, P., & Rexeis, M. (2003). Emission factors for heavy-duty vehicles and validation by tunnel measurements. *Atmospheric Environment*, *37*(37), 5237–5245. https://doi.org/10.1016/j.atmosenv.2003.05.002

Heinrich, J., Schwarze, P. E., Stilianakis, N., Momas, I., Medina, S., Totlandsdal, A. I., Bree, L. von, Kuna-Dibbert, B., & Krzyzanowski, M. (2005). Studies on health effects of transport-related air pollution. In M. Krzyzanowski, B. Kuna-Dibbert, & J. Schneider (Eds.), *Health effects of transport-related air pollution* (p. 190). WHO Regional Office for Europe.

Hirschmann, K., Zallinger, M., Fellendorf, M., & Hausberger, S. (2010). A new method to calculate emissions with simulated traffic conditions. *13th International IEEE Conference on Intelligent Transportation Systems, 2010*, 33–38. https://doi.org/10.1109/ITSC.2010.5625030

Hoffmann, S. (2014). *Mikroskopische Modellierung und Bewertung von Verkehrsicherheitskritischen Situationen, am Beispiel Kommunikationsbasierter Fahrerwartungen auf Autobahnen*. Technische Universität München.

Hu, J., Fontaine, M. D., Park, B. B., & Ma, J. (2016). Field evaluations of an adaptive traffic signal-using private-sector probe data. *Journal of Transportation Engineering*, *142*(1), 1–9. https://doi.org/10.1061/(ASCE)TE.1943-5436.0000806

Huang, D., & Huang, W. (2003). Traffic signal synchronization. *Physical Review E - Statistical Physics, Plasmas, Fluids, and Related Interdisciplinary Topics*, *67*(5), 7. https://doi.org/10.1103/PhysRevE.67.056124

Huang, Y., Ng, E. C. Y., Zhou, J. L., Surawski, N. C., Chan, E. F. C., & Hong, G. (2018). Eco-driving technology for sustainable road transport: A review. *Renewable and Sustainable Energy Reviews*, *93*, 596–609. https://doi.org/10.1016/j.rser.2018.05.030

Hülsmann, F. (2014). *Integrated agent-based transport simulation and air pollution modelling in urban areas - the example of Munich*.

Hülsmann, F., Gerike, R., & Ketzel, M. (2014). Modelling traffic and air pollution in an integrated approach - the case of Munich. *Urban Climate*, *10*, 732–744. https://doi.org/10.1016/j.uclim.2014.01.001

Jamshidnejad, A., Papamichail, I., Papageorgiou, M., & De Schutter, B. (2017). A mesoscopic integrated urban traffic flow-emission model. *Transportation Research Part C: Emerging Technologies*, *75*, 45–83. https://doi.org/10.1016/j.trc.2016.11.024

Jiang, R., & Wu, Q. S. (2005). The traffic flow controlled by the traffic lights in the speed gradient continuum model. *Physica A: Statistical Mechanics and Its Applications*, *355*(2–4), 551–564. https://doi.org/10.1016/j.physa.2005.04.001

Jimenez, F. (Ed.). (2017). *Intelligent Vehicles: Enabling technologies and future developments*. Butterworth-Heinemann.

Jing, P., Huang, H., & Chen, L. (2017). An adaptive traffic signal control in a connected vehicle environment: A systematic review. *Information*, *8*(3). https://doi.org/10.3390/info8030101

Joumard, R., & Andre, M. (1990). Cold start emissions of traffic. *Science of the Total Environment*, *93*, 175–182.

Kachroo, P., & Ozbay, K. (2003). Intelligent Approach to Congestion Problem: Ramp Metering. In *Feedback Ramp Metering in Intelligent Transportation Systems* (p. 352). Springer Science & Business Media.

Keller, M., Hausberger, S., Matzer, C., Wüthrich, P., & Notter, B. (2017). HBEFA Version 3.3. In *Background documentation, Berne*.

Kent, J. H., & Mudford, N. R. (1979). Motor vehicle emissions and fuel consumption modelling. *Transportation Research Part A: General*, *13*(6), 395–406. https://doi.org/10.1016/0191-2607(79)90003-7

Kerner, B. S., Hemmerle, P., Koller, M., Hermanns, G., Klenov, S. L., Rehborn, H., & Schreckenberg, M. (2014). Empirical synchronized flow in oversaturated city traffic. *Physical Review E - Statistical, Nonlinear, and Soft Matter Physics*, *90*(3), 1–5. https://doi.org/10.1103/PhysRevE.90.032810

Kiefer, J., & Wolfowitz, J. (1959). Optimum designs in regression problems. *The Annals of MathematicalStatistics*, *30*, 271–294.

Klunder, G., Stelwagen, U., & Taale, H. (2013). Integrating a macro emission model with a macroscopic traffic model. *In ETC 2013: European Transport Conference, 30 September-2 October 2013.*, 1–11.

Knorr, W., Hausberger, S., Helms, H., Lambrecht, U., Keller, M., & Steven, H. (2011). *Weiterentwicklung der Emissionsfaktoren für das Handbuch für Emissionsfaktoren (HBEFA)*.

Krajzewicz, D. (2010). Traffic Simulation with SUMO – Simulation of Urban Mobility. In J. Barceló (Ed.), *Fundamentals of Traffic Simulation, Series: International Series in Operations Research & Management Science*. Springer.

Krajzewicz, Daniel, Behrisch, M., Wagner, P., Luz, R., & Krumnow, M. (2015). Second generation of pollutant emission models for SUMO. In *Modeling Mobility with Open Data* (pp. 203–221). Springer International Publishing. https://doi.org/10.1007/978-3-319-15024-6_12

Krajzewicz, Daniel, Cyganski, R., Heinrichs, M., & Erdmann, J. (2016). Benefits of Using Microscopic Models for Simulating Air Quality Management Measures. *95th Annual Meeting of the Transportation Research Board*, 1–14.

Krajzewicz, Daniel, Heinrich, M., & Milano, M. (2013). COLOMBO: Investigating the Potential of V2X for Traffic Management Purposes assuming low penetration Rates. *9th ITS European Congress*. http://elib.dlr.de/83217/1/paper_200_1366355375.pdf

Krauß, S. (1998). *Microscopic Modeling of Traffic Flow: Investigation of Collision Free Vehicle Dynamics*.

Kun, C., & Lei, Y. U. (2007). Microscopic Traffic-Emission Simulation and Case Study for Evaluation of Traffic Control Strategies. *Journal of Transportation Systems Engineering and Information Technology*, *7*(1), 93–99. https://doi.org/https://doi.org/10.1016/S1570-6672(07)60011-7

Kuwahara, M., de Kievit, Martijn; Shladover, S., Zhang, W.-B., & Barth, M. (n.d.). *Guidelines for Assessing the Effects of ITS on CO 2 Emissions - International Joint Report -*.

Kwak, K. H., Woo, S. H., Kim, K. H., Lee, S. B., Bae, G. N., Ma, Y. Il, Sunwoo, Y., & Baik, J. J. (2018). On-road air quality associated with traffic composition and street-canyon ventilation: Mobile monitoring and CFD modeling. *Atmosphere*, *9*(3), 1–13. https://doi.org/10.3390/atmos9030092

Lateb, M., Meroney, R. N., Yataghene, M., Fellouah, H., Saleh, F., & Boufadel, M. C. (2016). On the use of numerical modelling for near-field pollutant dispersion in urban environments - A review. *Environmental Pollution*, *208*, 271–283. https://doi.org/10.1016/j.envpol.2015.07.039

Lebedevas, S., Dailydka, S., Jastremskas, V., & Rapalis, P. (2015). The influence of locomotive diesel engine transient operating modes on energy usage. *Transportation Research Part D: Transport and Environment*, *34*, 219–229. https://doi.org/10.1016/j.trd.2014.10.011

Lee, F., Lee, C. E., Machemehl, R. B., & Copeland, C. R. (1983). *Simulation of Vehicle Emissions at Intersections*.

Lejri, D., Can, A., Schiper, N., & Leclercq, L. (2018). Accounting for traffic speed dynamics when calculating COPERT and PHEM pollutant emissions at the urban scale. *Transportation Research Part D: Transport and Environment*, *63*, 588–603. https://doi.org/10.1016/j.trd.2018.06.023

Li, X., & Sun, J. (2014). Effect of interactions between vehicles and pedestrians on fuel consumption and emissions. *Physica A*, *416*, 661–675. https://doi.org/10.1016/j.physa.2014.09.028

Ligterink, N. E., & de Lange, R. (2009). Refined vehicle and driving-behaviour dependencies in the VERSIT + emission model. *ETAPP Symposium*, 1–8.

Lin, J., & Ge, Y. E. (2006). Impacts of traffic heterogeneity on roadside air pollution concentration. *Transportation Research Part D: Transport and Environment*, *11*(2), 166–170. https://doi.org/10.1016/j.trd.2005.12.001

Lozhkina, O. V., & Lozhkin, V. N. (2016). Estimation of nitrogen oxides emissions from petrol and diesel passenger cars by means of on-board monitoring: Effect of vehicle speed, vehicle technology, engine type on emission rates. *Transportation Research Part D: Transport and Environment*, *47*, 251–264. https://doi.org/10.1016/j.trd.2016.06.008

Lu, C., Zheng, F., Li, J., Zuylen, H. Van, & Lu, C. (2017). Influence of driver characteristics on emissions and fuel consumption. *Transportation Research Procedia*, *27*, 624–631. https://doi.org/10.1016/j.trpro.2017.12.142

Lüßmann, J., Vreeswijk, J., Katwijk, R. van, Blokpoel, R., & Fullerton, M. (2014). Impact assessment for cooperative urban traffic management applications based on microscopic traffic flow simulation. *21st World Congress on Intelligent Transport Systems, ITSWC 2014: Reinventing Transportation in Our Connected World*, 1–13.

Luz, R. ;, & Hausberger, S. (2011). *User Guide for Version 2011*.

Lv, J., & Zhang, Y. (2012). Effect of signal coordination on traffic emission. *Transportation Research Part D*, *17*(2), 149–153. https://doi.org/10.1016/j.trd.2011.10.005

M. Cormack, R & Cliff, Andrew & K. Ord, J. (1975). Spatial autocorrelation. *Journal of the Royal Statistical Society. Series A (General)*, *138*, 103–104. https://doi.org/10.2307/2345258

Macedo, E., Tomás, R., Fernandes, P., Coelho, M. C., & Bandeira, J. M. (2020). Quantifying road traffic emissions embedded in a multi-objective traffic assignment model. *Transportation Research Procedia*, *47*(2019), 648–655. https://doi.org/10.1016/j.trpro.2020.03.143

Maciejewski, M. (2010). A Comparison of Microscopic Traffic Flow Simulation systems for an urban area. *Transport Problems*, *5*(4).

Maerivoet, S., & De Moor, B. (2005). *Transportation Planning and Traffic Flow Models*. *32*(0). http://arxiv.org/abs/physics/0507127

Mahmod, M., Jonkers, E., Klunder, G. A., Benz, T., & Winder, A. (2015). Amitran methodology framework for evaluating the impact of information and communication technology-based measures on CO2 emissions in the transport field. *IET Intelligent Transport Systems*, *9*(4), 418–428. https://doi.org/10.1049/iet-its.2014.0058

MathWorks. (2020). *cordexch*. https://www.mathworks.com/help/stats/cordexch.html

Matthaios, V. N., Kramer, L. J., Sommariva, R., Pope, F. D., & Bloss, W. J. (2019). Investigation of vehicle cold start primary NO2 emissions inferred from ambient monitoring data in the UK and their implications for urban air quality. *Atmospheric Environment*, *199*, 402–414. https://doi.org/10.1016/j.atmosenv.2018.11.031

Matzoros, A., & Van Vliet, D. (1992). A model of air pollution from road traffic, based on the characteristics of interrupted flow and junction control: Part I - model description. *Transportation Research Part A*, *26*(4), 315–330. https://doi.org/10.1016/0965-8564(92)90019-4

Mera, Z., Fonseca, N., López, J. M., & Casanova, J. (2019). Analysis of the high instantaneous NOx emissions from Euro 6 diesel passenger cars under real driving conditions. *Applied Energy*, *242*, 1074–1089. https://doi.org/10.1016/j.apenergy.2019.03.120

Minitab Blog Editor. (2016). *When Should You Fit a Non-Hierarchical Regression Model?* https://blog.minitab.com/blog/adventures-in-statistics-2/when-should-you-fit-a-non-hierarchical-regression-model

Minitab Blog Editor. (2019). *How to Choose the Best Regression Model(Blog post)*. https://blog.minitab.com/blog/how-to-choose-the-best-regression-model

Minitab Statisticians. (n.d.). *Multiple Regression*.

Montazeri-Gh, M., & Fotouhi, A. (2011). Traffic condition recognition using the k-means clustering method. *Scientia Iranica*, *18*(4), 930–937. https://doi.org/10.1016/j.scient.2011.07.004

Montgomery, D. C. (2017). Design and analysis of experiments, 8th Edition. In *Design and analysis of experiments, 8th Edition*. John Wiley & Sons Inc.

Moran, P. A. P. (1948). The Interpretation of Statistical Maps. *Journal of the Royal Statistical Society. Series B (Methodological)*, *10*(2), 243–251.

Murena, F., Favale, G., Vardoulakis, S., & Solazzo, E. (2009). Modelling dispersion of traffic pollution in a deep street canyon: Application of CFD and operational models. *Atmospheric Environment*, *43*(14), 2303–2311. https://doi.org/10.1016/j.atmosenv.2009.01.038

Nagel, K., & Schreckenberg, M. (1992). A Cellular Automation Model for Freeway Traffic. *Journal de Physique*, *2*, 2221–2229.

Negrenti, E. (1999). The “Corrected Average Speed” approach in ENEA’s TEE model: An innovative solution for the evaluation of the energetic and environmental impacts of urban transport policies. *Science of the Total Environment*, *235*(1–3), 411–413. https://doi.org/10.1016/S0048-9697(99)00249-1

Negrenti, E, Carrese, S., Beltran, B., Parenti, A., Giovannini, F., & Lapolla, V. (2007). Modelling vehicles kinematics and parking processes relevance on pollutant emissions in the city of Florence. *WIT Transactions on Ecology and the Environment*, *101*, 341–350. https://doi.org/10.2495/AIR070341

Negrenti, Emanuele. (1996). TEE: the ENEA traffic emissions and energetics model micro-scale applications. *Science of the Total Environment*, *189–190*, 167–174. https://doi.org/10.1016/0048-9697(96)05206-0

Neunzig, D., Weilkes, M., Hochstädter, A., & Ludmann, J. (1998). Assessment of advanced vehicle control systems with the vehicle oriented traffic simulation tool PELOPS. *SAE Technical Papers*, *724*. https://doi.org/10.4271/981890

Ni, D. (2020). Traffic Signal Coordination. In *Signalized Intersections: Fundamentals to Advanced Systems* (p. 335). Springer International Publishing.

Ni, Daiheng. (2011). Multiscale Modeling of Traffic Flow. *Mathematica Aeterna*, *1*(01), 27–54.

Ni, Daiheng. (2016). Traffic Sensing Technologies. In *Traffic Flow Theory* (pp. 3–17). Butterworth-Heinemann. https://doi.org/10.1016/b978-0-12-804134-5.00001-5

NIST. (2013). *NIST/SEMATECH e-Handbook of Statistical Methods*. https://www.itl.nist.gov/div898/handbook/pmd/section3/pmd34.htm

Office of the Assistant Secretary for Research and Technology (OST-R). (n.d.). *Multi-Modal Intelligent Traffic Safety System (MMITSS)*. https://www.its.dot.gov/research_archives/dma/bundle/mmitss_plan.htm

Organ, B., Huang, Y., Zhou, J. L., Yam, Y. S., Mok, W. C., & Chan, E. F. C. (2020). Simulation of engine faults and their impact on emissions and vehicle performance for a liquefied petroleum gas taxi. *Science of the Total Environment*, *716*(2), 137066. https://doi.org/10.1016/j.scitotenv.2020.137066

Osorio, C., & Nanduri, K. (2015). Urban transportation emissions mitigation: Coupling high-resolution vehicular emissions and traffic models for traffic signal optimization. *Transportation Research Part B: Methodological*, *81*, 520–538. https://doi.org/10.1016/j.trb.2014.12.007

Pace, R. Di, Cantarella, G. E., De Luca, S., & Gangi, M. Di. (2017). Scheduled Synchronisation based on a mesoscopic flow model with speed dispersion. *Transportation Research Procedia*, *27*, 180–187. https://doi.org/10.1016/j.trpro.2017.12.107

Pandian, S., Gokhale, S., & Ghoshal, A. K. (2009). Evaluating effects of traffic and vehicle characteristics on vehicular emissions near traffic intersections. *Transportation Research Part D: Transport and Environment*, *14*(3), 180–196. https://doi.org/10.1016/j.trd.2008.12.001

Papson, A., Hartley, S., & Kuo, K. (2012). Analysis of Emissions at Congested and Uncongested Intersections with Motor Vehicle Emission Simulation 2010. *Transportation Research Record: Journal of the Transportation Research Board*, *2270*(1), 124–131. https://doi.org/https://doi.org/10.3141/2270-15

Pardoe, I., Simon, L., & Young, D. (2020). *Detecting Multicollinearity Using Variance Inflation Factors*. STAT 501. https://online.stat.psu.edu/stat501/lesson/12/12.4

Pasquale, C., Sacone, S., & Siri, S. (2014). Two-class emission traffic control for freeway systems. *19th World Congress The International Federation of Automatic Control*, *47*(3), 936–941. https://doi.org/10.3182/20140824-6-ZA-1003.01995

Pathak, S. K., Sood, V., Singh, Y., & Channiwala, S. A. (2016). Real world vehicle emissions: Their correlation with driving parameters. *Transportation Research Part D: Transport and Environment*, *44*, 157–176. https://doi.org/10.1016/j.trd.2016.02.001

Pelkmans, L., Debal, P., Hood, T., Hauser, G., & Delgado, M. R. (2004). Development of a simulation tool to calculate fuel consumption and emissions of vehicles operating in dynamic conditions. *SAE Technical Papers*, *724*. https://doi.org/10.4271/2004-01-1873

Perallos, A., Hernandez-jayo, U., Onieva, E., Julio, I., & Zuazola, G. (2015). Traffic Management Systems. In A. Perallos, U. Hernandez-Jayo, E. Onieva, & I. J. G. Zuazola (Eds.), *Intelligent Transport Systems: Technologies and Applications* (p. 368). John Wiley & Sons, Ltd.

Prakash, S., & Bodisco, T. A. (2019). An investigation into the effect of road gradient and driving style on NOX emissions from a diesel vehicle driven on urban roads. *Transportation Research Part D: Transport and Environment*, *72*(X), 220–231. https://doi.org/10.1016/j.trd.2019.05.002

Priemer, C., & Friedrich, B. (2009). A decentralized adaptive traffic signal control using V2I communication data. *IEEE Conference on Intelligent Transportation Systems, Proceedings, ITSC*, 765–770. https://doi.org/10.1109/ITSC.2009.5309870

PTV Planning Transport Verkehr AG. (2011). *VISSIM 5.40 User Manual*.

Rakha, H., Van Aerde, M., Ahn, K., & Trani, a. a. (2000). Requirements for evaluating traffic signal control impacts on energy and emissions based on instantaneous speed and acceleration measurements. *Transportation Research Record*, *1738*, 56–67. https://doi.org/10.3141/1738-07

Rakha, Hesham, Ahn, K., & Trani, A. (2004). Development of VT-Micro model for estimating hot stabilized light duty vehicle and truck emissions. *Transportation Research Part D: Transport and Environment*, *9*(1), 49–74. https://doi.org/10.1016/S1361-9209(03)00054-3

Rakha, Hesham, Yue, H., & Dion, F. (2011). VT-Meso model framework for estimating hot-stabilized light-duty vehicle fuel consumption and emission rates. *Canadian Journal of Civil Engineering*, *38*(11), 1274–1286. https://doi.org/10.1139/l11-086

Reuschel, A. (1950). Fahrzeugbewegungen in der kolonne bei gleichfoermig beschleunigtem oder verzoegertem leifahrzeug. Z. Oesterr.. [251]. *Zeitschrift Des Österreichischen Ingenieurund Architekten-Vereine*, *95*, 59–62,73–77.

Rexeis, M., Hausberger, S., Zallinger, M. S., & Kurz, C. (2007). PHEM and NEMO: Tools for micro and meso-scale emission modelling. *Abstracts of the 6th International Conference on Urban Air Quality*, S109.

Ritner, M., Westerlund, K. K., Cooper, C. D., & Claggett, M. (2013). Accounting for acceleration and deceleration emissions in intersection dispersion modeling using MOVES and CAL3QHC. *Journal of the Air and Waste Management Association*, *63*(6), 724–736. https://doi.org/10.1080/10962247.2013.778220

Robertson, D. I. (1969). *TRANSYT: A traffic network study tool*.

Rzeszutek, M., & Szulecka, A. (2016). Near-road air quality assessment for selected urban agglomerations in Poland. *Res. J. Univ. Gdańsk. Transp. Econ. Logist.*, *59*, 339–351(In Polish). https://doi.org/Logist. 59, 339–351 (In Polish) https://pbn.nauka.gov.pl/polindex-webapp/browse/article/article-1eede014-63cc-42fe-86d5-85469a6827f1

Rzeszutek, Mateusz, Bogacki, M., Bździuch, P., & Szulecka, A. (2019). Improvement assessment of the OSPM model performance by considering the secondary road dust emissions. *Transportation Research Part D: Transport and Environment*, *68*(April), 137–149. https://doi.org/10.1016/j.trd.2018.04.021

Saharan, S., Bawa, S., & Kumar, N. (2020). Dynamic pricing techniques for Intelligent Transportation System in smart cities: A systematic review. *Computer Communications*, *150*, 603–625. https://doi.org/10.1016/j.comcom.2019.12.003

Salamati, K., Rouphail, N. M., Frey, H. C., Liu, B., & Schroeder, B. J. (2015). A Simplified Method for Comparing Emissions in Roundabouts and at Signalized Intersections. *Transportation Research Record: Journal of the Transportation Research Board*, *2517*, 48–60.

Schreckenberg, M., Kerner, B. S., Rehborn, H., Koller, M., & Hemmerle, P. (2015). Fuel consumption in empirical synchronised flow in urban traffic. *IET Intelligent Transport Systems*, *10*, 1–8. https://doi.org/10.1049/iet-its.2015.0014

Sipos, T. (2017). Spatial Statistical Analysis of the Traffic Accidents. *Periodica Polytechnica Transportation Engineering*, *45*(2), 101–105. https://doi.org/10.3311/PPtr.9895

Slavin, C., Feng, W., Figliozzi, M., & Koonce, P. (2013). Statistical Study of the Impact of Adaptive Traffic Signal Control on Traffic and Transit Performance. *Transportation Research Record: Journal of the Transportation Research Board*, *2356*, 117–126. https://doi.org/10.1177/0361198113235600114

Smit, R. (2006). *An examination of congestion in road traffic emission models and their application to urban road networks*. Griffith University.

Smit, R. (2013). Development and performance of a new vehicle emissions and fuel consumption software (PΔP) with a high resolution in time and space. *Atmospheric Pollution Research*, *4*(3), 336–345. https://doi.org/10.5094/APR.2013.038

Smucker, B., Krzywinski, M., & Altman, N. (2018). Optimal experimental design. *Nature Methods*, *15*(8), 559–560. https://doi.org/10.1038/s41592-018-0083-2

So, J. (Jason), Motamedidehkordi, N., Wu, Y., Busch, F., & Choi, K. (2018). Estimating emissions based on the integration of microscopic traffic simulation and vehicle dynamics model. *International Journal of Sustainable Transportation*, *12*(4), 286–298. https://doi.org/10.1080/15568318.2017.1363328

Soltic, P., & Hausberger, S. (2004). Emission Measurements and Modelling of a Tractor-Semitrailer in Trans-Alpine Operation. *Conference: Transport and Air Pollution*.

Song, G., Yu, L., & Xu, L. (2013). Comparative Analysis of Car-Following Models for Emissions Estimation. *Transportation Research Record: Journal of the Transportation Research Board*, *2341*(1), 12–22. https://doi.org/10.3141/2341-02

Soulhac, L., Salizzoni, P., Mejean, P., Didier, D., & Rios, I. (2012). The model SIRANE for atmospheric urban pollutant dispersion; PART II, validation of the model on a real case study. *Atmospheric Environment*, *49*, 320–337. https://doi.org/10.1016/j.atmosenv.2011.11.031

Soulhac, Lionel, Salizzoni, P., Cierco, F. X., & Perkins, R. (2011). The model SIRANE for atmospheric urban pollutant dispersion; part I, presentation of the model. *Atmospheric Environment*, *45*(39), 7379–7395. https://doi.org/10.1016/j.atmosenv.2011.07.008

Sparmann, U. (1978). Spurwechselvorg¨ange auf zweispurigen BAB-Richtungsfahrbahnen. *Forschung, Straßenbau Und Straßenverkehrstechni*, *263*.

Stern, R. E., Chen, Y., Churchill, M., Wu, F., Delle Monache, M. L., Piccoli, B., Seibold, B., Sprinkle, J., & Work, D. B. (2019). Quantifying air quality benefits resulting from few autonomous vehicles stabilizing traffic. *Transportation Research Part D: Transport and Environment*, *67*(December 2018), 351–365. https://doi.org/10.1016/j.trd.2018.12.008

Stevanovic, A., Stevanovic, J., Zhang, K., & Batterman, S. (2009). Optimizing Traffic Control to Reduce Fuel Consumption and Vehicular Emissions:Optimizing traffic control to reduce fuel consumption and vehicular emissions: Integrated approach with VISSIM, CMEM, and VISGAOST. *Transportation Research Record: Journal of the Transportation Research Board*, *2128*, 105–113. https://doi.org/10.3141/2128-11

Sturm, P. J., Pucher, K., Sudy, C., & Almbauer, R. A. (1996). Determination of traffic emissions - Intercomparison of different calculation methods. *Science of the Total Environment*, *189–190*, 187–196. https://doi.org/10.1016/0048-9697(96)05209-6

Sun, D., Zhang, K., & Shen, S. (2018). Analyzing spatiotemporal traffic line source emissions based on massive didi online car-hailing service data. *Transportation Research Part D: Transport and Environment*, *62*(800), 699–714. https://doi.org/10.1016/j.trd.2018.04.024

Sun, J., Niu, D., Chen, S., & Li, K. (2013). Development and Investigation of a Dynamic Eco-Driving Speed Guidance Strategy for Signalized Highway Traffic. *TRB 92nd Annual Meeting Compendium of Papers*, 23.

Tang, K., Li, K., Li, M., & Liu, D. (2019). China. In K. Tang, M. Boltze, H. Nakamura, & Z. Tian (Eds.), *Global Practices on Road Traffic Signal Control: Fixed-Time Control at Isolated Intersections* (p. 344). Elsevier Science. https://doi.org/https://doi.org/10.1016/B978-0-12-815302-4.00011-X

Targino, A. C., Gibson, M. D., Krecl, P., Rodrigues, M. V. C., dos Santos, M. M., & de Paula Corrêa, M. (2016). Hotspots of black carbon and PM 2.5 in an urban area and relationships to traffic characteristics. *Environmental Pollution*, *218*, 475–486. https://doi.org/10.1016/j.envpol.2016.07.027

Tate, J., & Connors, R. (2012). *Mapping vehicle emissions through urban streets and intersections*. 2011–2012.

Tate, J., & Connors, R. (2014). Mapping vehicle emissions through urban streets and intersections. *20th International Transport and Air Pollution Conference, 2014*.

Tielert, T., Killat, M., Hartenstein, H., Luz, R., Hausberger, S., & Benz, T. (2010). The impact of traffic-light-to-vehicle communication on fuel consumption and emissions. *2010 Internet of Things (IOT)*, 1–8. https://doi.org/10.1109/IOT.2010.5678454

Tominaga, Y., & Stathopoulos, T. (2011). CFD modeling of pollution dispersion in a street canyon: Comparison between LES and RANS. *Journal of Wind Engineering and Industrial Aerodynamics*, *99*(4), 340–348. https://doi.org/10.1016/j.jweia.2010.12.005

Transportation Research Board. (2002). *The Congestion Mitigation and Air Quality Improvement Program: assessing 10 years of experience*.

Transportation Research Board (TRB). (2010). *Highway capacity manual*.

Tripathy, S., & Hota, S. (2012). A survey on partitioning and parallel partitioning clustering algorithms. *Studies in Regional Science*, *42*(4), 897–909. https://doi.org/10.1007/s11115-013-0241-z

Turkensteen, M. (2017). The accuracy of carbon emission and fuel consumption computations in green vehicle routing. *European Journal of Operational Research*, *262*(2), 647–659. https://doi.org/10.1016/j.ejor.2017.04.005

Unal, A, Christopher Frey, H., Rouphail, N. M., & Colyar, J. D. (2001). Hot spot analysis of real world vehicle emissions based upon a portable on-board measurement system. *Proceedings of the Air & Waste Management Association 94th Annual Meeting and Exhibition*, *x*, Paper No.42159.

Unal, Alper, Frey, H. C., & Rouphail, N. M. (2004). Quantification of Highway Vehicle Emissions Hot Spots Based upon On-Board Measurements. *Journal of the Air and Waste Management Association*, *54*(2), 130–140. https://doi.org/10.1080/10473289.2004.10470888

van Katwijk, R. . (2012). Using I2V Communication to Reduce Traffic Emissions at Urban Signalized Intersections. *Procedia - Social and Behavioral Sciences*, *48*, 2385–2392. https://doi.org/10.1016/j.sbspro.2012.06.1209

Vardoulakis, S., Fisher, B. E. A., Pericleous, K., & Gonzalez-Flesca, N. (2003). Modelling air quality in street canyons: A review. *Atmospheric Environment*, *37*(2), 155–182. https://doi.org/10.1016/S1352-2310(02)00857-9

Vieira da Rocha, T., Can, A., Parzani, C., Jeanneret, B., Trigui, R., & Leclercq, L. (2013). Are vehicle trajectories simulated by dynamic traffic models relevant for estimating fuel consumption? *Transportation Research Part D: Transport and Environment*, *24*, 17–26. https://doi.org/10.1016/j.trd.2013.03.012

Wang, A., Fallah-Shorshani, M., Xu, J., & Hatzopoulou, M. (2016). Characterizing near-road air pollution using local-scale emission and dispersion models and validation against in-situ measurements. *Atmospheric Environment*, *142*, 452–464. https://doi.org/10.1016/j.atmosenv.2016.08.020

Wang, M., Hoogendoorn, S., Daamen, W., & van Arem, B. (2014). Potential impacts of ecological adaptive cruise control systems on traffic and environment. *IET Intelligent Transport Systems*, *8*(2), 77–86. https://doi.org/10.1049/iet-its.2012.0069

Wang, Y., Szeto, W. Y., Han, K., & Friesz, T. L. (2018). Dynamic traffic assignment: A review of the methodological advances for environmentally sustainable road transportation applications. *Transportation Research Part B: Methodological*, *111*, 370–394. https://doi.org/10.1016/j.trb.2018.03.011

Wiedemann, R. (1974). *Simulation des Straßenverkehrsflusses*. Universität Karlsruhe.

Wolfermann, A., Friedrich, B., & Fellendorf, M. (2019). Germany and Austria. In K. Tang, M. Boltze, H. Nakamura, & Z. Tian (Eds.), *Global Practices on Road Traffic Signal Control:*

Fixed-Time Control at Isolated Intersections (p. 344). Elsevier Science. https://doi.org/https://doi.org/10.1016/C2017-0-02878-1

Wong, W. K. (1994). Comparing robust properties of A, D, E and G-optimal designs. *Computational Statistics and Data Analysis*, *18*(4), 441–448. https://doi.org/10.1016/0167-9473(94)90161-9

Woodward, H., Stettler, M., Pavlidis, D., Aristodemou, E., ApSimon, H., & Pain, C. (2019). A large eddy simulation of the dispersion of traffic emissions by moving vehicles at an intersection. *Atmospheric Environment*, *215*(August), 116891. https://doi.org/10.1016/j.atmosenv.2019.116891

World Health Organization. (2018). *9 out of 10 people worldwide breathe polluted air, but more countries are taking action*. https://www.who.int/news-room/detail/02-05-2018-9-out-of-10-people-worldwide-breathe-polluted-air-but-more-countries-are-taking-action

Wu, K., Chen, Y., Ma, J., Bai, S., & Tang, X. (2017). Traffic and emissions impact of congestion charging in the central Beijing urban area: A simulation analysis. *Transportation Research Part D: Transport and Environment*, *51*, 203–215. https://doi.org/10.1016/j.trd.2016.06.005

Yale University. (n.d.). *Experimentation*. http://www.stat.yale.edu/Courses/1997-98/101/expdes.htm

Yang, G., & Tian, Z. (2019). An exploratory investigation of the impact of ramp metering on driver acceleration behavior. *IATSS Research*, *43*(4), 277–285. https://doi.org/10.1016/j.iatssr.2019.03.002

Yang, H., Zhai, X., & Zheng, C. (2018). Effects of variable speed limits on traffic operation characteristics and environmental impacts under car-following scenarios: Simulations in the framework of Kerner's three-phase traffic theory. *Physica A: Statistical Mechanics and Its Applications*, *509*, 567–577. https://doi.org/10.1016/j.physa.2018.05.032

Ye, B. L., Wu, W., & Mao, W. (2015). A Method for Signal Coordination in Large-Scale Urban Road Networks. *Mathematical Problems in Engineering*, *2015*. https://doi.org/10.1155/2015/720523

Yusof, N. N., Mohamed, A., & Abdul-Rahman, S. (2015). Implementation of Dynamic Traffic Routing for Traffic Congestion: A Review. In M. Berry, A. Mohamed, & B. Yap (Eds.), *Soft Computing in Data Science* (pp. 174–186). Springer. https://doi.org/10.1007/978-981-287-936-3

Zachiotis, A. T., & Giakoumis, E. G. (2019). Non-regulatory parameters effect on consumption and emissions from a diesel-powered van over the WLTC. *Transportation Research Part D: Transport and Environment*, *74*(August), 104–123. https://doi.org/10.1016/j.trd.2019.07.019

Zallinger, M. S., Le Anh, T., & Hausberger, S. (2005). Improving an Instantaneous Emission Model for Passenger Cars. *14th Symposium Transport and Air Pollution*.

Zegeye, S. K., De Schutter, B., Hellendoorn, J., Breunesse, E. A., & Hegyi, A. (2013). Integrated macroscopic traffic flow, emission, and fuel consumption model for control

purposes. *Transportation Research Part C: Emerging Technologies*, *31*, 158–171. https://doi.org/10.1016/j.trc.2013.01.002

Zhang, K., & Batterman, S. (2013). Air pollution and health risks due to vehicle traffic. *Science of the Total Environment*, *450–451*, 307–316. https://doi.org/10.1016/j.scitotenv.2013.01.074

Zhang, Y., & Ioannou, P. A. (2016). Environmental Impact of Combined Variable Speed Limit and Lane Change Control: A Comparison of MOVES and CMEM Model. IFAC-PapersOnLine, 49(3), 323–328. https://doi.org/10.1016/j.ifacol.2016.07.054

Abbreviations

NO_x	nitrogen oxides
PM	particulate matter
PM2.5	fine particulate matter
CO	carbon monoxide
CFD	computational fluid dynamics
HCs	hydrocarbons
SO_x	sulfur oxides
a_r	ratio of the right turns
C	cycle time of the signal [s]
c	capacity [veh/hour]
c_e	capacity of the east approach [veh/hour]
c_n	capacity of the north approach [veh/hour]
c_sr	capacity of the lane with straight-through and right-turning traffic [veh/hour]
cold spot_s	cold spot of the straight-through lane
cold spot_sr	cold spot of the lane with straight-through and right-turning traffic
cold spot_slr	cold sport on the lane with mixed traffic
crossing_s_s	crossing of the straight-through traffic from the straight-through lane
crossing_s_sr	crossing of the straight-through traffic from the lane with straight-through and right-turning traffic
EF	emission factor [g/km]
EF_NO_x	average emission factor of NO_x [g/km]
hot spot_l	hot spot of the left-turning lane
hot spot_s	hot spot of the straight-through lane
hot spot_sr	hot spot of the lane with straight-through and right-turning traffic

ITS	intelligent transportation systems
local Getis' Gi	Local Gi*
OLS	ordinary least squares
PF	percentage error
Q	traffic volume [veh/hour]
q_c	conflicting traffic volume [veh/hour]
q_es	traffic volume of the straight-through traffic on the east approach [veh/hour]
q_l	traffic volume of left turns [veh/hour]
q_nr	traffic volume of the right turns from the north approach [veh/hour]
q_r	traffic volume of right turns [veh/hour]
q_s	traffic volume of straight going [veh/hour]
q_sl	traffic volume of the left turns on the south approach [veh/hour]
q_total	total traffic volume of the straight-through and right-turning traffic [veh/hour]
RMSE	root mean square error
Truck_c	truck percentage of the conflicting traffic
Truck_es	truck percentage of the straight-through traffic on the east approach
Truck_l	truck percentage of the left-turning traffic
Truck_r	truck percentage of the right-turning traffic
Truck_s	truck percentage of the straight-through traffic
truck_sl	truck percentage of the left turns on the south approach
truck_nr	truck percentage of the right turns on the north approach
V	speed limit [km/hour]
VIF	variance inflation factors
$\bar{v}$	average speed [km/hour]

List of figures

List of tables

Appendix：emission functions for upper parts, crossing lanes and after crossing

Upper part on the straight-through lane

The truck percentage, speed limit, hourly traffic volume, and capacity are used as predictors. The stepwise model is chosen to be the best model since the residuals of the linear model distribute as a curve, and the full interaction model includes some interaction terms statistically insignificant. The effect of each predictor is seen in Fig. A. 1.

- The truck percentage has a positive relation to the emission factor of NO_x.
- The emission factor of NO_x is positively related to traffic volume.
- The speed limit has a negative relation to the emission factor of NO_x.
- With higher capacity, the emission factor of NO_x gets lower.

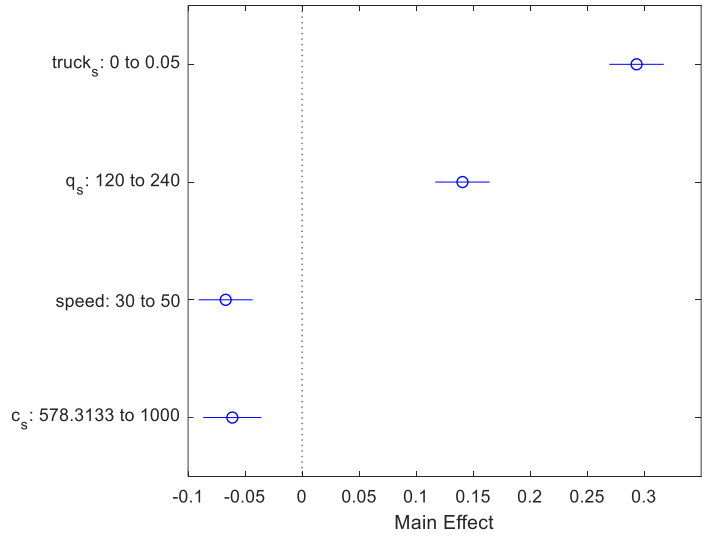

Fig. A. 1 Effect on upstream of the straight-through lane

Upper part on the left-turning lane

As shown in Fig. A. 2,

- The percentage of the truck has a positive relationship with the emission factor of NO_x. The size gets bigger in case of bigger traffic volume, smaller capacity, and slower speed limit. The difference in emission factors between the truck and car is bigger during acceleration than during other driving modes. When there is more queue due to bigger volume or smaller capacity, the higher truck percentage can cause a higher emission factor of NO_x. With a higher speed limit, there are more decelerations upstream on which the emission factor between trucks and passengers is smaller. Consequently, the effect size of the truck percentage gets smaller.

- Traffic volume has a positive relationship with the emission factor. The size gets smaller when there is less truck percentage, or there is a higher capacity that causes the queue shorter.

- Capacity has a negative effect on the emission factor. The absolute effect size gets bigger when there are more trucks, traffic volume, and opposite traffic.

- When the speed limit is higher, the emission factor drops. The absolute effect size gets bigger in case of the high truck percentages.

- Opposite traffic volume has a negative relation with the emission factor of NO_x. And the absolute effect size gets bigger when more traffic volume or less capacity.

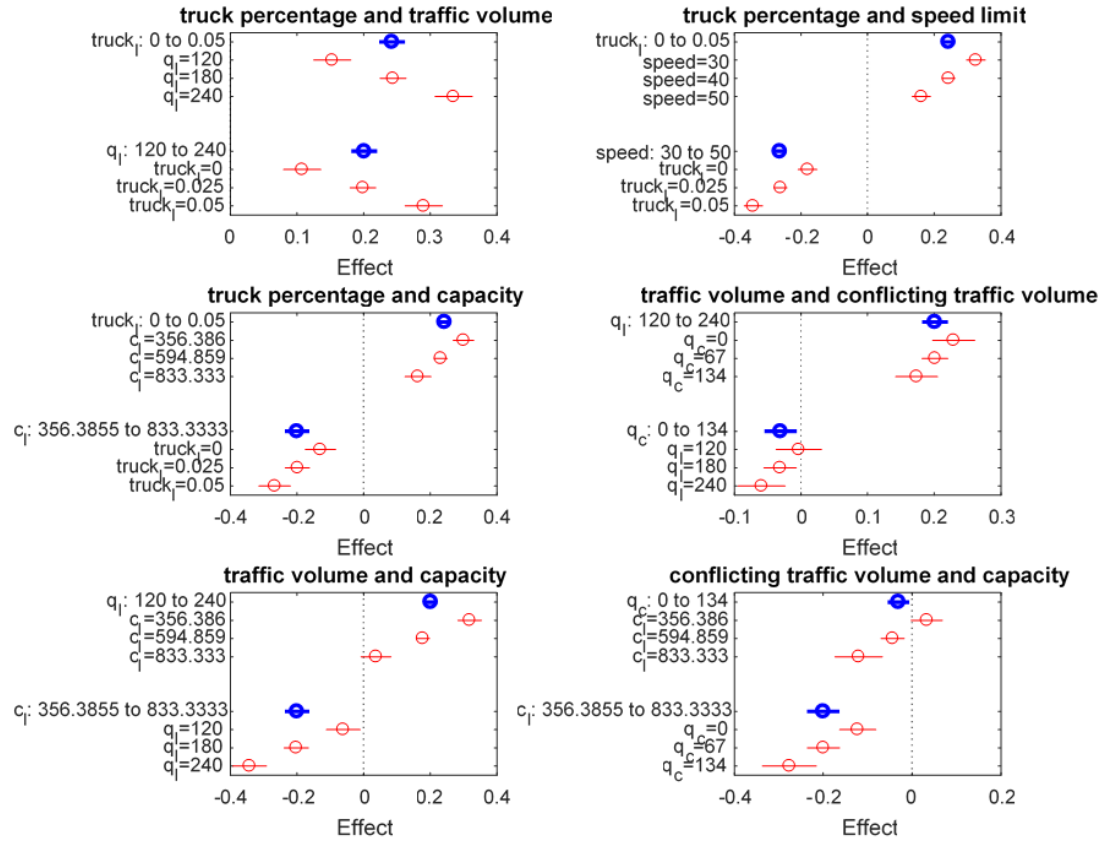

Fig. A. 2 Interaction effect of upstream on the left-turning lane

The upper part before the turning lane

After checking each intersection effect of the stepwise model (Fig. A. 3 - Fig. A. 6), the findings are below:

- The truck percentage of each driving direction has a positive relationship with the emission factor of NO_x. The effect size is smaller when there is more traffic volume from the other two directions. The effect size is bigger when more traffic in the same direction. With a slower speed limit, the positive effect of truck percentage gets much bigger. The effect of truck percentage of straight-through traffic is negatively dependent on the truck percentage of right-turning and left-turning.

- With more right-turning traffic volume, the emission factor of NO_x is lower. Its absolute effect size gets higher with the bigger truck percentage of left-turning or straight-through, or smaller truck percentage of right turns. The absolute effect size gets smaller with higher traffic volume of the straight-through or left-turning traffic, but with lower average speed.

- With more traffic volume of left turns, the emission factor of NO_x is higher. The effect size gets bigger with more truck percentage of left turns, while with less truck percentage of straight-through or right-turning traffic. The effect size gets higher with more traffic volume of straight-through or right-turning traffic, but with lower average speed.

- With more straight-through traffic volume, the emission factor of NO_x is higher. The effect size gets bigger with more truck percentage of the straight-through or left-turning traffic, while with less right-turning trucks. The effect size gets higher with more left-or right-turning traffic volume.

- In the case of a higher speed limit, the emission factor of NO_x is higher. Its effect size becomes smaller when there are higher truck percentages.

- In the case of lower average speed, the emission factor of NO_x is higher. Its absolute effect size becomes bigger when there is more turning traffic.

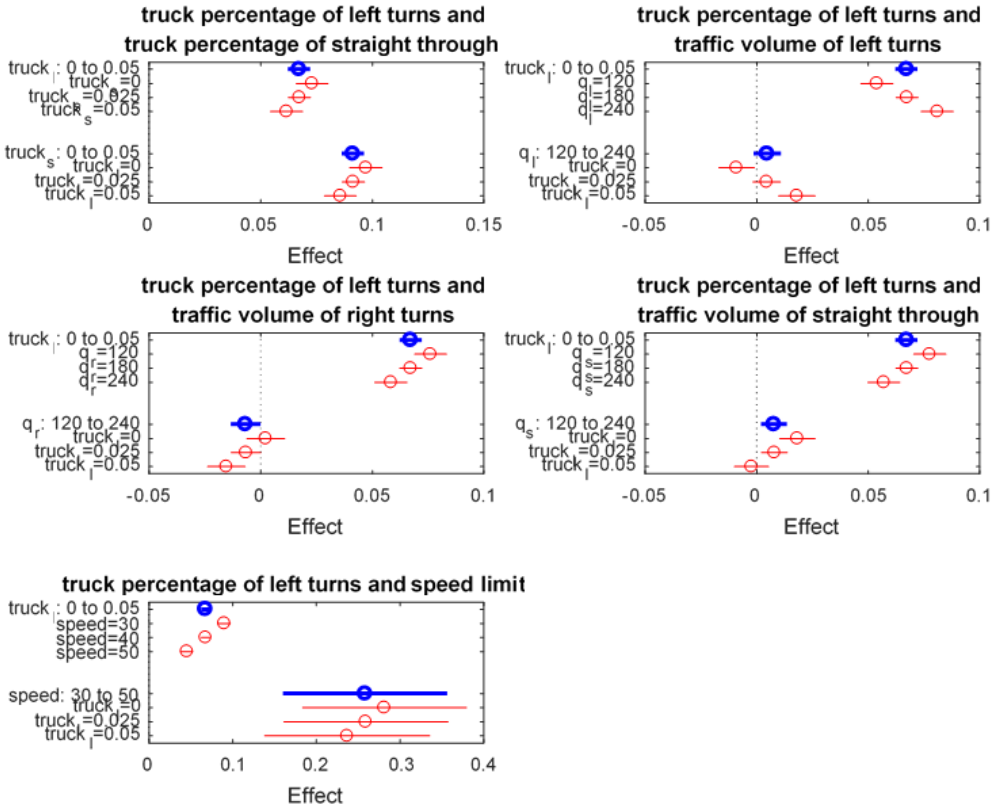

Fig. A. 3 Interaction effect between the truck percentage of the left turns with others

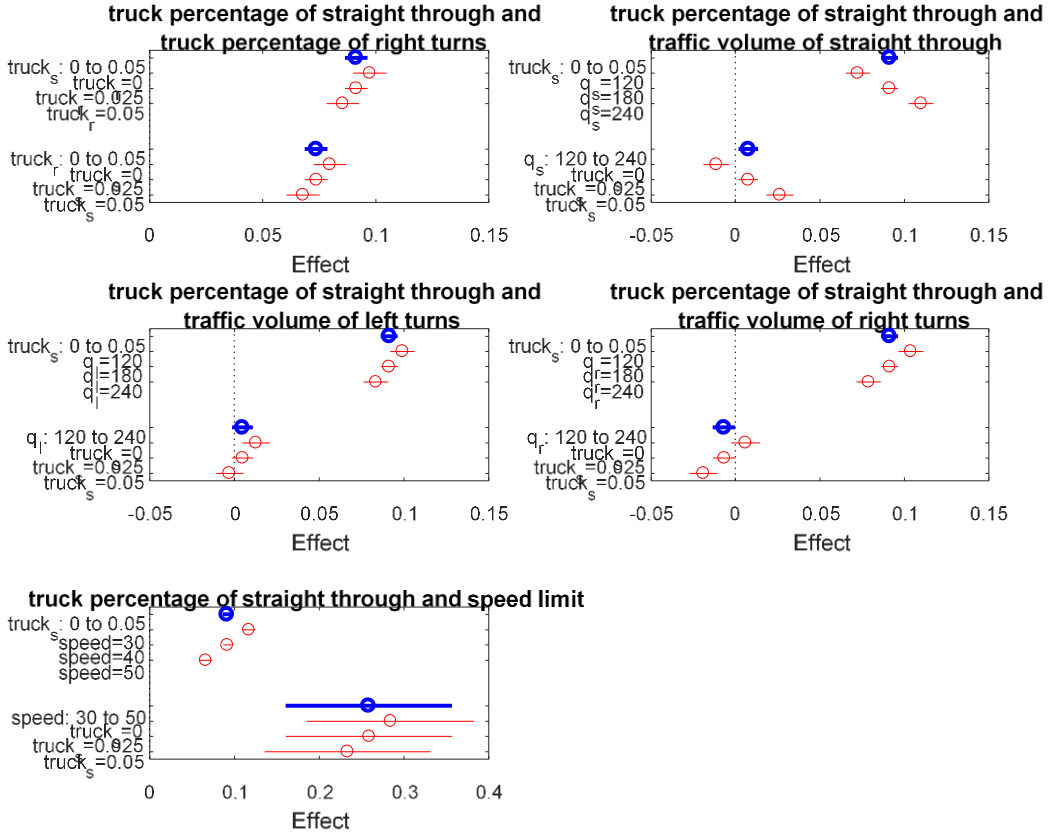

Fig. A. 4 Interaction effect between the truck percentage of straight going and the others

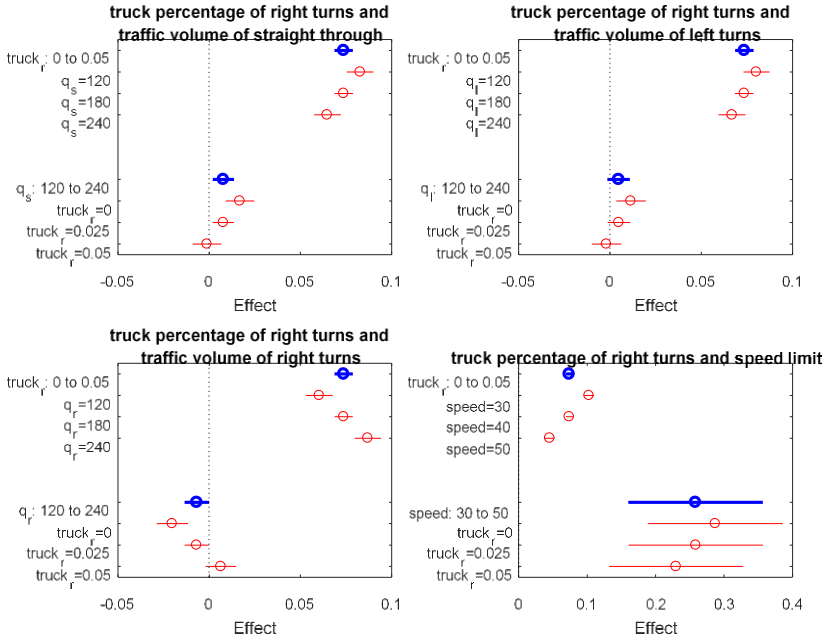

Fig. A. 5 Interaction effect between the truck percentage of the right turns and the others

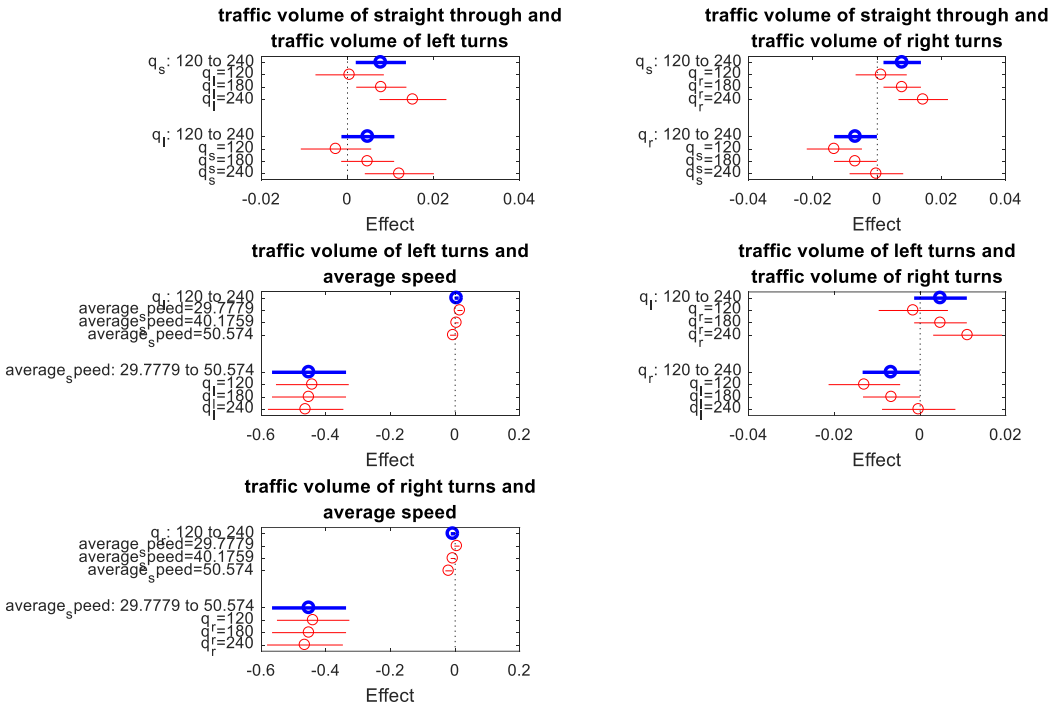

Fig. A. 6 Rest of the interaction effect

Upper part on the lane with right-turning and straight-through traffic

For the upper part of the lane, the final stepwise model shows in Fig. A. 7.

- With a higher right-turning ratio, the emission factor of NO_x gets lower. It decreases more when fewer truck percentages of right turns, less traffic, or lower average speed.
- The truck percentage of right-turning traffic has a positive effect on the emission factor of NO_x, and the effect size gets bigger with a bigger right-turning ratio.
- The traffic volume has a positive effect on the emission factor of NO_x. The effect size gets bigger, with a higher right-turning ratio.
- With lower average speed, the emission factor of NO_x gets higher. It increases more when a bigger right-turning ratio.
- The truck percentage of straight-through traffic, cycle time, and total traffic volume have positive effects on the emission factor of NO_x. Capacity is negatively related to the emission factor of NO_x.

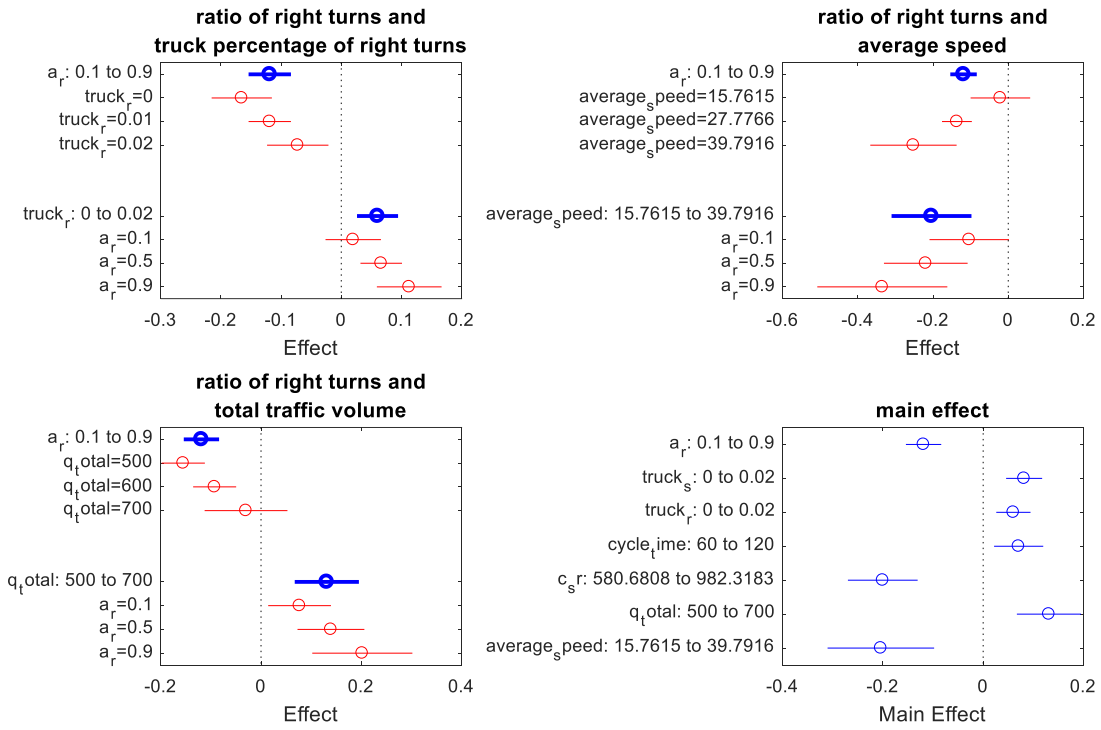

Fig. A. 7 Interaction effect of upper part on the lane with right-turning and straight-through traffic

The upper part of the right-turning lane (seen in Fig. A. 8)

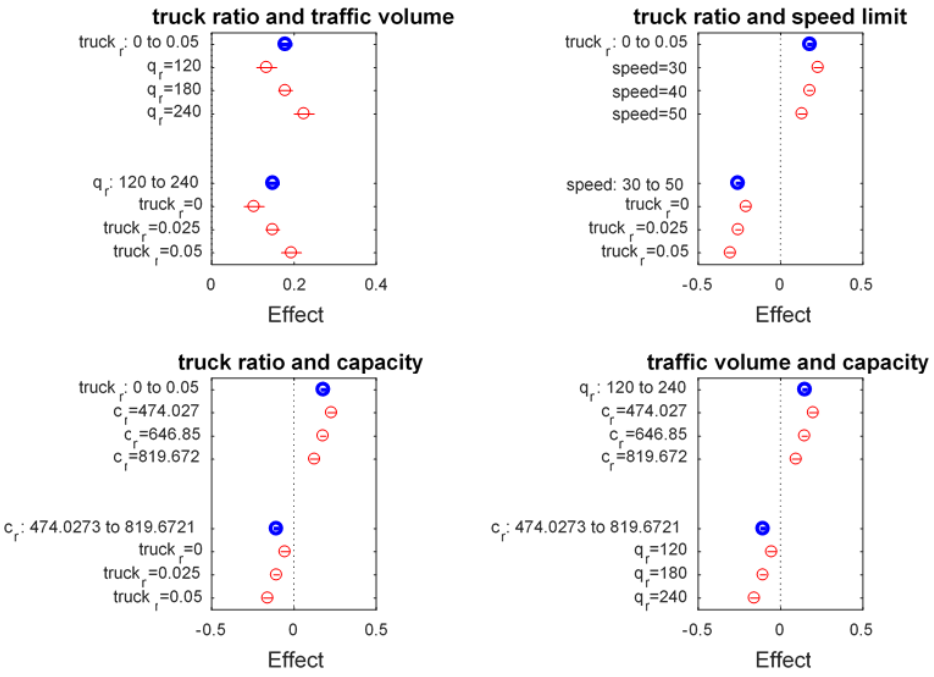

Fig. A. 8 Interaction effect on the upper part of the right-turning lane

The upper part of the right-turning lane

Since the residuals increase with the response, the log transformation is used. The stepwise model is chosen to test, and the effect of each predictor from the model is below (Fig. A. 9):

- The truck percentage is positively related to the emission factor of NO_x, and the effect size is larger in case of lower capacity or less traffic volume.
- Traffic volume has a positive relation with the emission factor of NO_x, and the effect size is larger when lower truck percentage.
- Capacity has a negative relation to the emission factor of NO_x. The absolute effect size gets bigger when higher truck percentages and a lower speed limit.
- The emission factor of NO_x gets bigger with the lower speed limit, and the absolute effect size gets bigger with large truck percentages.

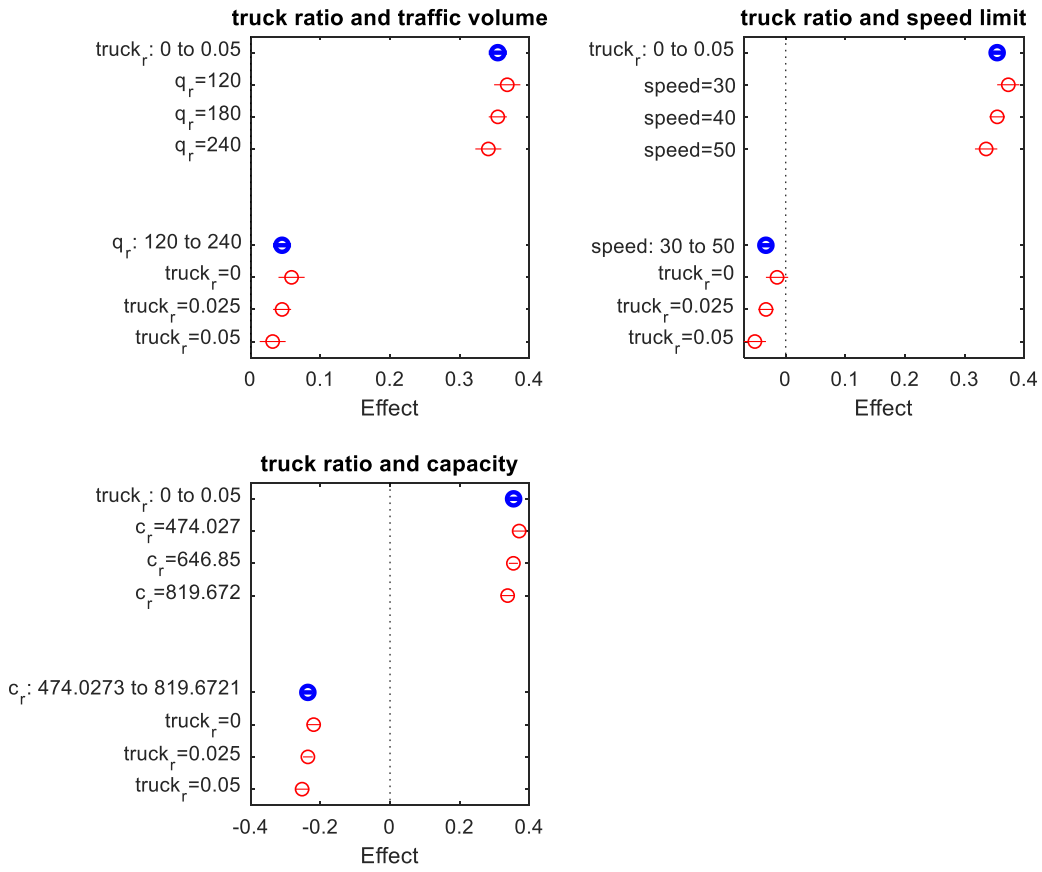

Fig. A. 9 Interaction effect after log transformation near stop line on the right-turning lane

Right turning from the right-turning lane

Using the traffic volume, truck percentage, capacity, speed limit, conflict volume, and truck percentage as predictors, it shows no multilinearity. The linear interaction and stepwise linear regression have better residual distribution. Since the full interaction regression has many statistically insignificant terms, the simpler model by the stepwise method is chosen for further check. The capacity and speed are statistically significant. Since they have interaction effects with other variables, the major effect terms would be kept. The coefficient signs of these terms show the average emission factor has positive relations with the truck percentage and volume, while negative relations to the conflict volume, speed, and capacity. The average speed is added for the stepwise regression. Its residual shows a trend to higher absolute residuals as the value of the response increases. The transformation of the response by logarithm and square root might help. To keep simple, the linear regression model is used to test (Fig. A. 10).

- The truck percentage has a positive relationship with the emission factor of NO_x since the average emission factor of NO_x of trucks is higher than passenger cars. The absolute effect size decreases with a higher speed limit. The vehicles decelerate while turning right. When the upstream speed is higher, more decelerations lead to a lower emission factor. Thus, the effect of the truck percentage on the emission factor is negatively dependent on the speed limit.

- When there is no truck, the higher speed limit upstream can lead to a higher emission factor of NO_x. When there are trucks, the emission factor can decrease at a higher speed. Since the emission factor of the truck is more sensitive to speed than passenger cars, when the truck's ratio is high, the emission actor drops more due to higher speed upstream.

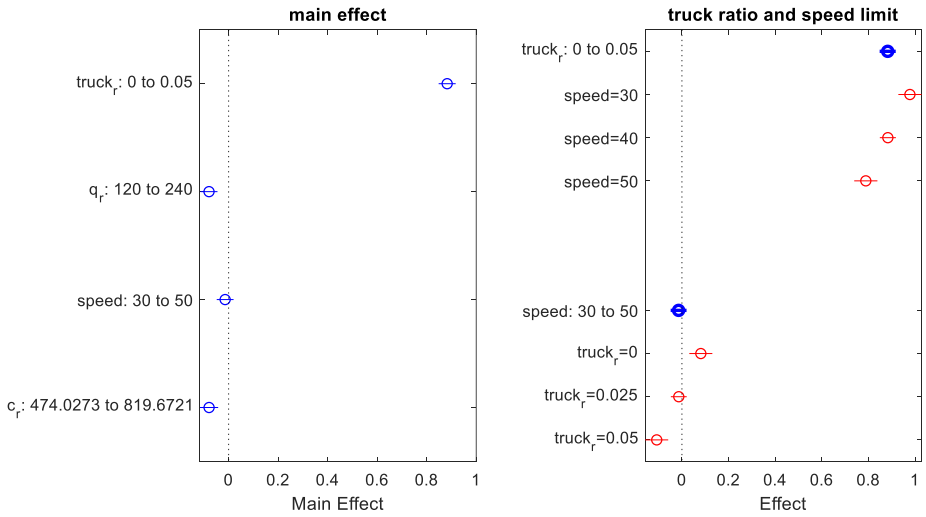

Fig. A. 10 Main and interaction effect for right-turning

Left turns from the left-turning lane

- When the truck percentage increases, the emission factor of NO_x gets bigger, the effect size would be larger with less conflicting volume, higher speed limit, and higher capacity.
- The emission factor of NO_x decreases with higher traffic volume, and the effect size gets bigger with lower capacity.
- More conflicting traffic can lead to a higher emission factor of NO_x and when more trucks turn left. The size due to conflict volume gets bigger while the bigger capacity leads to the effect decreases (the effect of conflict volume on the emission factors is majorly explained by more acceleration time and idling time.)
- A higher speed limit upstream can lead to a higher emission factor of NO_x, and the size would decrease when there are more trucks.
- With the bigger capacity of the left-turning approach, the emission factor drops, and size is bigger in case of higher truck percentage, more conflicting volume, and less left-turning traffic.

Right turning from the lane with the straight-through and right-turning traffic

Both two models (shown in Fig. A. 11 and Fig. A. 12 separately) show the truck percentage and speed limit have a positive relationship with the emission factor of NO_x while traffic volume negatively to the emission factor of NO_x. In the stepwise model, when more right-turning traffic, the positive effect size of truck percentage will decrease. When more trucks, the negative effect of traffic volume would be bigger. When cycle time is longer, the vehicles can have a lower emission factor. And it decreases more with a higher speed limit. The positive effect of the speed limit would be bigger when a shorter cycle time.

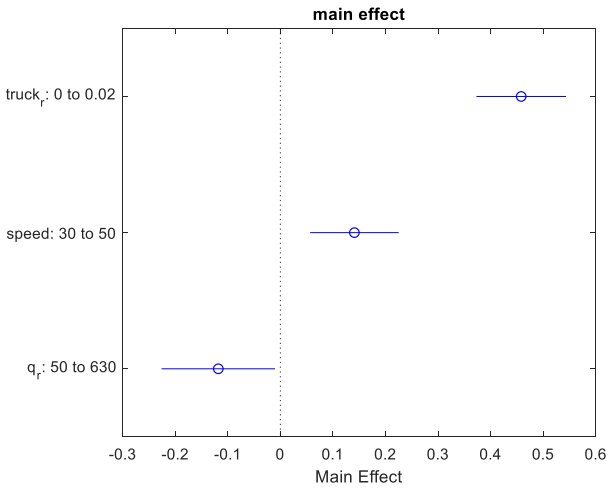

Fig. A. 11 Effect of linear regression for right turning from the lane with straight-through and right-turning traffic

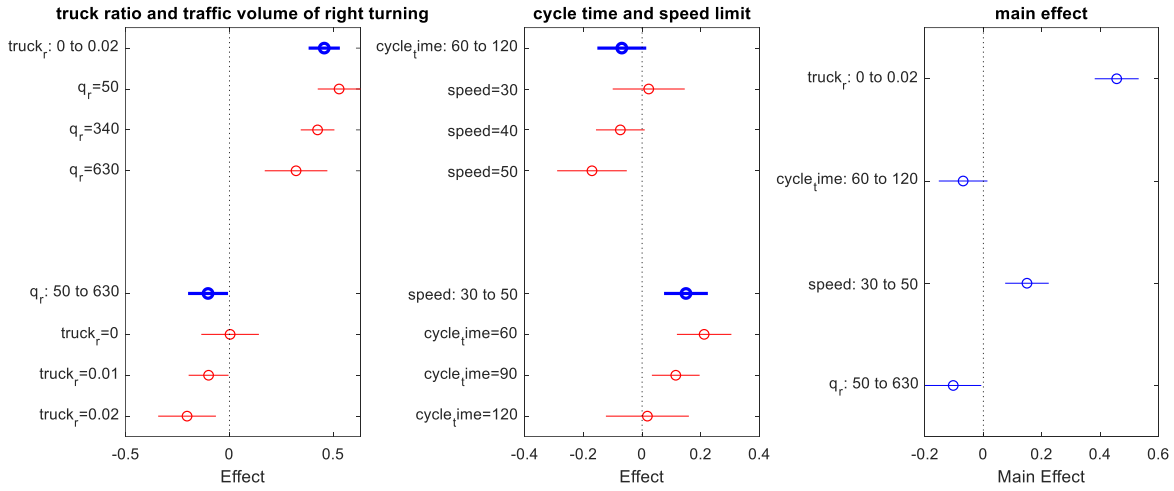

Fig. A. 12 Effect of step-wise regression for right turning from the lane with straight-through and right-turning traffic

Crossing from the lane only with straight-through traffic (seen in Fig. A. 13)

- When the truck percentage increases, the emission factor of NO_x gets bigger. The effect size is smaller when there is a higher capacity or higher speed limit.
- The emission factor of NO_x decreases with higher traffic volume. The size of decreasing gets bigger in case of a lower speed limit.
- The emission factor of NO_x decreases with bigger capacity since there are fewer accelerations from queued vehicles. When there is a bigger truck percentage or higher speed limit, the decreasing size of the emission factor of NO_x gets bigger.
- A higher speed limit can lead to a higher emission factor of NO_x. The effect size decreases when there are more trucks, higher capacity, or less straight-through traffic.

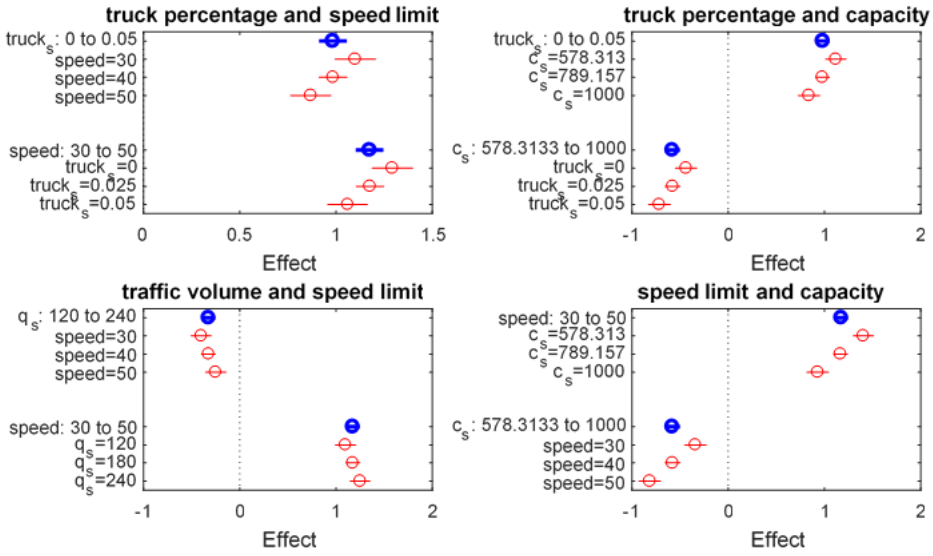

Fig. A. 13 Effect for the crossing traffic from the lane with straight-through traffic

Straight crossing from the lane with straight-through and right-turning traffic

The effect on the emission factor of NO_x is seen in Fig. A. 14. With a longer cycle time, the emission factor of NO_x becomes bigger. The effect size gets bigger with more traffic volume before the stop line. The total traffic volume has a positive effect on the emission factor of NO_x, and the effect size gets bigger with longer cycle time. The straight-through traffic and capacity have negative effects on the emission factor of NO_x, while the truck percentage of straight-through and speed limit as positive effects on the emission factor of NO_x.

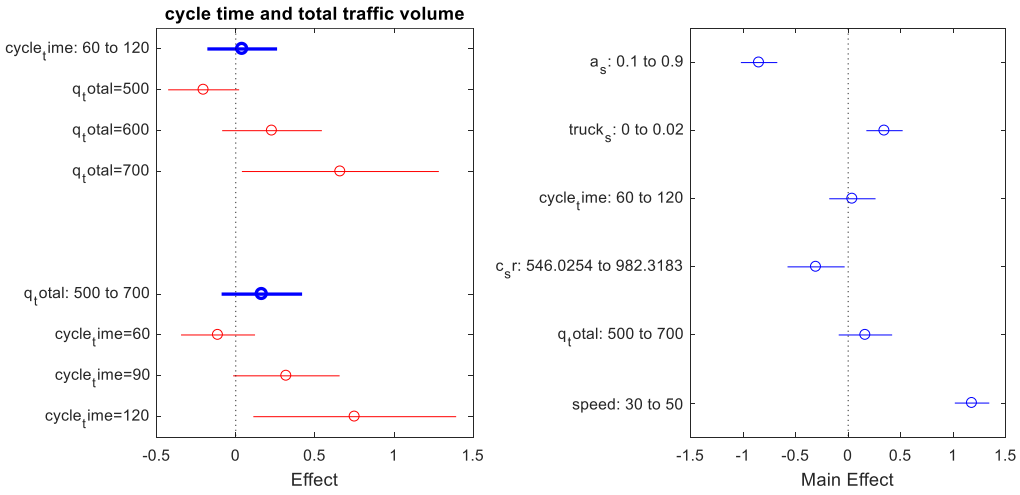

Fig. A. 14 Effect for the crossing from the lane with straight-through and right-turning traffic

After crossing the intersection

Using the traffic volume, truck percentage, capacity of right-turning north, left-turning south, and straight-through of the east, average speed, and speed limit as predictors, the stepwise model is selected (Fig. A. 15, Fig. A. 16, Fig. A. 17).

- The truck percentage of left turns has a bigger positive effect when the capacity of the straight-through lane is bigger, or the left-turning volume is larger.
- The truck percentage of right turns has a positive effect. The effect size gets bigger, with a higher speed limit and higher straight-through traffic.
- The left-turning volume is positively related to the emission factor of NO_x. The effect size increases with a longer cycle time or higher speed limit.
- The right-turning volume has a positive effect. The effect size decreases with the bigger capacity of the straight-through lane, more left turns, and a higher speed limit.
- The volume of the straight-through traffic has a negative relationship to the emission factor of NO_x. The effect size gets smaller with more right-turning trucks or a lower speed limit.
- The cycle time has a negative effect. The absolute effect size increases with higher average speed or fewer left turns.
- The capacity of the straight-through lane is negatively related to the emission factor of NO_x. The absolute effect size increases with more right turns or higher average speed.
- The average speed has a positive relationship with the emission factor of NO_x. The effect size increases when a shorter cycle time, less straight-through traffic, higher capacity of the straight-through lane, or a higher speed limit.
- The speed limit has a positive effect. The effect size increases with more right-turning trucks or more straight-through traffic.

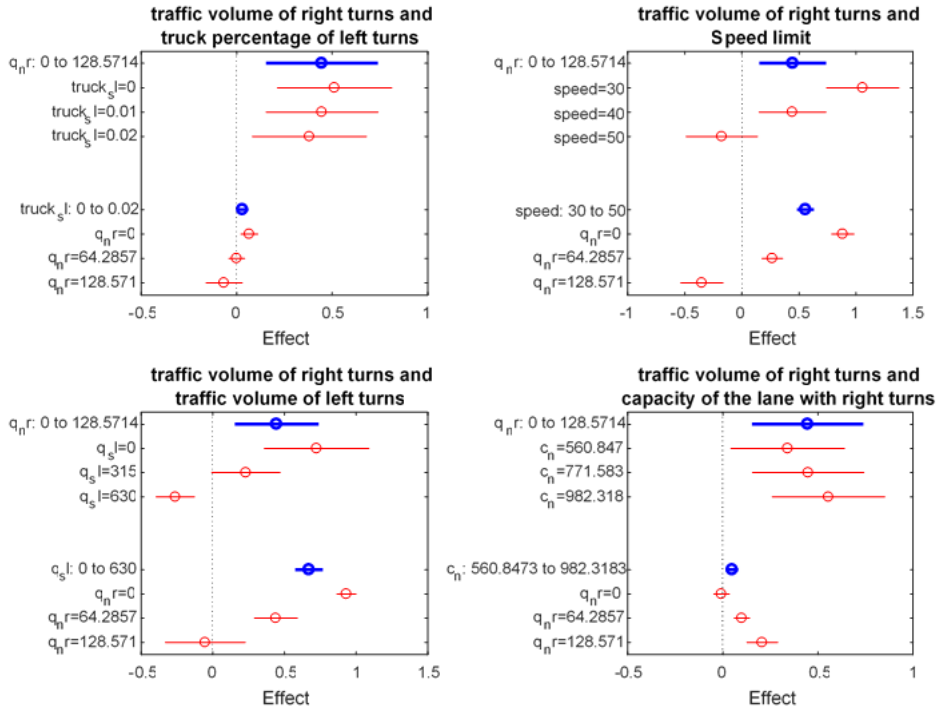

Fig. A. 15 Effects after crossing (a)

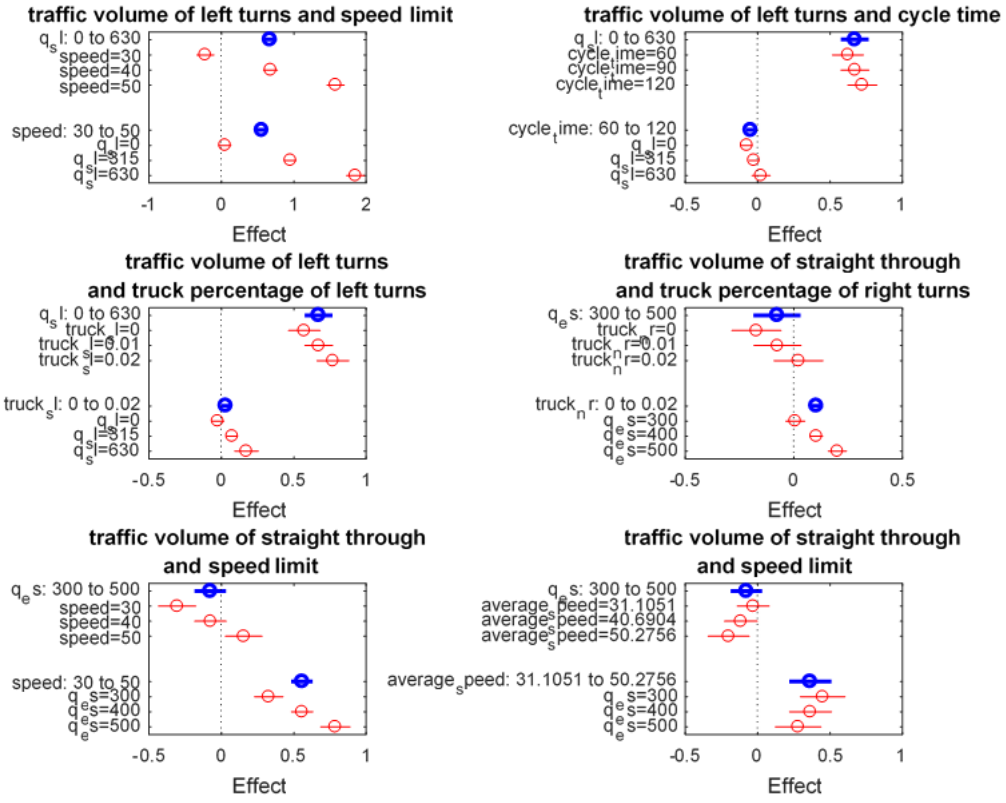

Fig. A. 16 Effect after crossing (b)

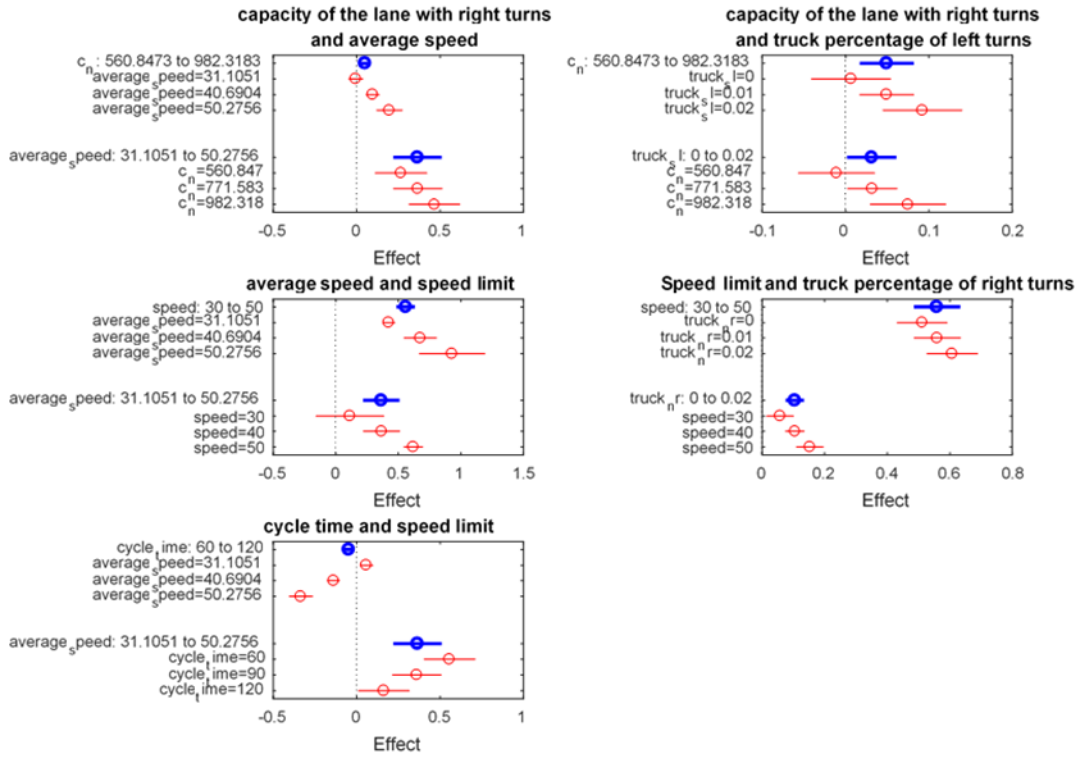

Fig. A. 17 Effect after crossing (c)